THE WORLD BANK
IBRD • IDA | WORLD BANK GROUP

ESMAP
Energy Sector Management Assistance Program

SOLAR RESOURCE AND PV POTENTIAL OF ZAMBIA

24 MONTH SITE RESOURCE REPORT

August 2018

This report was prepared by Solargis, under contract to the World Bank.

It is one of several outputs from the solar resource mapping component of the activity "Capacity Building for Renewable Energy Resource Mapping and Grid Integration in Zambia" [Project ID: P145271]. This activity is funded and supported by the Energy Sector Management Assistance Program (ESMAP), a multi-donor trust fund administered by the World Bank, under a global initiative on Renewable Energy Resource Mapping. Further details on the initiative can be obtained from the ESMAP website.

The content of this document is the sole responsibility of the consultant authors. Any improved or validated solar resource data will be incorporated into the Global Solar Atlas.

Washington DC 20433
Telephone: +1-202-473-1000
Internet: www.worldbank.org

Attribution

Please cite the work as follows: World Bank. 2018. Solar resource and PV potential of Zambia: 24 Month site resource report. Washington, DC: World Bank.

Annual Solar Resource Report

Six solar meteorological stations after completion of ground measuring campaign (24 months)

Republic of Zambia

Solargis reference	**128-07/2017**
Date:	**15 August 2018**

Customer

World Bank
Energy Sector Management Assistance Program
Contact: Mr. Oliver Knight
1818 H St NW, Washington DC, 20433, USA
Phone: +1-202-473-3159
E-mail: oknight@worldbank.org
http://www.esmap.org/RE_Mapping

Consultant

Solargis s.r.o.
Contact: Mr. Marcel Suri
Mytna 48, 811 07 Bratislava, Slovakia
Phone +421 2 4319 1708
E-mail: marcel.suri@solargis.com
http://solargis.com

TABLE OF CONTENTS

ACRONYMS

AP	Atmospheric Pressure
CFSR	Climate Forecast System Reanalysis. The meteorological model operated by the US service NOAA (National Oceanic and Atmospheric Administration)
CFSv2	Climate Forecast System Version 2 CFSv2 model is the operational extension of the CFSR (NOAA, NCEP)
DIF	Diffuse Horizontal Irradiation, if integrated solar energy is assumed. Diffuse Horizontal Irradiance, if solar power values are discussed
DNI	Direct Normal Irradiation, if integrated solar energy is assumed. Direct Normal Irradiance, if solar power values are discussed.
GFS	Global Forecast System. The meteorological model operated by the US service NOAA (National Oceanic and Atmospheric Administration)
GHI	Global Horizontal Irradiation, if integrated solar energy is assumed. Global Horizontal Irradiance, if solar power values are discussed.
MACC	Monitoring Atmospheric Composition and Climate – meteorological model operated by the European service ECMWF (European Centre for Medium-Range Weather Forecasts)
Meteosat MFG and MSG	Meteosat satellite operated by EUMETSAT organization. MSG: Meteosat Second Generation; MFG: Meteosat First Generation
PWAT	Precipitable water (water vapour)
QC	Quality control
RH	Relative Humidity at 2 metres
TEMP	Air Temperature at 2 metres
WD	Wind Direction at 10 metres
WS	Wind Speed at 10 metres

GLOSSARY

Aerosols	Small solid or liquid particles suspended in air, for example desert sand or soil particles, sea salts, burning biomass, pollen, industrial and traffic pollution.
All-sky irradiance	The amount of solar radiation reaching the Earth's surface is mainly determined by Earth-Sun geometry (the position of a point on the Earth's surface relative to the Sun which is determined by latitude, the time of year and the time of day) and the atmospheric conditions (the level of cloud cover and the optical transparency of atmosphere). All-sky irradiance is computed with all factors taken into account
Bias	Represents systematic deviation (over- or underestimation) and it is determined by systematic or seasonal issues in cloud identification algorithms, coarse resolution and regional imperfections of atmospheric data (aerosols, water vapour), terrain, sun position, satellite viewing angle, microclimate effects, high mountains, etc.
Clear-sky irradiance	The clear sky irradiance is calculated similarly to all-sky irradiance but without taking into account the impact of cloud cover.
Long-term average	Average value of selected parameter (GHI, DNI, etc.) based on multiyear historical time series. Long-term averages provide a basic overview of solar resource availability and its seasonal variability.
P50 value	Best estimate or median value represents 50% probability of exceedance. For annual and monthly solar irradiation summaries it is close to average, since multiyear distribution of solar radiation resembles normal distribution.
P90 value	Conservative estimate, assuming 90% probability of exceedance (with the 90% probability the value should be exceeded). When assuming normal distribution, the P90 value is also a lower boundary of the 80% probability of occurrence. P90 value can be calculated by subtracting uncertainty from the P50 value. In this report, we apply a simplified assumption of normal distribution of yearly values.
Root Mean Square Deviation (RMSD)	Represents spread of deviations given by random discrepancies between measured and modelled data and is calculated according to this formula: $$RMSD = \sqrt{\frac{\sum_{k=1}^{n}\left(X^{k}{}_{measured} - X^{k}_{modeled}\right)^{2}}{n}}$$ On the modelling side, this could be low accuracy of cloud estimate (e.g. intermediate clouds), under/over estimation of atmospheric input data, terrain, microclimate and other effects, which are not captured by the model. Part of this discrepancy is natural - as satellite monitors large area (of approx. 3.2 x 4.0 km for MSG satellite), while sensor sees only micro area of approx. 1 sq. centimetre. On the measurement side, the discrepancy may be determined by accuracy/quality and errors of the instrument, pollution of the detector, misalignment, data loggers, insufficient quality control, etc.
Solar irradiance	Solar power (instantaneous flow of energy) falling on a unit area per unit time [W/m^2]. Solar resource or solar radiation is used when considering both irradiance and irradiation.
Solar irradiation	Amount of solar energy falling on a unit area over a stated time interval [Wh/m^2 or kWh/m^2].
Uncertainty of estimate, U_{est}	Is a parameter characterizing the possible dispersion of the values attributed to an estimated irradiance/irradiation values. In this report, uncertainty assessment of the solar resource model estimate is based on a detailed understanding of the achievable accuracy of the solar radiation model and its data inputs (satellite, atmospheric and other data), which is confronted by an extensive data validation experience. The second source of uncertainty is ground measurements. Their quality depends on accuracy of instruments, their maintenance and data quality control. Third contribution to the uncertainty is from the site adaptation method where ground-measured and satellite-based data are correlated.

EXECUTIVE SUMMARY

This report is prepared within Phase 2 of the project *Renewable Energy Resource Mapping for the Republic of Zambia*. The project objectives is to deliver high quality solar resource mapping and measurement services for renewable energy development implemented by the World Bank in Zambia.

This report describes results of 24+ months of the measuring campaign at six solar meteorological stations, installed in Zambia. The report accompanies delivery of site-specific measurements and model data prepared for six sites, where meteorological measurement campaign has been conducted. These solar meteorological stations were installed and operated by GeoSUN Africa (South Africa) with their partner SGS Zambia, and commissioned by the World Bank over the years 2015 to 2017 under the same activity. The data quality control and further processing and integration to the solar models has been conducted by Solargis (Slovakia) under the same project.

The 2-year campaign brought a unique set of solar resource measurements for a region in Africa, and climate zone, that have been mapped insufficiently so far. The data helps specialists to better understand solar resource availability and variability, as both are crucial for development of solar power plants and for their efficient integration into existing energy infrastructure. This campaign also contributes to better understanding of performance and uncertainty of solar measuring sensors in tropical conditions. The knowledge based on the analysis of measured and modelled data in this region improves confidence of engineers, designing solar power plants, and investors and banks, providing the financing.

One of key benefits of having these type of measurements is that they can be used for improving the solar and meteorological models. We used data from six meteo sites for adaption of Solargis model to the regional climate, and this results in reduced uncertainty of the model outputs, see the summary table below. This way, the improved model is able to generate more accurate solar and meteorological historical data, which reduces uncertainties in technical and financial evaluation of any solar energy project in Zambia.

This report describes technical parameters of the measurement campaign, features of the measured data, adaptation of models, summary statistics for the outputs at six meteorological sites, and relevant uncertainties.

Summary table: Uncertainty of solar model estimates for original and site-adapted annual long-term values at 80% probability of occurrence

Uncertainty of long-term annual values	Acronym	Uncertainty of the original Solargis model	Uncertainty of the Solargis model after site adaptation based on solar measured data	
			After 1st year	After 2nd year
Global Horizontal Irradiation	GHI	±7.5% (up to ±10.0%*)	±4.5%	±4.0%
Direct Normal Irradiance	DNI	±12.0% (up to ±18.0%*)	±6.0%	±5.5%

* in complex microclimate

1 INTRODUCTION

1.1 Background

This report is prepared within Phase 2 of the project *Renewable Energy Resource Mapping for the Republic of Zambia*. This part of the project focuses on solar resource mapping and measurement services as part of a technical assistance in the renewable energy development implemented by the World Bank in Zambia. It is being undertaken in close coordination with the Department of Energy (DoE) of Zambia, the World Bank's primary country counterpart for this project, and Zambia Meteorological Department (ZMD). This project is funded by the Energy Sector Management Assistance Program (ESMAP), administered by the World Bank and supported by bilateral donors.

This report summarizes results of 24+ months of the measuring campaign at six solar meteorological stations, installed as part of the World Bank's ESMAP mission in Zambia. The report describes delivery of site-specific measurements, and site-adaptation model data. Data uncertainty and summary statistics are also described in this report.

This report accompanies delivery of site-specific solar resource and meteorological data for six sites, where solar meteorological stations have been in operation. High-quality measurements were used for the adaptation of the Solargis model for regional climate of Zambia. The model was run for the six sites and delivered high accuracy time series and Typical Meteorological Year.

The improved model can be used for delivery of similar type of data for any location in Zambia, for the needs of technical and financial evaluation of solar energy projects.

The measurements are provided by GeoSUN Africa company (South Africa). The model data for the same sites and related calculations, together with this report are supplied by Solargis company (Slovakia).

1.1 Delivered data sets

The site-specific data, provided as part of this delivery, include:

- Solar and meteorological ground measurements, after data quality assessment, 25+ months of data (11/2015 – 12/2017)
- Time series of satellite-based model data, adapted for regional climate, representing last 24+ years (1994 to 2017)
- Typical Meteorological Year data, representing 24 calendar years (1994 to 2017)

The data is delivered in formats ready to use in solar energy simulation software. This report provides detailed insight into the methodologies and results.

Table 1.1 Characteristics of the delivered data

Feature	Time coverage	Primary time step	Delivered files
Measurements (GeoSUN Africa)	Nov 2015 to Dec 2017	1 minute	Quality controlled measurements: 1- minute time resolution
Model data – original (Solargis)	Jan 1994 to Dec 2017	15 minutes	Time series: hourly, monthly and yearly time aggregation
Model data – site adapted (Solargis)	Jan 1994 to Dec 2017	15 minutes	Time series: hourly, monthly and yearly time aggregation
Model data – site adapted (Solargis)	Jan 1994 to Dec 2017	hourly	Typical Meteorological Year for P50 and P90

Table 1.2 Parameters in the delivered time series (TS) and TMY data (hourly time step)

Parameter	Acronym	Unit	TS	TMY P50	TMY P90
Global horizontal irradiance	GHI	W/m^2	X	X	X
Direct normal irradiance	DNI	W/m^2	X	X	X
Diffuse horizontal irradiance	DIF	W/m^2	X	X	X
Global tilted irradiance (at optimum angle)	GTI	W/m^2	X	-	-
Solar azimuth	SA	°	X	X	X
Solar elevation	SE	°	X	X	X
Air temperature at 2 metres	TEMP	°C	X	X	X
Wind speed at 10 metres	WS	m/s	X	X	X
Wind direction at 10 metres	WD	°	X	X	X
Relative humidity	RH	%	X	X	X
Air Pressure	AP	hPa	X	X	X
Precipitable Water	PWAT	kg/m^2	X	X	X

1.2 Information included in this report

This report presents:

- Solar resource and meteorological measurements after 24 months of operation
  - Review and quality check of the measured data
  - Calibration procedures and results
  - List and explanation of the occurred disturbances and failures
- Comparison of the measurements with the Solargis model; uncertainty analysis
  - Comparison of solar and meteo measurements with the model data
  - Site adaptation of satellite data based on ground measurements and uncertainty estimate
  - Estimate of model data uncertainty
- Data analysis (measured vs. modelled)
  - Monthly summaries of solar and meteorological parameters captured at the site
  - Variability of measured solar parameters
  - Frequency of occurrence of GHI and DNI 1-minute and 15-minute values
  - Frequency of occurrence of GHI and DNI 1-minute and 15-minute ramps

2 POSITION OF SOLAR METEOROLOGICAL SITES

In Zambia, six measuring stations were installed within the ESMAP Solar initiative. They have been located within the premises of Zambia Meteorological Department (ZMD), Zambia Agriculture Research Institute (ZARI) and School of Agricultural Sciences at University of Zambia (UNZA) (Figure 2.1, Table 2.1).

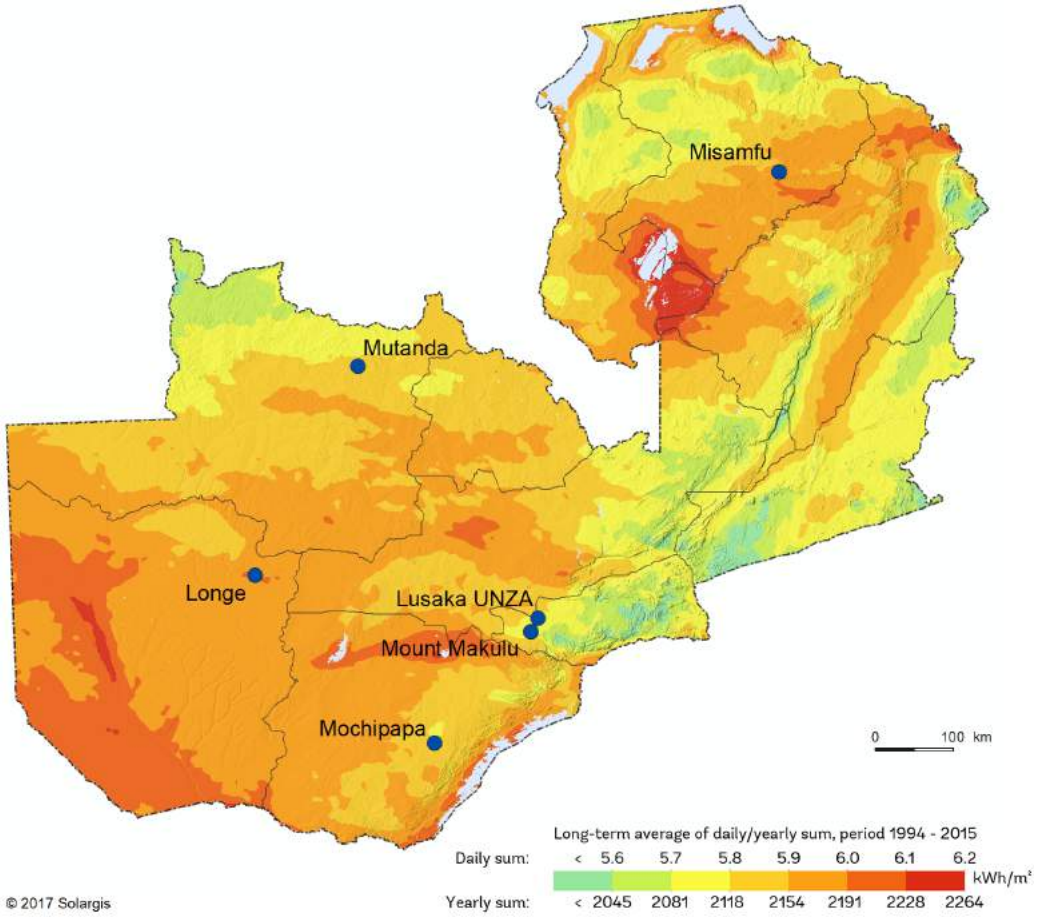

Figure 2.1: Position of solar meteorological stations in Zambia
Map of global horizontal irradiation in the background

Table 2.1 Solar meteorological stations installed in Zambia: Overview

Site name	Closest town	Latitude [°]	Longitude [°]	Altitude [m a.s.l.]	Host of measurement station
Lusaka UNZA	Lusaka	-15.39463°	28.33722°	1263	UNZA
Mount Makulu	Chilanga	-15.54830°	28.24817°	1227	ZARI/ZMD
Mochipapa	Choma	-16.83828°	27.07046°	1282	ZARI/ZMD
Longe	Kaoma	-14.83900°	24.93100°	1169	ZARI
Misamfu	Kasama	-10.17165°	31.22558°	1380	ZARI/ZMD
Mutanda	Mutanda	-12.42300°	26.21500°	1316	ZARI/ZMD

The position of solar meteorological station is selected to achieve a representative geographical distribution within the territory of Zambia, as well as in proximity to the population centres, where solar energy installations will be mostly deployed.

In addition to geographical and socio-economic criteria, the sites fulfil the criteria for the operation and maintenance of the solar measuring stations:

- Existence of free horizon,
- Availability of GSM networks,
- Availability of local work force for maintenance,
- Easy to access and high level of security

During two years of the measurements, the measured data was analysed and harmonized with the objective to acquire reference solar radiation data for reducing the uncertainty of the model Chapter 6). The quality measurements from one Tier 1 and five Tier 2 meteorological stations is available for this assessment (Chapter 3).

Position and detailed information about the measurement sites is available also in the Global Solar Atlas by the World Bank: https://globalsolaratlas.info/.

3 GROUND MEASUREMENTS IN ZAMBIA

3.1 Instruments and measured parameters

Basic information about measurements sites is in Table 3.1. Solar parameters at stations are measured by high accuracy equipment (CMP 10 for GHI measurements and CHP 1 for DNI measurements) at Tier 1 station, and by CMP 10 and additional medium accuracy equipment (RSR, for GHI, DNI and DIF, Tables 3.2 to 3.4) at all other stations. The measurement campaign in Zambia has been performed by GeoSUN Africa company (South Africa).

Table 3.1 Overview information on measurement stations operated in the region

ID	Site name	Closest town	Station type	Installation date
1	Lusaka UNZA	Lusaka	Tier 1	7 November 2015
2	Mount Makulu	Chilanga	Tier 2	13 November 2015
3	Mochipapa	Choma	Tier 2	5 November 2015
4	Longe	Kaoma	Tier 2	10 November 2015
5	Misamfu	Kasama	Tier 2	18 November 2015
6	Mutanda	Mutanda	Tier 2	21 November 2015

Table 3.2 Solar instruments installed at the solar meteorological stations

Site name	GHI	DIF	DNI	GHI 2	DIF 2	DNI 2
Lusaka UNZA	CMP 10	CMP 10	CHP 1	RSR 2	RSR 2	RSR 2
Mount Makulu	CMP 10	-	-	RSR 2	RSR 2	RSR 2
Mochipapa	CMP 10	-	-	RSR 2	RSR 2	RSR 2
Longe	CMP 10	-	-	RSR 2	RSR 2	RSR 2
Misamfu	CMP 10	-	-	RSR 2	RSR 2	RSR 2
Mutanda	CMP 10	-	-	RSR 2	RSR 2	RSR 2

Table 3.3 Meteorological instruments installed at the solar meteorological stations

Site name	WS	WD	TEMP	RH	AP	PWAT
Lusaka UNZA	05103	05103	CS215	CS215	PTB110	TE525
Mount Makulu	03002	03002	CS215	CS215	PTB110	TE525
Mochipapa	03002	03002	CS215	CS215	PTB110	TE525
Longe	03002	03002	CS215	CS215	PTB110	TE525
Misamfu	03002	03002	CS215	CS215	PTB110	TE525
Mutanda	03002	03002	CS215	CS215	PTB110	TE525

Table 3.4 Technical parameters and accuracy class of the instruments at Tier 1 and Tier 2 stations

Parameter	Instrument	Type	Manufacturer	Uncertainty
GHI	Secondary standard pyranometer	CMP 10	Kipp & Zonen	< ±2 % (daily)
DIF	Tier 1 station Secondary standard pyranometer	CMP 10	Kipp & Zonen	< ±2 % (daily)
DNI	Tier 1 station Pyrheliometer	CHP 1	Kipp & Zonen	< 1 % (daily)
GHI 2	Rotating Shadowband Radiometer with LI200	RSR 2	Irradiance Inc.	Indicatively ±5 %
DIF 2	Rotating Shadowband Radiometer with LI200	RSR 2	Irradiance Inc.	Indicatively ±8 %
DNI 2	Rotating Shadowband Radiometer with LI200	RSR 2	Irradiance Inc.	Indicatively ±5 %
WS	Tier 1 station wind speed sensor (at 10 m)	05103	R.M. Young	±0.3 m/s
	Tier 2 station wind speed sensor (at 3 m)	03002	R.M. Young	±0.5 m/s
WD	Tier 1 station wind direction sensor (at 10 m)	05103	R.M. Young	±3 °
	Tier 2 station wind direction sensor (at 3 m)	03002	R.M. Young	±5 °
TEMP	Temperature probe (at 2 m)	CS215	Campbell Scientific	±0.9°C
RH	Relative humidity probe	CS215	Campbell Scientific	±4% RH
AP	Atmospheric pressure sensor	PTB110	Vaisala	±1.5 hPa
PWAT	Tipping-bucket rain gage	TE525	Texas Instrument	±1%
-	Data logger	CR1000	Campbell Scientific	± (0.06% of reading + offset)

3.2 Station operation and calibration of instruments

In this report, complete set of data from of 2-year measurement campaign is analysed. As the measurement stations have been installed during November 2015, the period for the data analysis starts in November 2015 and ends in November 2017. On some stations, where limit of 95% of high quality data availability was not fulfilled by the end 2-year campaign, the measurements continued until December 2017. Overview of the data availability, time step and measured parameters is shown in Tables 3.5 to 3.8.

Table 3.5 Overview information on solar meteorological stations operating in the region

Site name	Closest town	Measurement period	Primary time step
Lusaka UNZA	Lusaka	7 November 2015 – 31 December 2017	1 minute
Mount Makulu	Chilanga	13 November 2015 – 31 December 2017	1 minute
Mochipapa	Choma	5 November 2015 – 31 December 2017	1 minute
Longe	Kaoma	10 November 2015 – 31 December 2017	1 minute
Misamfu	Kasama	18 November 2015 – 31 December 2017	1 minute
Mutanda	Mutanda	21 November 2015 – 31 December 2017	1 minute

Table 3.6 show data recovery statistics for the whole measurement period for each station. In this statistics, only serious issues (missing data for a longer period, erroneous data - initial installation problem or shading ring problem) are accounted. Short-term operational issues (shading by surrounding objects, morning dew on the instrument, etc.) are not considered. The column *Data loss* represents amount of missing data or data excluded during quality control process. *Percentage* share is calculated from daytime values and *days* represent cumulative amount of missing data (one day may be composed from several shorter missing data periods). The column *influenced days* represents number of days with fully or partially missing data or days excluded by quality control process. The column *Exceeding two years* show count of days of measurements exceeding the two years period.

All stations fulfilled criteria of 2-years availability of high quality ground measurements. Periods of missing or erroneous data were substituted by additional measurement days, beyond the originally assigned measurement campaign.

Table 3.6 Data recovery statistics of the measurement campaign

Zambia	Data loss*			Influenced days**		Exceeding	Acceptance criteria	
Measurement period	Erroneous + Missing data			Total	Length of individual periods	two years ***	95%	15+ days
11/2015-12/2017	[%]	(days)	Description	(days)	(days)	(days)		
Lusaka	0	**0**	-	**0**		54	OK	OK
Mount Makulu	0.5	**4**	initial RSR instrument problem (mornings)	**13**	1, 1, 1, 10	48	OK	OK
Mochipapa	0	**0**	-	**0**		56	OK	OK
Longe	2.5	**18**	missing data	**18**	1, 8, 9	51	OK	OK
Misamfu	1.9	**14**	missing/NAN data, battery failure	**14**	14	43	OK	OK
Mutanda	0	**0**	-	**0**		40	OK	OK

Table 3.7 Period of measurements analysed in this report

Year, month	2015												2016												2017											
Station	1	2	3	4	5	6	7	8	9	10	11	12	1	2	3	4	5	6	7	8	9	10	11	12	1	2	3	4	5	6	7	8	9	10	11	12
Lusaka																																				
Mount Makulu																																				
Mochipapa																																				
Longe																																				
Misamfu																																				
Mutanda																																				

During measurement campaign, the local staff of Zambia Meteorological Department, Zambia Agriculture Research Institute and School of Agricultural Sciences at University of Zambia was fully trained by GeoSUN and provided instruments inspection, monitoring and cleaning, with frequency of 1 to 5 days.

All stations measured a rare phenomenon of dip in solar irradiance on 1 September 2016 - the solar eclipse.

Table 3.8 Meteorological stations maintenance and instruments field verification

Lusaka UNZA		**Comments and issues**
Station type	Tier 1	• Occasional distortions of GHI and DNI values occurred for some mornings due to dew.
Instruments cleaning interval [days]	Average: 2.1 Longest: 12	
Verification visits date by GeoSUN Africa	6 Jun 2016 1 Nov 2016 23 Jun 2017 3 to 10 April 2018	
Instruments field verification	GHI – reference CMP 10 DIF – reference CMP10 DNI – reference CHP1 GHI 2 – reference Li200	
Mount Makulu - Chilanga		**Comments and issues**
Station type	Tier 2	• The station did not face North in November and December 2015. This affects the DIF and the DNI reading, especially in the mornings. • Atmospheric pressure data was lost in November 2016 due to sensor verification. • The station is located between trees, which causes minimum shading on the instruments during some mornings and afternoons. • Dew on the instruments cause inaccurate readings in some mornings.
Instruments cleaning interval [days]	Average: 1.4 Longest: 8	
Verification visits date by GeoSUN Africa	6 Jun 2016 1 Nov 2016 23 Jun 2017 3 to 10 April 2018	
Instruments field verification	GHI – reference CMP 10 GHI 2 – reference Li200	

Mochipapa - Choma		**Comments and issues**
Station type	Tier 2	• Shading from a tree in late afternoon. • Several distortions of GHI and DNI occurred in some mornings due to dew. • During February, March and April 2016, malfunction of TEMP and RH sensor occurred (CS215); thus datalogger internal temperature sensor readings were used for correction of RSR measurements (GHI, DNI, DIF).
Instruments cleaning interval [days]	Average: 2.2 Longest: 9	
Verification visits date by GeoSUN Africa	27 Apr 2016 2 Nov 2016 24 Jun 2017 3 to 10 April 2018	
Instruments field verification	GHI – reference CMP 10 GHI 2 – reference Li200	
Longe – Kaoma		**Comments and issues**
Station type	Tier 2	• The station is located close to trees, which cause slight shading in the mornings and afternoons. • Several distortions of GHI and DNI values occurred on some mornings due to dew. • Short data period loss occurred in February and May 2016 due to lost connection with datalogger. • Several longer periods without cleaning (9 to 17 days) • Unknown shadow cast over the CMP 10 instrument on 6 June 2017 causing inaccurate measurements for a couple of minutes.
Instruments cleaning interval [days]	Average: 4.3 Longest: 17	
Verification visits date by GeoSUN Africa	7 Jun 2016 4 Nov 2016 25 June 2017 3 to 10 April 2018	
Instruments field verification	GHI – reference CMP 10 GHI 2 – reference Li200	
Misamfu – Kasama		**Comments and issues**
Station type	Tier 2	• Shading on the irradiance sensors every morning due to overhead utility power cables close to the station. • Several distortions of GHI and DNI values occurred on some mornings due to dew. • Incorrect readings from RSR and CMP10 in February 2016 due to faulty RSR and battery • Small data loss in February 2016 due to faulty battery
Instruments cleaning interval [days]	Average: 2.1 Longest: 9	
Verification visits date by GeoSUN Africa	7 Nov 2016 29 Jun 2017 2 March 2017 3 to 10 April 2018	
Instruments field verification	GHI – reference CMP 10 GHI 2 – reference Li200	
Mutanda – Solwezi		**Comments and issues**
Station type	Tier 2	• Several distortions of GHI and DNI values occurred on some mornings due to dew.
Instruments cleaning interval [days]	Average: 3.0 Longest: 17	
Verification visits date by GeoSUN Africa	8 Jun 2016 5 Nov 2016 27 Jun 2017 3 to 10 April 2018	
Instruments field verification	GHI – reference CMP 10 GHI 2 – reference Li200	

GeoSUN Africa performed detailed visits and station maintenance after 6, 12, 18 and 24 months of operation. Instruments field verification [26], i.e. comparative measurements of solar radiation parameters and cross check with the reference instruments was performed by GeoSUN Africa after first year of operation (Table 3.8). The objective was to proof that calibration constants remained stable within the instrument specifications. At the end of measurement campaign, the re-calibration of instruments was performed.

To perform a verification of the measurements, the spare instruments of the same category were used. The solar sensors (thermopile pyrheliometer and thermopile pyranometer) were side-by-side compared and only clear-sky

values were used. In case of RSR, the GHI values of the RSR were compared to the GHI of the reference thermopile pyranometer for a 12-month period, to assess possible drift. Results of field instruments verification are listed in Table 3.9. During the data analysis, it was found that incorrect multipliers were applied on RSR sensors, thus the calibration coefficients at all meteorological stations had been updated and the measurements have been post-processed to correct this issue. The detailed results and discussion is supplied in *Sensor verification report* delivered in July 2017 [26]. The sensors are found to operate within the expected uncertainty limits.

Table 3.9 Results of field instruments verification performed by GeoSUN Africa on April 2018

Site name	Station type	Measured bias							
		GHI		DNI		DIF		GHI 2	
		[W/m²]	[%]	[W/m²]	[%]	[W/m²]	[%]	[W/m²]	[%]
Lusaka UNZA	Tier 1	-11.42	-1.10	-6.75	-0.77	-1.83	-1.32	2.05	0.21
Mount Makulu	Tier 2	-3.74	-1.38	-	-	-	-	-11.79	-4.42
Mochipapa	Tier 2	-6.44	-0.72	-	-	-	-	-2.57	-0.33
Longe	Tier 2	-3.60	-0.35	-	-	-	-	-6.98	-0.73
Misamfu	Tier 2	-4.59	-0.55	-	-	-	-	-15.07	-1.85
Mutanda	Tier 2	-17.27	-1.99	-	-	-	-	-22.79	-2.74

On the April 2018 GeoSUN Africa swopped the pyranometers with newly-calibrated ones. A field verification was performed on the meteorological instruments. Swap of the pyrheliometer at UNZA remains to be done. The data from all stations is regularly downloaded on a PC at the ZMD headquarters. After the end of Phase 2 (24-months of the measuring campaign) the operation of the stations is still overseen by GeoSUN Africa. All is ready for final hand-over of the equipment to ZMD.

3.3 Quality control of measured solar resource data

Prior to correlation with satellite-based solar data, the ground-measured solar radiation was quality-controlled by Solargis. Quality control (QC) was based on methods defined in SERI QC procedures and Younes et al. [1, 2] and the in-house developed tests. The ground measurements were inspected also visually, mainly for identification of shading and other error patterns such as RSR shading ring malfunction.

Figures 3.1, 3.2, 3.4, 3.9, 3.12, 3.16 and 3.18 show results of quality control for individual stations. The colours in the quality control pictures indicate the following flags:

- Blue: data excluded by visual inspection - mainly shading, shading ring issues and effect of dew
- Green: data passed all tests
- Grey: un below horizon
- White and brown strips: missing data
- Red and violet: GHI, DNI and DIF consistency issue or exceedance of physical limits

The data records not passing the quality control test were flagged and excluded from further processing. The results show relatively small amount of excluded data readings (Tables 3.11, 3.14, 3.17, 3.20, 3.23 and 3.26), predominantly during first year of operation. The most frequent is the shading from surrounding trees and the GHI values affected by dew.

3.3.1 University of Zambia (UNZA) Lusaka

Table 3.10 Occurrence of data readings for UNZA Lusaka meteorological station

Data availability	DNI CHP1, GHI CMP10		GHI, DNI RSR	
Sun below horizon	555 472	49.3%	555 472	49.3%
Sun above horizon	570 244	50.7%	570 244	50.7%
Total data readings	1 125 716	100.0%	1 125 716	100.0%

Table 3.11 Excluded ground measurements after quality control (Sun above horizon) in UNZA Lusaka

Type of test	Occurrence of data samples (Sun above horizon)							
	DNI CHP1		GHI CMP10		DNI RSR		GHI RSR	
Physical limits test	232	0.0%	3652	0.6%	0	0.0%	3041	0.5%
Consistency test (GHI – DNI – DIF)	4091	0.7%	4091	0.7%	12	0.0%	12	0.0%
Visual test (incorrect data)	12726	2.2%	10581	1.9%	11172	2.0%	10663	1.9%
Other (non-valid data)	0	0.0%	0	0.0%	17280	3.0%	0	0.0%
Total excluded data samples	17 049	3.0%	18 324	3.2%	28 464	5.0%	13 716	2.4%
Total samples	570 244	100.0%	570 244	100.0%	570 244	100.0%	570 244	100.0%

Main findings:

- Occurrence of morning dew on sensors influencing mainly the measurements from thermopile instruments (CMP10 and CHP1)
- Short periods of inconsistency between independent GHI, DNI and DIF measurements is present in the data (Figure 3.1 and 3.2). This might be a result of morning dew occurrence and insufficient cleaning.
- Seasonal early morning and late afternoon shading from the surrounding objects.
- A systematic difference between GHI measurements from the secondary standard pyranometer CMP10 and RSR (Figure 3.3 right). GHI from CMP10 is in average higher by 1.6% than GHI from RSR. The difference was 1.9% in 2016 and 1.2% in 2017. In the noon time, it can exceed 3% to 4%.
- A systematic difference between DNI measurements from first class pyrheliometer CHP1 and RSR (Figure 3.3 left). DNI from CHP1 is in average higher by 2.0% than DNI from RSR. The difference was 2.4% in 2016 and 1.5% in 2017. In the noon time, it can exceed 4% to 5%.

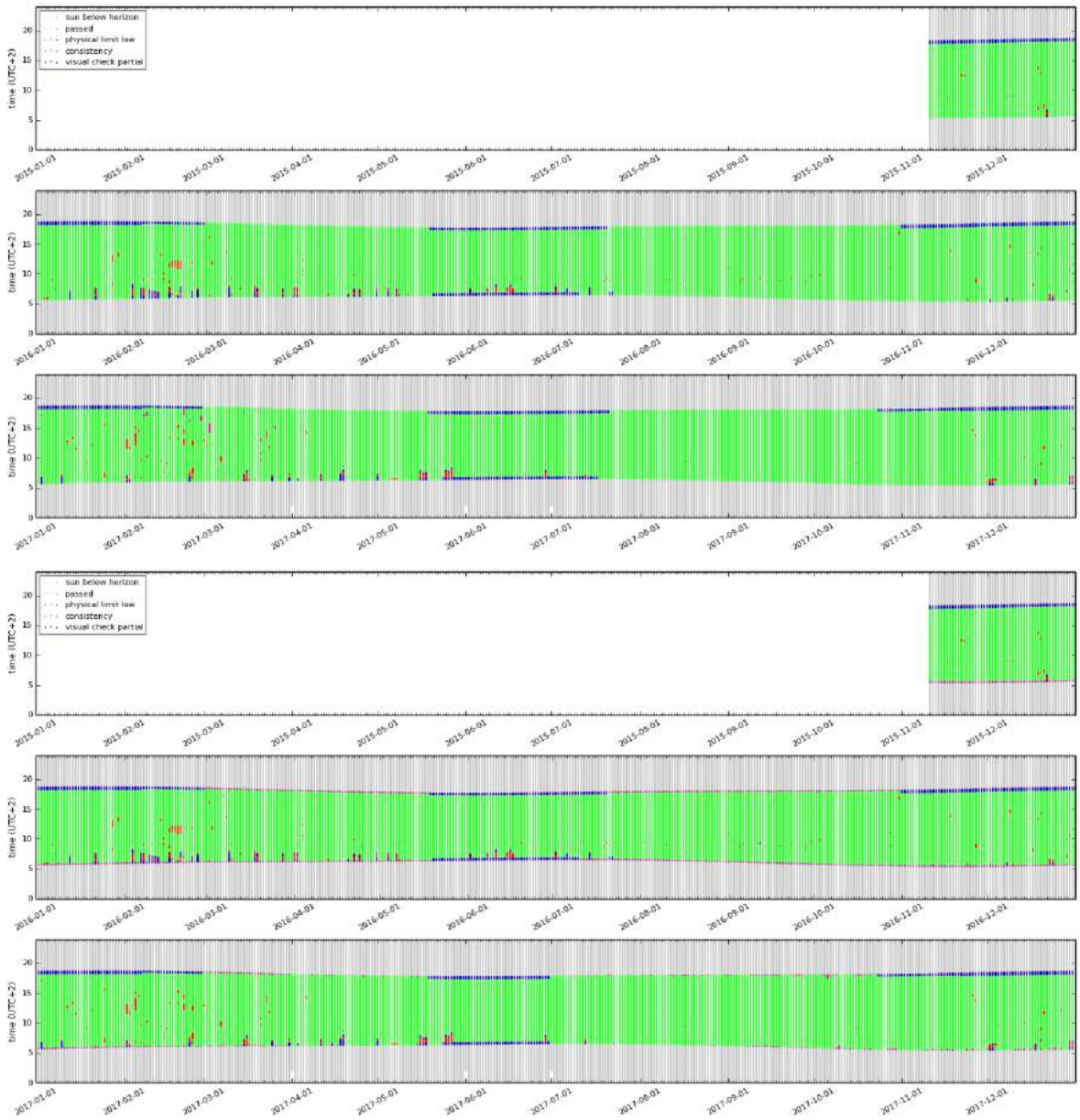

Figure 3.1 Results of DNI (CHP1) and GHI (CMP10) quality control at UNZA Lusaka.
Green – data passing all tests; grey – sun below horizon; red – consistency issue, violet – physical limit, blue excluded by visual inspection. Top: DNI (CHP1); bottom: GHI (CMP10)

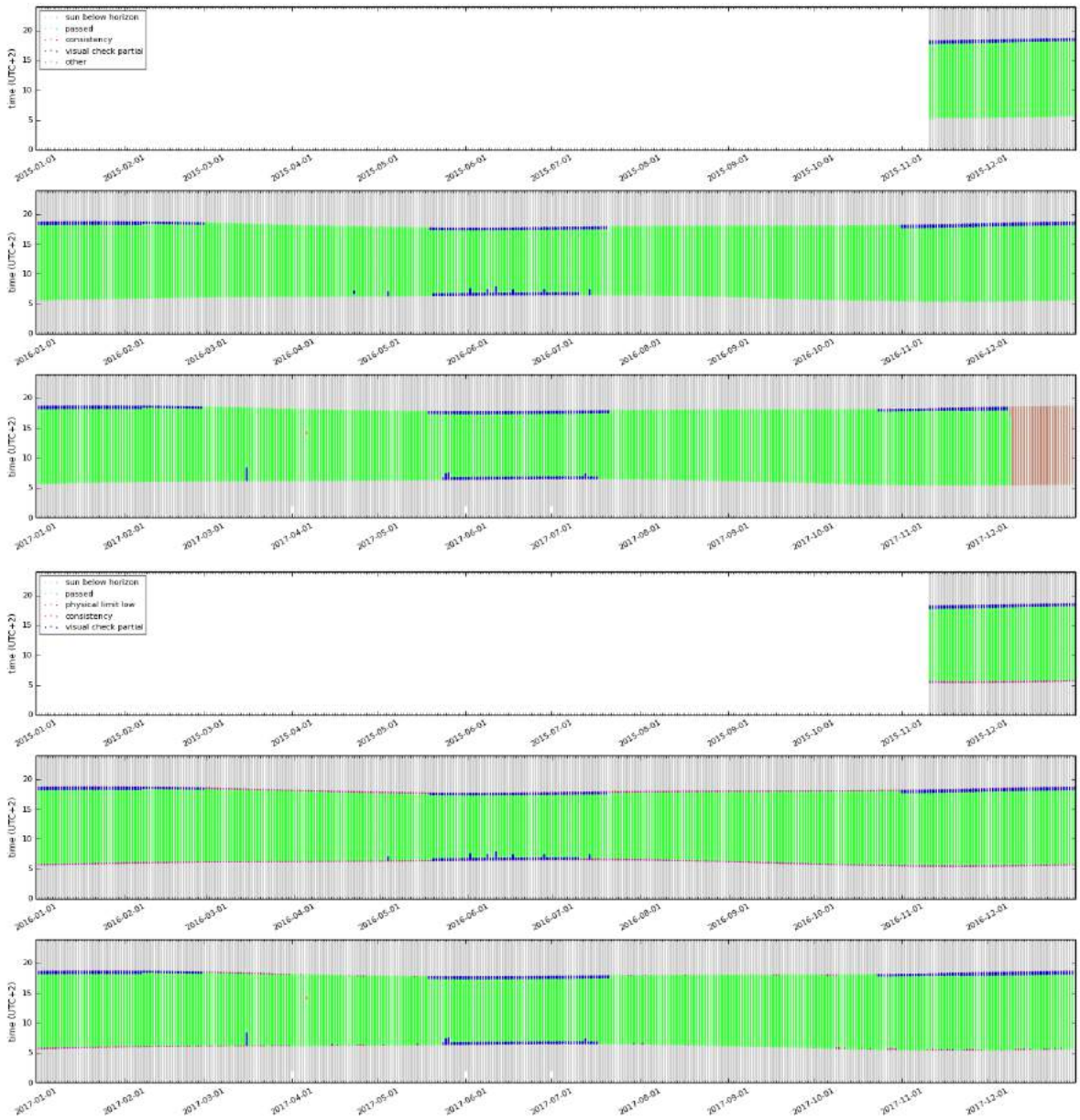

Figure 3.2 Results of DNI (RSR) and GHI (RSR) quality control at UNZA Lusaka.
Green – data passing all tests; grey – sun below horizon; red – consistency issue, violet – physical limit, blue excluded by visual inspection. Top: DNI (RSR); bottom: GHI (RSR)

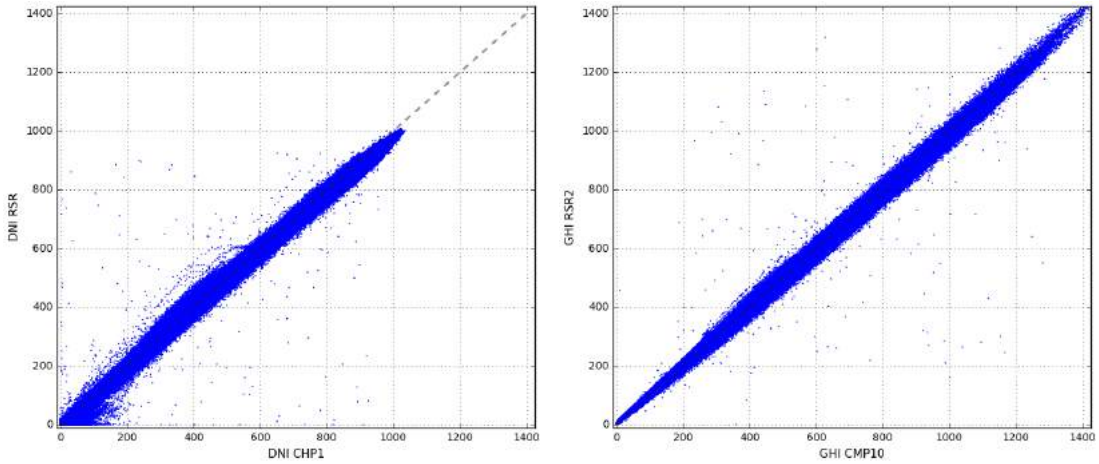

Figure 3.3 Difference of DNI and GHI between two sensors – UNZA Lusaka.
Left: DNI from CHP1 and RSR; right: GHI from CMP10 and RSR

Table 3.12 Quality control summary – UNZA Lusaka

Indicator	Flag	Description
Station description, metadata		Installation report available
Instrument accuracy		2x Secondary standard pyranometer CMP10 (GHI, DIF) 1x First class pyrheliometer CHP1 (DNI)
		1x Rotating Shadowband Radiometer RSR 2 (GHI, DIF, DNI)
Instrument calibration		Instruments were calibrated and calibration verified after 12 months
Data structure		Clear
Cleaning and maintenance information		Cleaning log available Diligent cleaning and maintenance
Time reference		Correct and clear time reference
Quality control complexity		RSR data, full QC CMP10 and CHP1 data, with (GHI-DNI-DIF) consistency test, comparison of GHI and DNI from RSR and CHP1 and CMP10
Quality control results		Occurrence of morning dew influencing mainly data from CMP10 and CHP1 Small issues with early morning and late afternoon shading Small inconsistency of RSR and CMP10/CHP1 measurements
Period		More than 25 months
Other issues		-

Legend: Quality flag

Very good	Good	Sufficient	Problematic	Insufficient	Not specified

3.3.2 Mount Makulu (Chilanga)

Table 3.13 Occurrence of data readings for Mount Makulu meteorological station

Data availability	GHI CMP10		GHI, DNI RSR	
Sun below horizon	553 295	49.3%	553 295	49.3%
Sun above horizon	567 963	50.7%	5679 63	50.7%
Total data readings	1 121 258	100.0%	1 121 258	100.0%

Table 3.14 Excluded ground measurements after quality control (Sun above horizon) in Mount Makulu

Type of test	Occurrence of data samples (Sun above horizon)					
	GHI CMP10		DNI RSR		GHI RSR	
Physical limits test	5 063	0.9%	0	0.0%	3 756	0.7%
Consistency test (GHI – DNI – DIF)	0	0.0%	0	0.0%	0	0.0%
Visual test (incorrect data)	29 406	5.2%	32 748	5.8%	30 148	5.3%
Other (non-valid data)	19	0.0%	19	0.0%	19	0.0%
Total excluded data samples	34 488	6.1%	32 767	5.8%	33 923	6.0%
Total samples	567 963	100.0%	567 963	100.0%	567 963	100.0%

Main findings:

- Incorrect orientation of RSR instrument towards the North results in incorrect data (Figure 3.5). This issue influenced morning data readings in the initial period of operation (November and December 2015).
- Early morning shading (Figure 3.6) from the surrounding objects or trees.
- A systematic difference between GHI measurements from the secondary standard pyranometer CMP10 and RSR (Figure 3.7). GHI from CMP10 is in average higher by 2.2% than GHI from RSR. The difference was 2.3% in 2016 and 2.0% in 2017. In the noon time, the difference can exceed 3% to 4%.
- Occurrence of morning dew on the sensors influencing mainly GHI from the thermopile instrument (CMP10).

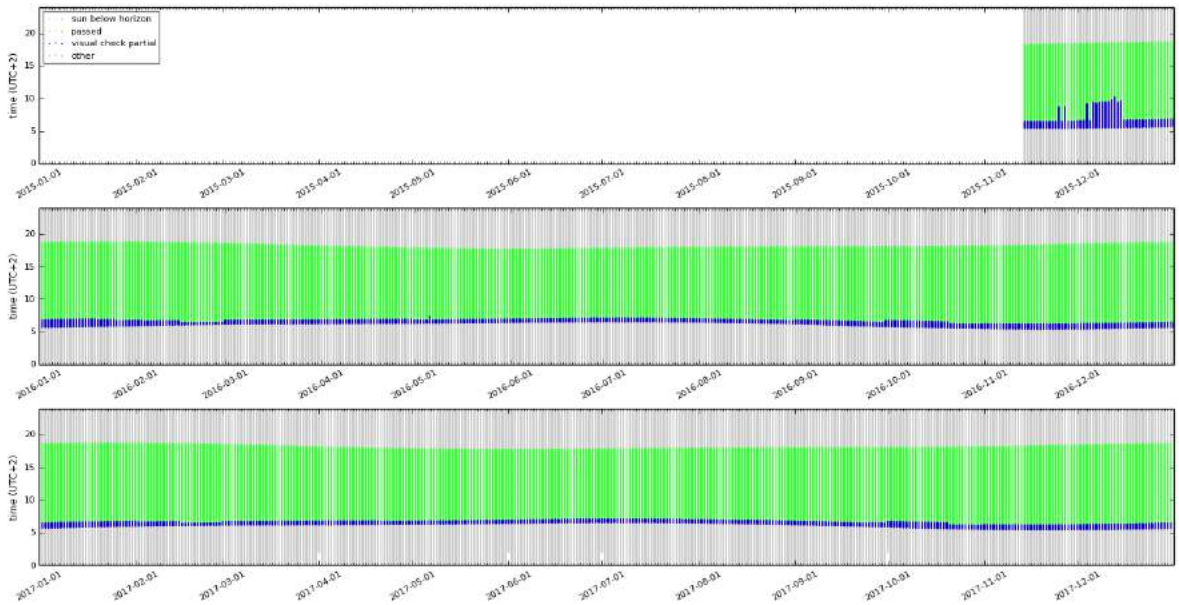

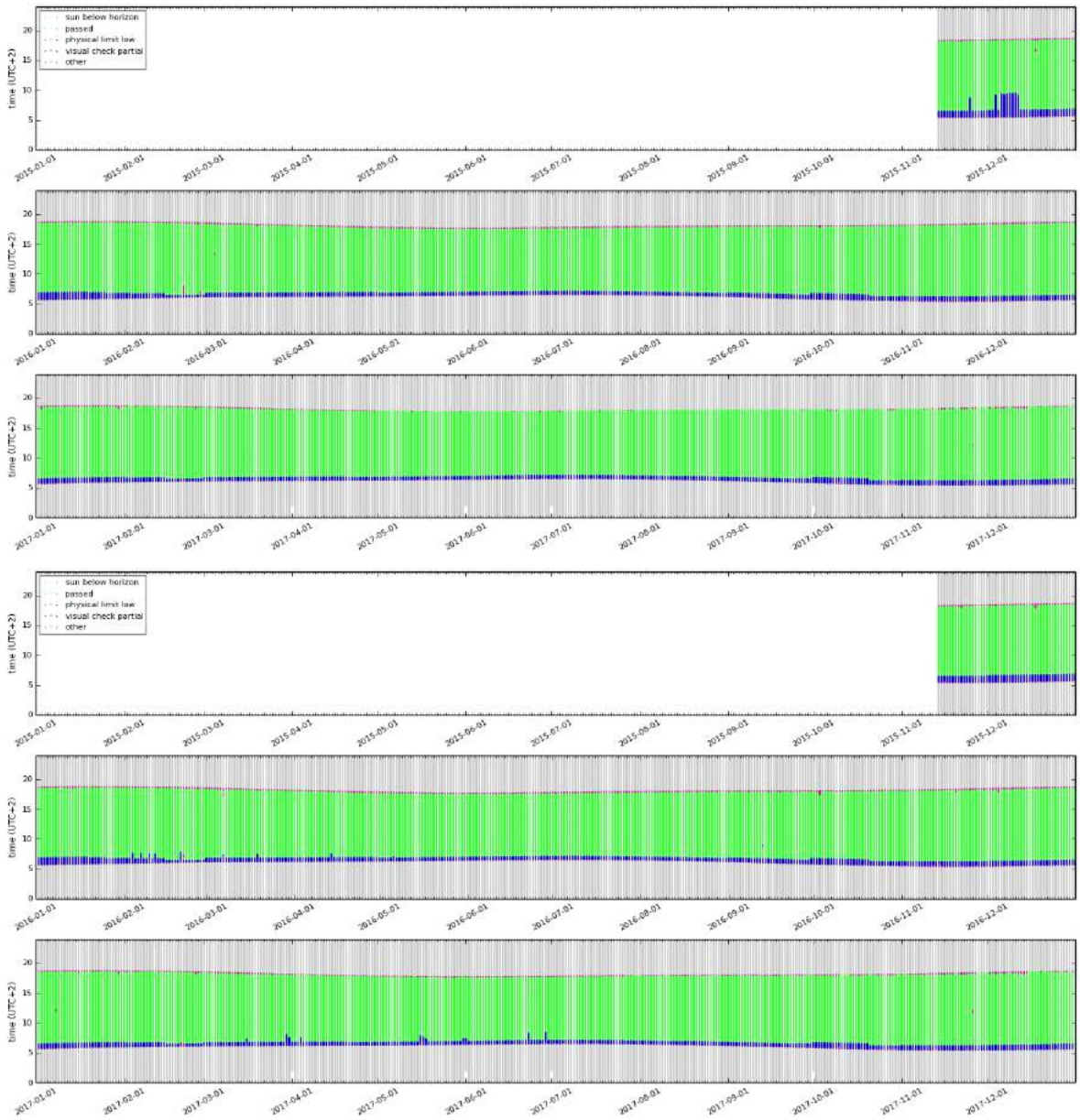

Figure 3.4 Results of GHI and DNI quality control in Mount Makulu.
Green – data passing all tests; grey – sun below horizon; violet – physical limit issue, blue excluded by visual inspection; brown – missing data.
Top: DNI (RSR); middle: GHI (RSR); bottom: GHI (CMP10)

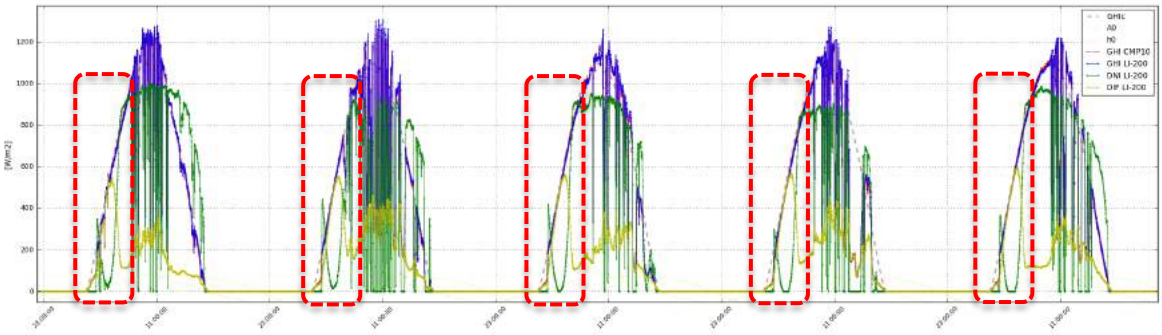

Figure 3.5 Effect of RSR alignment issues – drop of DNI in Mount Makulu
Green: DNI RSR; red: GHI CMP10; blue: GHI RSR; yellow: DIF RSR; dashed: theoretical clear-sky profile

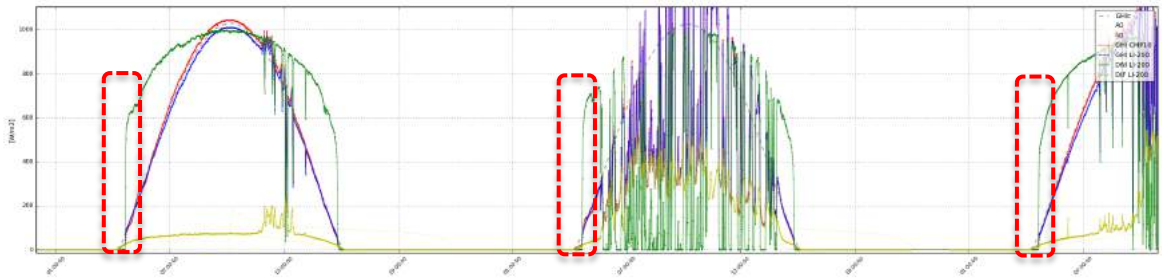

Figure 3.6 Effect of morning shading - Mount Makulu
Green: DNI RSR; red: GHI CMP10; blue: GHI RSR; yellow: DIF RSR; dashed: theoretical clear-sky profile

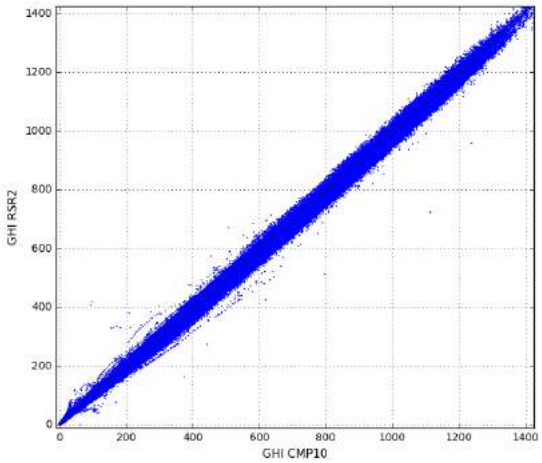

Figure 3.7 Systematic difference between GHI from CMP10 and RSR - Mount Makulu

Table 3.15 Quality control summary – Mount Makulu

Indicator	Flag	Description
Station description, metadata		Installation report available
Instrument accuracy		1x Secondary standard pyranometer CMP10 (GHI)
		1x Rotating Shadowband Radiometer RSR 2 (GHI, DIF, DNI)
Instrument calibration		Instruments were calibrated, and calibration was verified after 12 months
Data structure		Clear
Cleaning and maintenance information		Cleaning log available Diligent cleaning and maintenance
Time reference		Correct and clear time reference
Quality control complexity		RSR data, full QC comparison of GHI from RSR and CMP10
Quality control results		Incorrect orientation of RSR instrument in initial phase of measurements Occurrence of morning dew influencing mainly data from CMP10 Early morning shading Small inconsistency of RSR and CMP10 measurements
Period		More than 25 months
Other issues		

Legend: Quality flag

Very good	Good	Sufficient	Problematic	Insufficient	Not specified

3.3.3 Mochipapa (Choma)

Table 3.16 Occurrence of data readings for Mochipapa meteorological station

Data availability	GHI CMP10		GHI, DNI RSR	
Sun below horizon	558 340	49.3%	5583 40	49.3%
Sun above horizon	574 316	50.7%	574 316	50.7%
Total data readings	1 132 656	100.0%	1 132 656	100.0%

Table 3.17 Excluded ground measurements after quality control (Sun above horizon) in Mochipapa

Type of test	Occurrence of data samples (Sun above horizon)					
	GHI CMP10		DNI RSR		GHI RSR	
Physical limits test	5 184	0.9%	0	0.0%	3 322	0.6%
Consistency test (GHI – DNI – DIF)	0	0.0%	0	0.0%	0	0.0%
Visual test (incorrect data)	34 992	6.1%	32 417	5.6%	30 785	5.4%
Other (non-valid data)	0	0.0%	0	0.0%	0	0.0%
Total excluded data samples	40 176	7.0%	32 417	5.6%	34 107	5.9%
Total samples	574 316	100.0%	574 316	100.0%	574 316	100.0%

Main findings:

- Late afternoon shading from surrounding objects or trees (Figure 3.9)
- A systematic difference between GHI measurements from secondary standard pyranometer CMP10 and RSR (Figure 3.10). GHI from CMP10 is in average higher by 1.8% than GHI from RSR. The difference was 2.1% in 2016 and 1.5% in 2017. In the noon time it can exceed 4%.
- Occurrence of morning dew on sensors influencing mainly the GHI from thermopile instrument (CMP10)
- Slight asymmetry of diurnal profiles may indicate problems with misalignment of instruments (Figure 3.11).

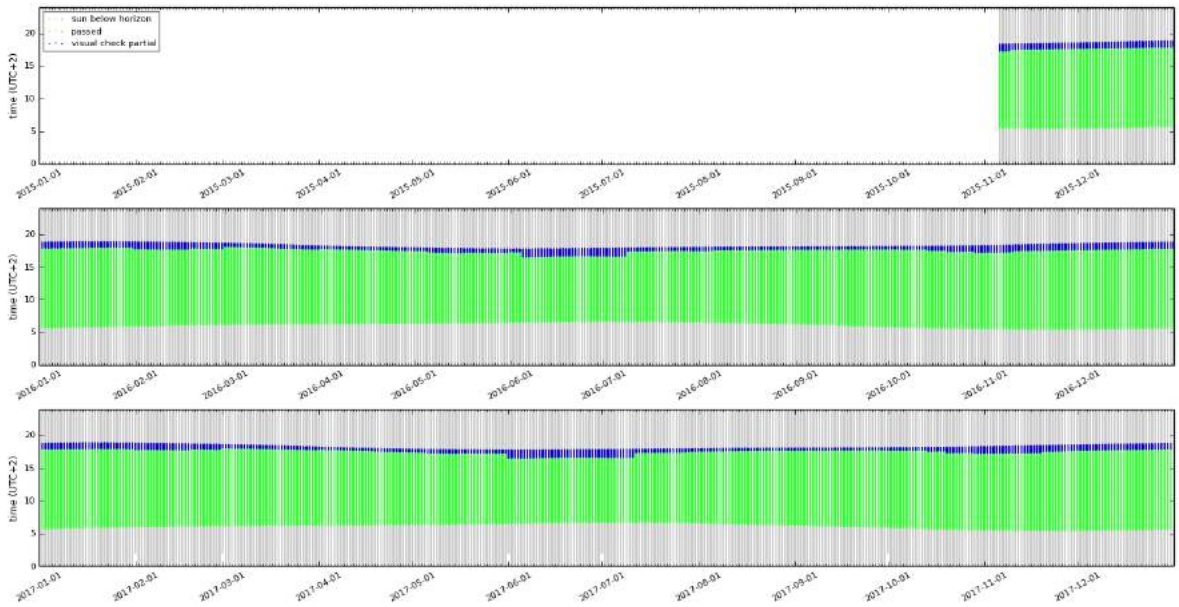

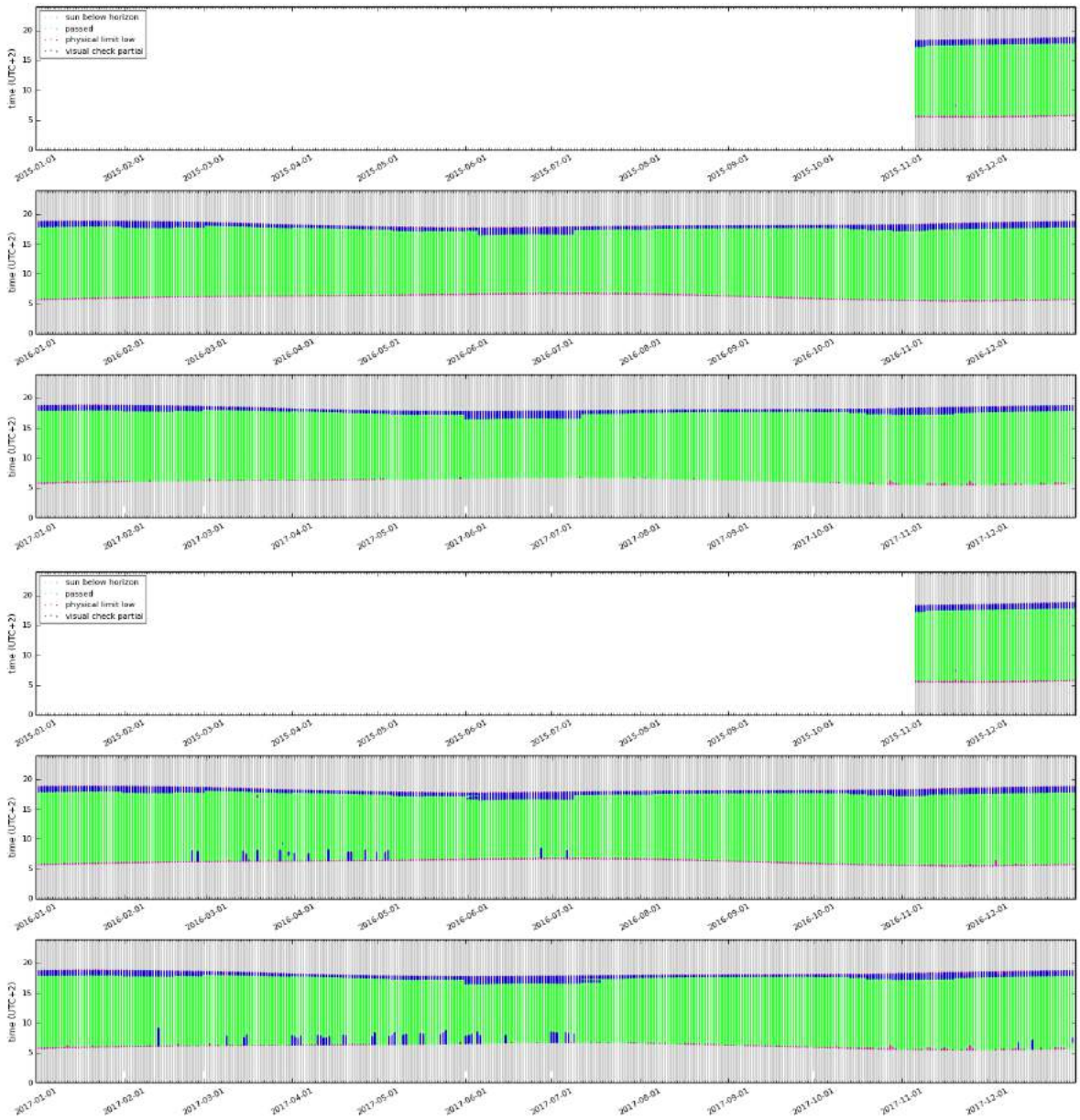

Figure 3.8 Results of GHI and DNI quality control – Mochipapa.
Green – data passing all tests; grey – sun below horizon; violet – physical limit issue, blue - excluded by visual inspection. Top: DNI (RSR); middle: GHI (RSR); bottom: GHI (CMP10)

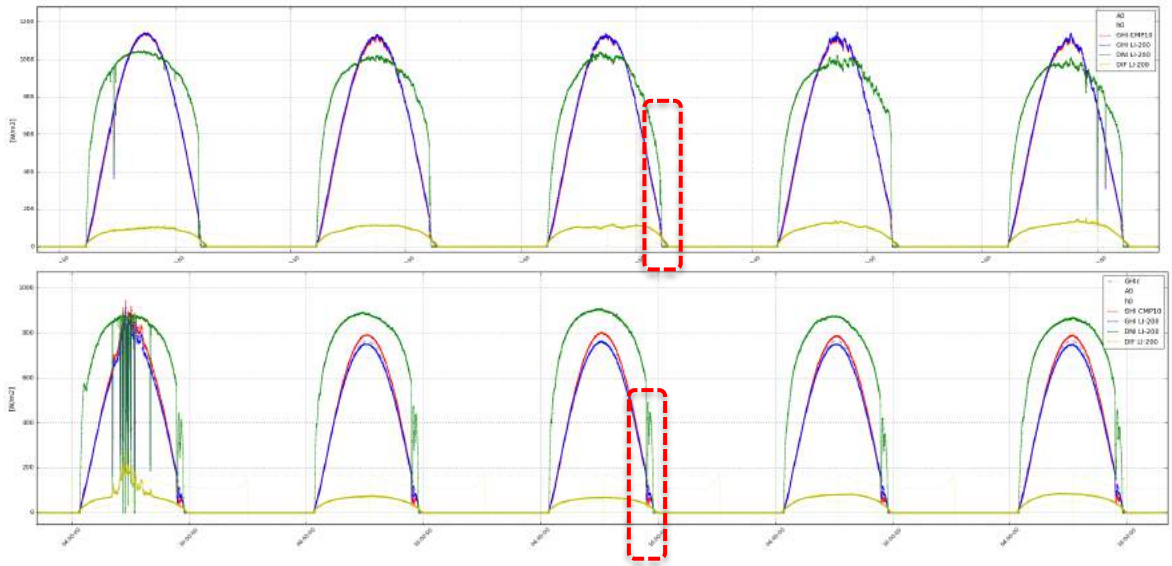

Figure 3.9 Shading effects on GHI and DNI in Mochipapa
Green: DNI RSR; red: GHI CMP10; blue: GHI RSR; yellow: DIF RSR; dashed: theoretical clear-sky profile

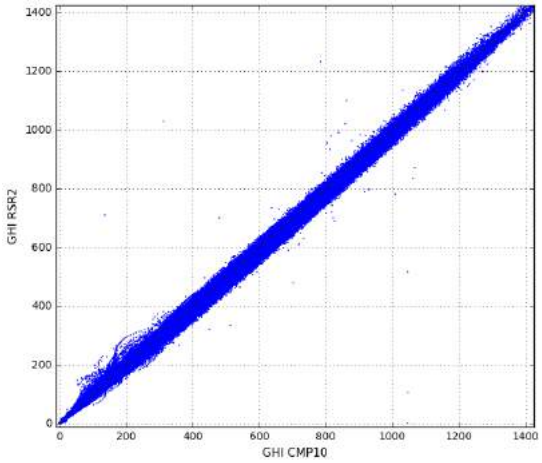

Figure 3.10 Systematic difference between GHI from CMP10 and RSR – Mochipapa

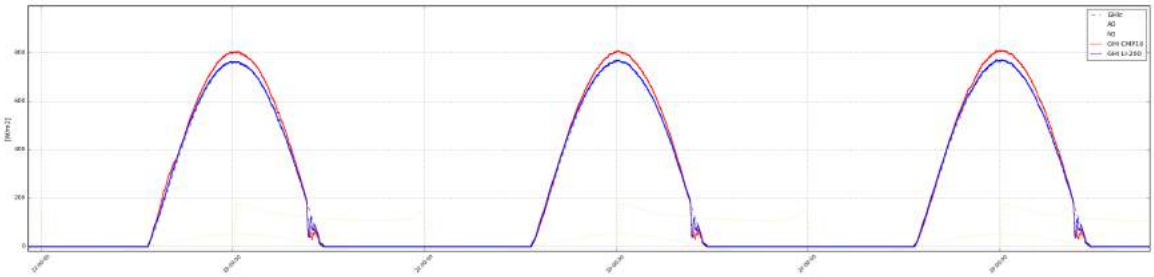

Figure 3.11 Asymmetry of GHI diurnal profiles from CMP10 and RSR – Mochipapa
Red: GHI CMP10; blue: GHI RSR; dashed: theoretical clear-sky profile

Table 3.18 Quality control summary – Mochipapa

Indicator	Flag	Description
Station description, metadata		Installation report available
Instrument accuracy		1x Secondary standard pyranometer CMP10 (GHI)
		1x Rotating Shadowband Radiometer RSR 2 (GHI, DIF, DNI)
Instrument calibration		Instruments were calibrated, and calibration was verified after 12 months
Data structure		Clear
Cleaning and maintenance information		Cleaning log available Diligent cleaning and maintenance
Time reference		Correct and clear time reference
Quality control complexity		RSR data, full QC comparison of GHI from RSR and CMP10
Quality control results		Occurrence of morning dew influencing mainly data from CMP10 Late afternoon shading Small inconsistency of RSR and CMP10 measurements Slight instrument misalignment
Period		More than 25 months
Other issues		

Legend: Quality marker

Very good	Good	Sufficient	Problematic	Insufficient	Not specified

3.3.4 Longe (Kaoma)

Table 3.19 Occurrence of data readings for Longe meteorological station

Data availability	GHI CMP10		GHI, DNI RSR	
Sun below horizon	534 958	49.4%	534 958	49.4%
Sun above horizon	548 940	50.6%	548 940	50.6%
Total data readings	1 083 898	100.0%	1 083 898	100.0%

Table 3.20 Excluded ground measurements after quality control (Sun above horizon) in Longe

Type of test	Occurrence of data samples (Sun above horizon)					
	GHI CMP10		DNI RSR		GHI RSR	
Physical limits test	6 216	1.1%	0	0.0%	3 080	0.6%
Consistency test (GHI – DNI – DIF)	0	0.0%	0	0.0%	0	0.0%
Visual test (incorrect data)	47 163	8.6%	45 888	8.4%	42 726	7.8%
Other (non-valid data)	26	0.0%	0	0.0%	0	0.0%
Total excluded data samples	53 405	9.7%	45 888	8.4%	45 806	8.3%
Total samples	548 940	100.0%	548 940	100.0%	548 940	100.0%

Main findings:

- Several periods with missing data, due to issues with the datalogger (Figure 3.12)
- Early morning and late afternoon shading from the surrounding trees (Figure 3.13) for the whole period of measurements.
- A systematic difference between GHI measurements from secondary standard pyranometer CMP10 and RSR (Figure 3.14). GHI from CMP10 is in average higher by 1.2% than GHI from RSR. The difference was 1.1% in 2016 and 1.3% in 2017. In the noon time, it can exceed 4%.
- Higher occurrence of morning dew on sensors influencing mainly GHI from the thermopile instrument (Figure 3.15)

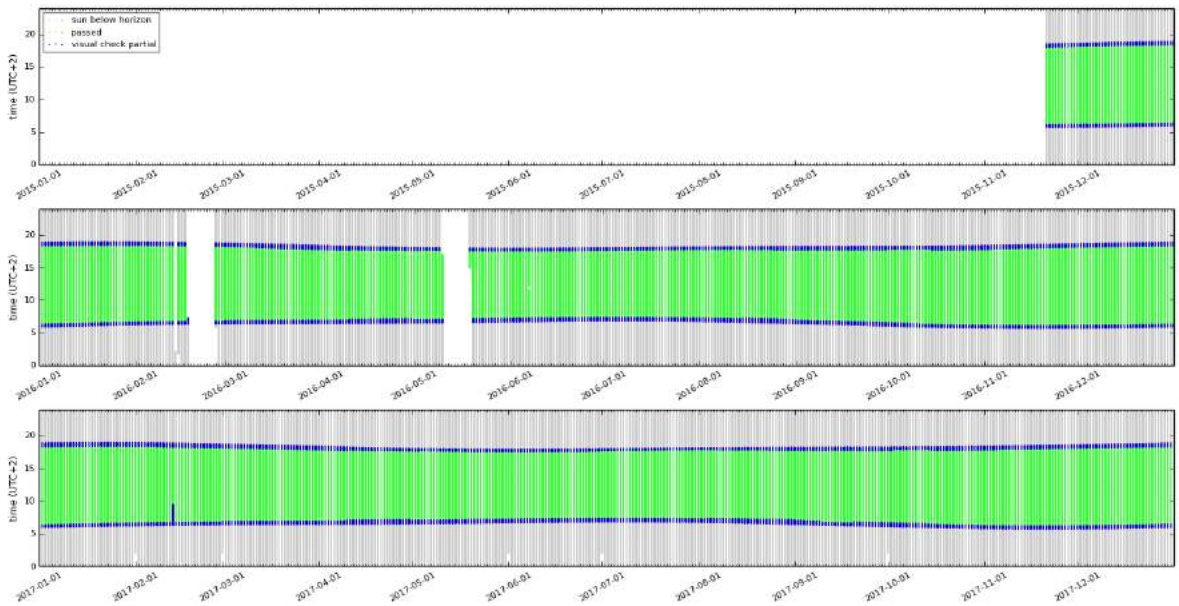

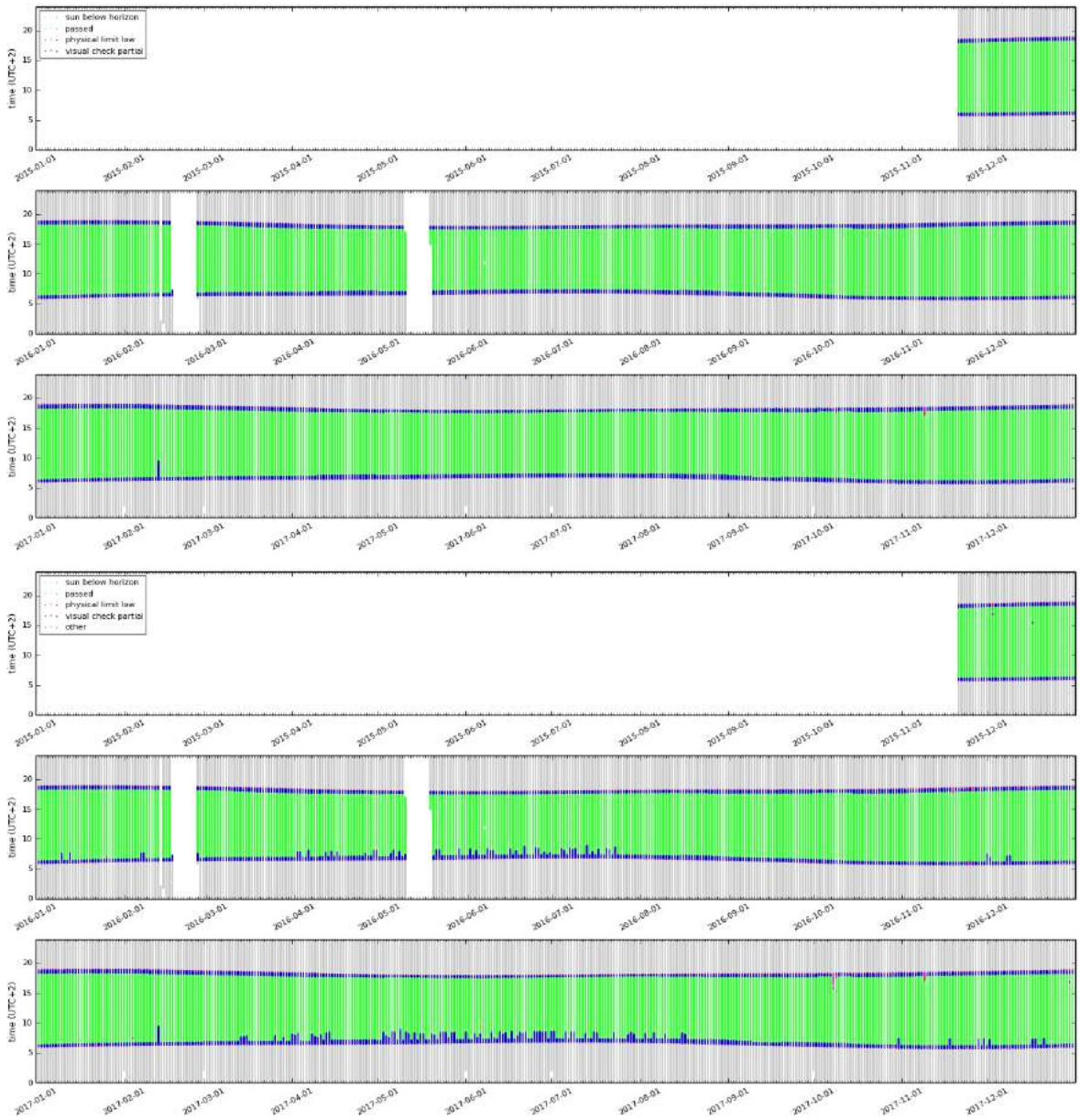

Figure 3.12 Results of GHI and DNI quality control – Longe
Green – data passing all tests; grey – sun below horizon; violet – physical limit issue, blue – excluded by visual inspection; Top: DNI (RSR); middle: GHI (RSR); bottom: GHI (CMP10)

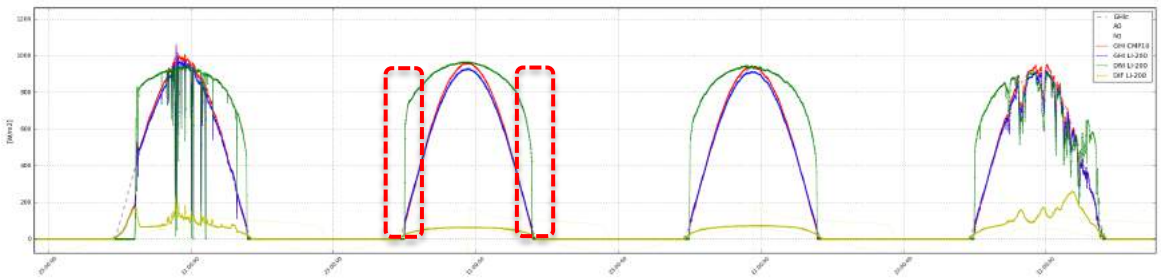

Figure 3.13 Systematic shading effects on GHI and DNI in Longe.
Green: DNI RSR; red: GHI CMP10; blue: GHI RSR; yellow: DIF RSR; dashed: theoretical clear-sky profile

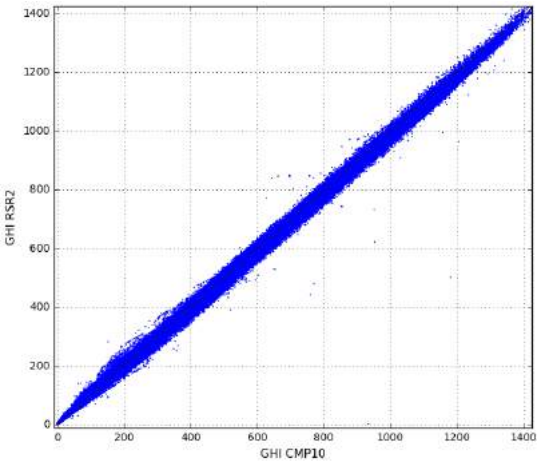

Figure 3.14 Systematic difference between GHI from CMP10 and RSR - Longe.

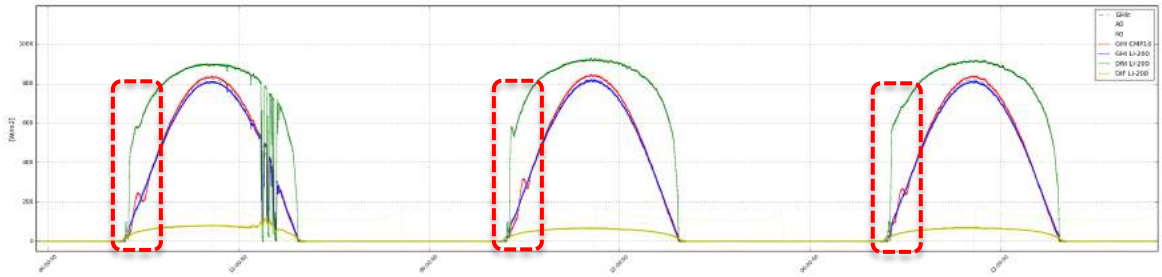

Figure 3.15 Morning dew effect on GHI and DNI measurements in Longe.
Green: DNI RSR; red: GHI CMP10; blue: GHI RSR; yellow: DIF RSR; dashed: theoretical clear-sky profile

Table 3.21 Quality control summary – Longe

Indicator	Flag	Description
Station description, metadata		Installation report available
Instrument accuracy		1x Secondary standard pyranometer CMP10 (GHI)
		1x Rotating Shadowband Radiometer RSR 2 (GHI, DIF, DNI)
Instrument calibration		Instruments were calibrated, and calibration was verified after 12 months
Data structure		Clear
Cleaning and maintenance information		Cleaning log available Several periods without cleaning (9 to 17 days)
Time reference		Correct and clear time reference
Quality control complexity		RSR data, full QC comparison of GHI from RSR and CMP10
Quality control results		Occurrence of morning dew influencing mainly data from CMP10 Early morning and late afternoon shading Small inconsistency of RSR and CMP10 measurements Missing data
Period		More than 24 months
Other issues		

Legend: Quality flag

Very good	Good	Sufficient	Problematic	Insufficient	Not specified

3.3.5 Misamfu (Kasama)

Table 3.22 Occurrence of data readings for Misamfu meteorological station

Data availability	GHI CMP10		GHI, DNI RSR	
Sun below horizon	545 304	49.3%	545 304	49.3%
Sun above horizon	560 524	50.7%	560 524	50.7%
Total data readings	1 105 828	100.0%	1 105 828	100.0%

Table 3.23 Excluded ground measurements after quality control (Sun above horizon) in Misamfu

Type of test	Occurrence of data samples (Sun above horizon)					
	GHI CMP10		DNI RSR		GHI RSR	
Physical limits test	5 733	1.0%	0	0.0%	3208	0.6%
Consistency test (GHI – DNI – DIF)	0	0.0%	0	0.0%	0	0.0%
Visual test (incorrect data)	33 459	6.0%	30 335	5.4%	29 276	5.2%
Other (non-valid data)	205	0.0%	6376	1.1%	280	0.0%
Total excluded data samples	39 397	7.0%	36 711	6.5%	32 764	5.8%
Total samples	560 524	100.0%	560 524	100.0%	560 524	100.0%

Main findings:

- Early morning shading for the whole period of measurements.
- Missing data in February 2016, due to faulty RSR and battery (Figure 3.16).
- A systematic difference between GHI measurements from the secondary standard pyranometer CMP10 and RSR (Figure 3.17). GHI from CMP10 is in average higher by 2.2% than GHI from RSR. The difference was 2.0% in 2016 and 2.4% in 2017. In the noon time, it can exceed 4%.
- Occurrence of morning dew on sensors influencing mainly the GHI from thermopile instrument

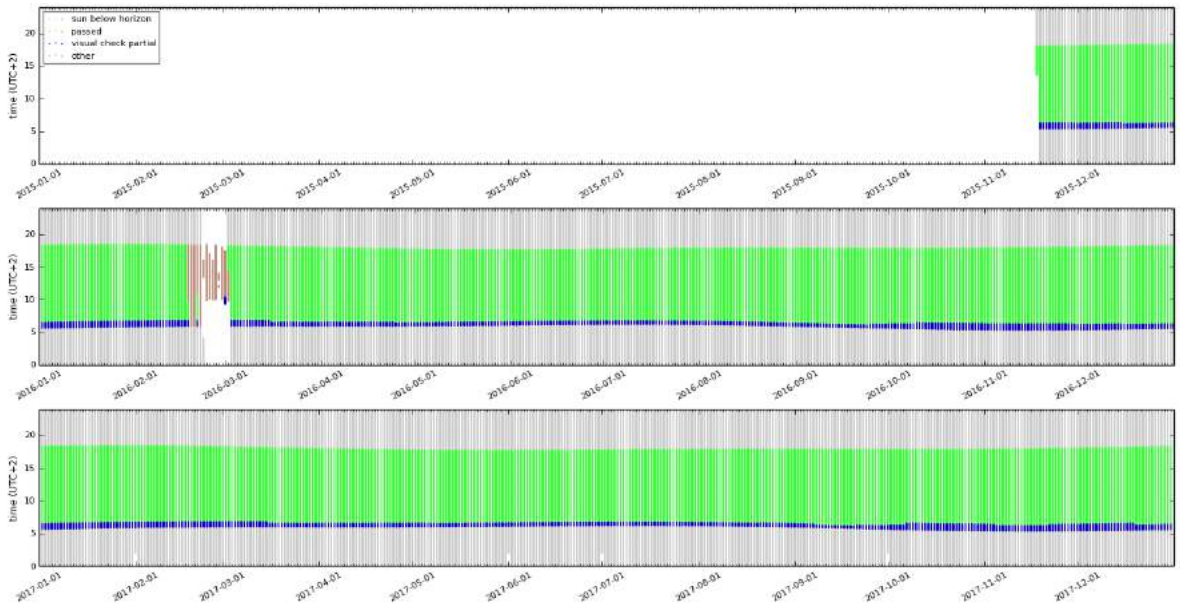

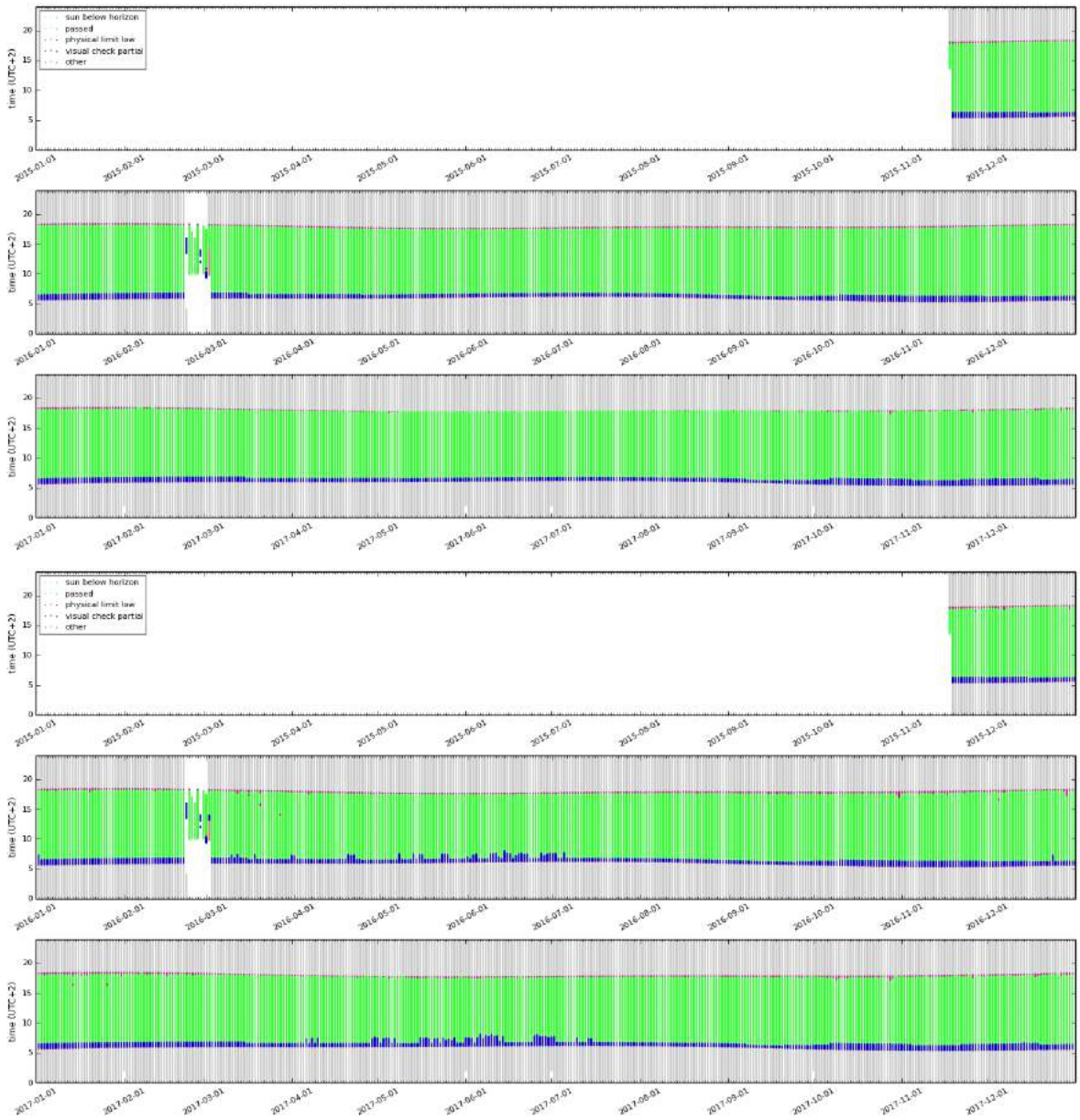

Figure 3.16 Results of GHI and DNI quality control – Misamfu.
Green – data passing all tests; grey – sun below horizon; violet – physical limit issue, blue excluded by visual inspection, brown – missing or non-valid values; Top: DNI (RSR); middle: GHI (RSR); bottom: GHI (CMP10)

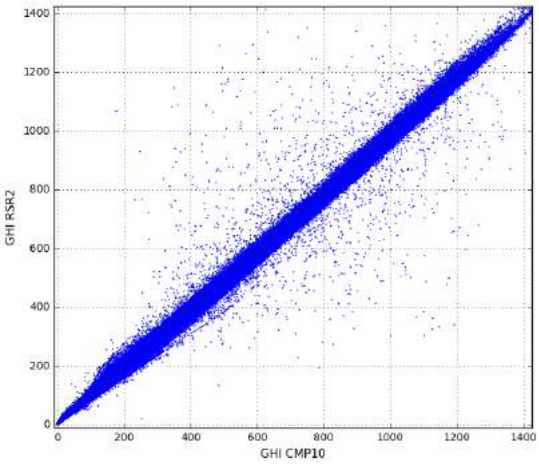

Figure 3.17 Systematic difference between GHI from CMP10 and RSR - Misamfu.

Table 3.24 Quality control summary – Misamfu

Indicator	Flag	Description
Station description, metadata		Installation report available
Instrument accuracy		1x Secondary standard pyranometer CMP10 (GHI)
		1x Rotating Shadowband Radiometer RSR 2 (GHI, DIF, DNI)
Instrument calibration		Instruments were calibrated, and calibration was verified after 12 months
Data structure		Clear
Cleaning and maintenance information		Cleaning log available Diligent cleaning and maintenance
Time reference		Correct and clear time reference
Quality control complexity		RSR data, full QC comparison of GHI from RSR and CMP10
Quality control results		Occurrence of morning dew influencing mainly data from CMP10 Early morning shading Small inconsistency of RSR and CMP10 measurements Missing data
Period		25 months
Other issues		

Legend: Quality flag

Very good	Good	Sufficient	Problematic	Insufficient	Not specified

3.3.6 Mutanda

Table 3.25 Occurrence of data readings for Mutanda meteorological station

Data availability	GHI CMP10		GHI, DNI RSR	
Sun below horizon	548 670	49.4%	548 670	49.4%
Sun above horizon	561 866	50.6%	561 866	50.6%
Total data readings	1 110 536	100.0%	1 110 536	100.0%

Table 3.26 Excluded ground measurements after quality control (Sun above horizon) in Mutanda

Type of test	Occurrence of data samples (Sun above horizon)					
	GHI CMP10		DNI RSR		GHI RSR	
Physical limits test	6 541	1.2%	20	0.0%	3 228	0.6%
Consistency test (GHI – DNI – DIF)	0	0.0%	0	0.0%	0	0.0%
Visual test (incorrect data)	28 855	5.1%	18 301	3.3%	16 696	3.0%
Other (non valid data)	0	0.0%	0	0.0%	0	0.0%
Total excluded data samples	35 396	6.3%	18 321	3.3%	19 924	3.5%
Total samples	561 866	100.0%	561 866	100.0%	561 866	100.0%

Main findings:

- Late afternoon shading for the whole period of measurements (Figure 3.18).
- Negligible systematic difference between GHI measurements from secondary standard pyranometer CMP10 and RSR. GHI from CMP10 is in average higher by 0.6% than GHI from RSR. The difference was 0.3% in 2016 and 0.9% in 2017. In the noon time, it can exceed 3% (Figure 3.19).
- High occurrence of morning dew on sensors influencing mainly the GHI from thermopile instrument (Figure 3.20).

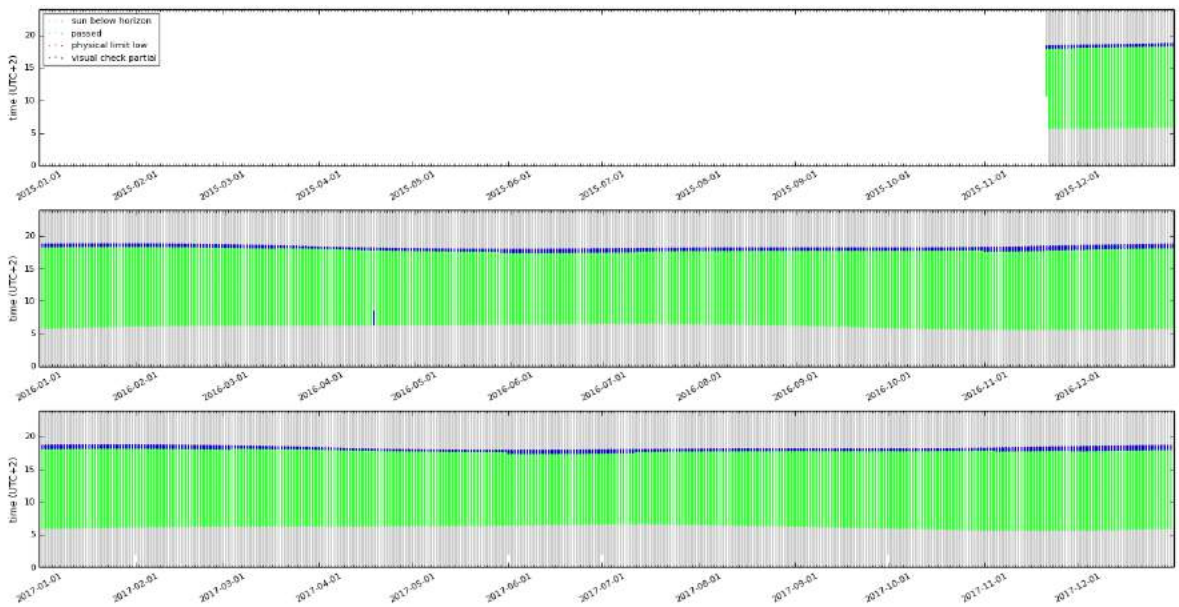

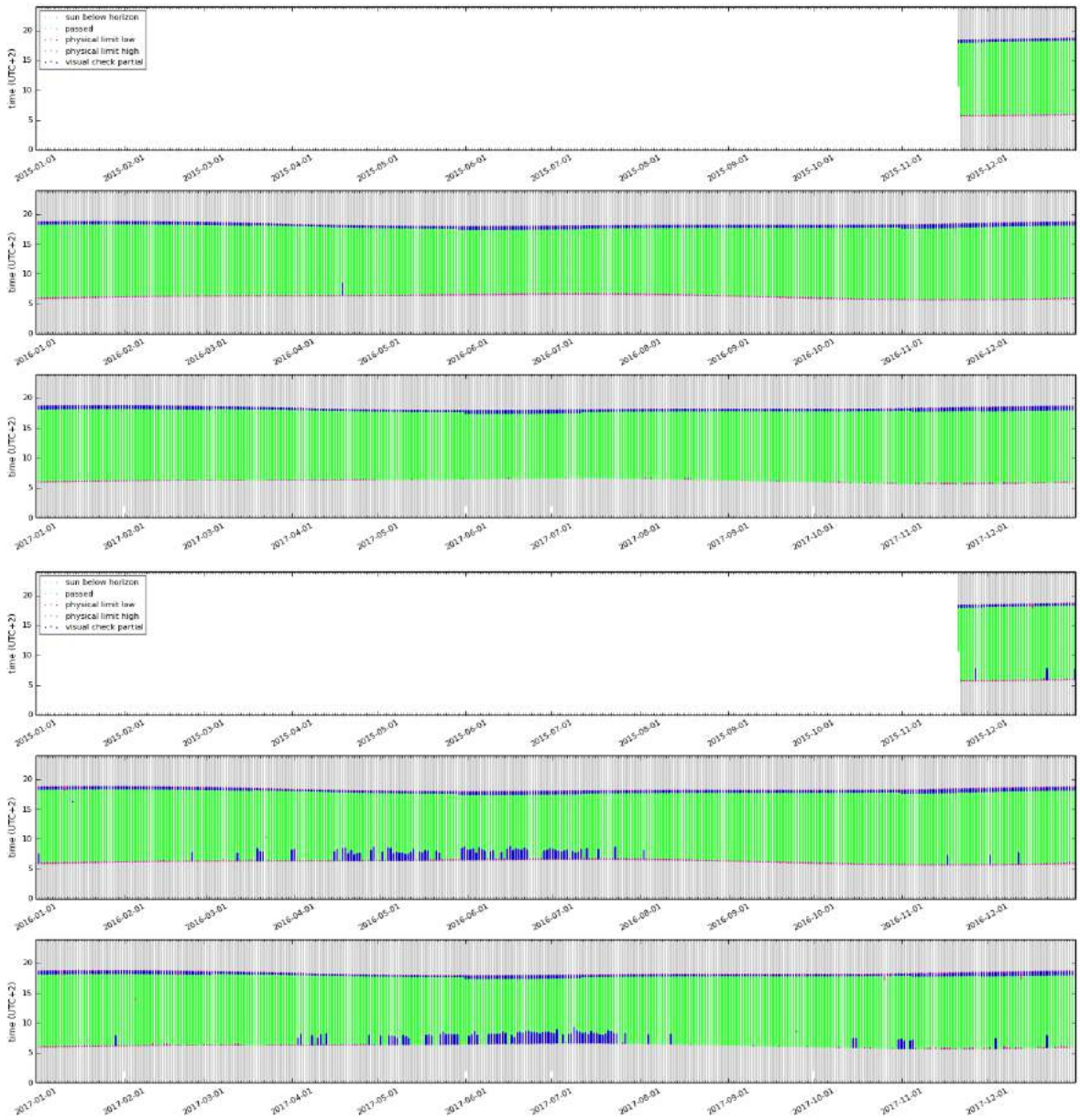

Figure 3.18 Results of GHI and DNI quality control – Mutanda.
Green – data passing all tests; grey – sun below horizon; violet – physical limit issue, blue excluded by visual inspection; Top: DNI (RSR); middle: GHI (RSR); bottom: GHI (CMP10)

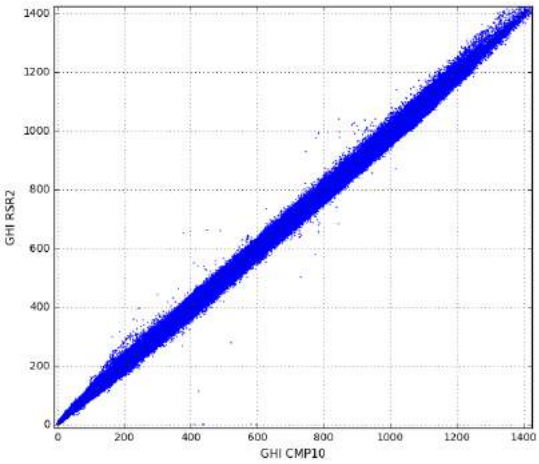

Figure 3.19 Systematic difference between GHI from CMP10 and RSR - Mutanda.

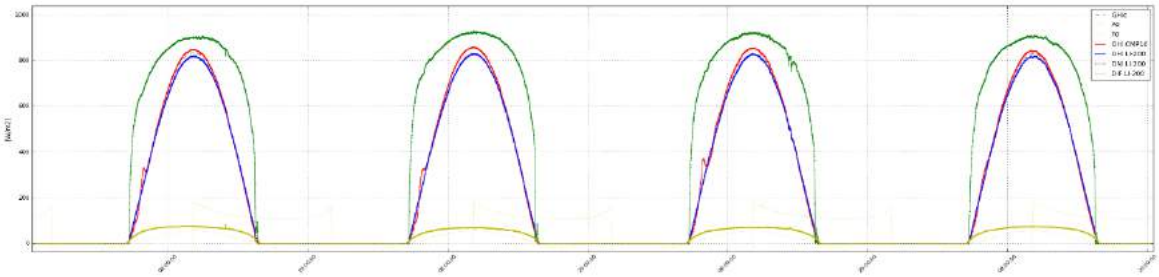

Figure 3.20 Morning dew effect on GHI measurements in Mutanda.
Green: DNI RSR; red: GHI CMP10; blue: GHI RSR; yellow: DIF RSR; dashed: theoretical clear-sky profile

Table 3.27 Quality control summary – Mutanda

Indicator	Flag	Description
Station description, metadata		Installation report available
Instrument accuracy		1x Secondary standard pyranometer CMP10 (GHI)
		1x Rotating Shadowband Radiometer RSR 2 (GHI, DIF, DNI)
Instrument calibration		Instruments were calibrated, and calibration was verified after 12 months
Data structure		Clear
Cleaning and maintenance information		Cleaning log available Diligent cleaning and maintenance
Time reference		Correct and clear time reference
Quality control complexity		RSR data, full QC comparison of GHI from RSR and CMP10
Quality control results		High occurrence of morning dew influencing mainly data from CMP10 Late afternoon shading
Period		More than 25 months
Other issues		

Legend: Quality flag

Very good	Good	Sufficient	Problematic	Insufficient	Not specified

3.4 Recommendations on the operation and maintenance of the meteorological stations in Zambia

Based on the results of quality control (Tables 3.11, 3.14, 3.17, 3.20, 3.23 and 3.26), we conclude that the solar radiation measurements come from the high accuracy (CMP10, CHP1) and medium accuracy (RSR) measuring equipment that is professionally installed, diligently operated and carefully maintained. Small issues were identified during the data quality control:

- Higher occurrence of the measurements by the thermopile instruments that are affected by dew. These data values were flagged and excluded from further processing.
- Early morning and late afternoon shading from surrounding objects in several sites. The data were flagged and excluded from further processing.
- Several short periods with insufficient cleaning at Longe and Mutanda station.

For future works, we recommend:

- Maintain and improve the cleaning frequency of solar sensors
- Consider installation of ventilation units for the pyranometers to reduce data records affected by morning dew.

4 SOLAR RESOURCE MODEL DATA

4.1 Solar model

Solar radiation is calculated by Solargis model, which are parameterized by a set of inputs characterizing the cloud transmittance, state of the atmosphere and terrain conditions. A comprehensive **overview of the Solargis model** is made available in the recent book publication [3]. The methodology is also described in [4, 5]. The related uncertainty and requirements for bankability are discussed in [6, 7].

In Solargis approach, the **clear-sky irradiance** is calculated by the simplified SOLIS model [8]. This model allows fast calculation of clear-sky irradiance from the set of input parameters. Sun position is deterministic parameter, and it is described by the algorithms with satisfactory accuracy. Stochastic variability of clear-sky atmospheric conditions is determined by changing concentrations of atmospheric constituents, namely aerosols, water vapour and ozone. Global atmospheric data, representing these constituents, are routinely calculated by world atmospheric data centres:

- In Solargis, the new generation **aerosol data set** representing Atmospheric Optical Depth (AOD) is used. The calculation accuracy is strongly determined by quality of aerosols, especially for cloudless conditions. The aerosol data implemented by MACC-II/CAMS and MERRA-2 projects are used [9, 10].
- **Water vapour** is also highly variable in space and time, but it has lower impact on the values of solar radiation, compared to aerosols. The GFS and CFSR databases (NOAA NCEP) are used in Solargis, and the data represent the daily variability from 1994 to the present time [11, 12, 13].
- **Ozone** absorbs solar radiation at wavelengths shorter than 0.3 μm, thus having negligible influence on the broadband solar radiation.

The clouds are the most influencing factor, modulating clear-sky irradiance. Effect of clouds is calculated from the satellite data in the form of a **cloud index** (cloud transmittance). The cloud index is derived by relating radiance recorded by the satellite in spectral channels and surface albedo to the cloud optical properties. In Solargis, the modified calculation scheme of Cano has been adopted to retrieve cloud optical properties from the satellite data [14].

To calculate **all-sky irradiance** in each time step, the clear-sky global horizontal irradiance is coupled with cloud index. Direct Normal Irradiance (DNI) is calculated from Global Horizontal Irradiance (GHI) using modified Dirindex model [15]. Diffuse irradiance for tilted surfaces, which is calculated by Perez model [16]. The calculation procedure includes also terrain disaggregation, the spatial resolution is enhanced with use of the digital terrain model to 250 meters [17]. Solargis model version 2.1 has been used. Table 4.1 summarizes technical parameters of the model inputs and of the primary data outputs.

Table 4.1 Input data used in the Solargis and related GHI and DNI outputs for Zambia

Inputs into the Solargis model	Source of input data	Time representation	Original time step	Approx. grid resolution
Cloud index (satellite data)	Meteosat MFG Meteosat MSG (EUMETSAT)	1994 to 2004 2005 to date	30 minutes 15 minutes	2.7 x 3.3 km 3.2 x 4.0 km
Atmospheric optical depth (aerosols)*	MACC-II/CAMS* (ECMWF) MERRA-2 (NASA)	2003 to date 1994 to 2002	3 hours 1 hour	75 km and 125 km 50 km
Water vapour	CFSR/GFS (NOAA)	1994 to date	1 hour	35 and 55 km
Elevation and horizon	SRTM-3 (SRTM)	-	-	250 m
Solargis primary data (GHI, DNI)	-	1994 to date	15 minutes	250 m

** Aerosol data for 2003-2012 come from the reanalysis database; the data representing years 2013-present are derived from near-real time operational model*

Figure 4.1: Sites with solar meteorological stations used for site adaptation of Solargis model in Zambia

4.2 Site adaptation of the solar model – method

This chapter describes accuracy improvement of the delivered model time series for six sites. This improvement has been achieved by site adaptation of the model, based on the use of local measurements.

The fundamental difference between a satellite observation and a ground measurement is that signal received by the satellite radiometer integrates a large area, while a ground station represents a pinpoint measurement. This results in a mismatch when comparing instantaneous values from these two observation instruments, mainly during intermittent cloudy weather and changing aerosol load. Nearly half of the hourly Root Mean Square Deviation (RMSD) for GHI and DNI can be attributed to this mismatch (value at sub-pixel scale), which is also known as the "nugget effect" [18].

The satellite pixel is not capable describing the inter-pixel variability in complex regions, where within one pixel diverse natural conditions mix-up (e.g. fog in narrow valleys or along the coast). In addition, the coarse spatial resolution of atmospheric databases such as aerosols or water vapour is not capable to describe local patterns of the state of atmosphere. These features can be seen in the satellite GHI and DNI data by increased bias due to imperfect description of aerosol load and satellite GHI mainly due to inaccurate identification of highly variable clouds. Satellite data have inherent inaccuracies, which have certain degree of geographical and time variability.

Especially DNI is strongly sensitive to variability of cloud information, aerosols, water vapour, and terrain shading. The relation between uncertainty of global and direct irradiance is nonlinear. Often, a negligible error in global irradiance may have high counterpart in the direct irradiance component. This relation may be present also in opposite order.

The solar energy projects require representative and accurate GHI and DNI time series. The satellite-derived databases are used to describe long-term solar resource for a specific site. However, their problem when compared to the high-quality ground measurements is a slightly higher bias and partial disagreement of frequency distribution functions, which may limit their potential to record the occurrence of extreme situations (e.g. very low atmospheric turbidity resulting in a high DNI and GHI). A solution is to correlate satellite-derived data with ground measurements to understand the source of discrepancy and subsequently to improve the accuracy of the resulting time series.

The Solargis satellite-derived data are correlated with ground measurement data with two objectives:

- Improvement of the overall bias (removal of systematic deviations)

- Improvement of the fit of the frequency distribution of values.

Limited spatial and temporal resolution of the input data and simplified nature of the models results in the occurrence of systematic and random deviations of the model outputs when compared to the ground observations. The deviations in the satellite-computed data, which have *systematic nature*, can be reduced by site adaptation or regional adaptation methods.

The terminology related to the procedure improving accuracy of the satellite data is not harmonized, and various terms are used:

- Correlation of ground measurements and satellite-based data;
- Calibration of the satellite model (its inputs and parameters);
- Site adaptation or regional adaptation of satellite-based data.

The term *site adaptation* is more general and best explains the concept of adapting the satellite-based model (by correlation, calibration, fitting and recalculation) to the ground measured data. **Site adaptation** aims to adapt the characteristics of the satellite-based time series to the site-specific conditions described by local measurements.

Three conditions are important for successful adaptation of the satellite-based model:

1. High quality DNI and GHI ground measurements for at least 12 months must be available; optimally data for 2 or 3 years should be used;
2. High quality satellite data must be used, with consistent quality over the whole period of data;
3. There must be identified a systematic difference between both data sources.

Systematic difference can be stable over the year or it can slightly change seasonally for certain meteorological conditions (e.g. typical cloud formation during a day, seasonal air pollution). The data analysis should distinguish systematic differences from those arising at occasional events, such as extreme sand storms or forest fires. The episodically-occurring differences may mislead the results of adaptation, especially if short period of ground measurements is only available.

If one of the three above-mentioned conditions is not fulfilled, site adaptation (regional adaptation) will not provide the expected results. On the contrary, such an attempt may provide worse results.

For the quantitative assessment of the accuracy enhancement procedures, the following metrics is used:

- Metrics based on the comparison of all pairs of the hourly daytime data values: Mean Bias, and Root Mean Square Deviation (RMSD), histogram, in an absolute and relative form (divided by the daytime mean DNI values);
- Metrics based on the difference of the cumulative distribution functions: KSI (Kolmogorov-Smirnov test Integral) [19]

The normalized KSI is defined as an integral of absolute differences of two cumulative distribution functions *D* normalized by the integral of critical value $a_{critical}$:

$$KSI\% = \frac{\int_{x\,\min}^{x\,\max} D_n dx}{a_{critical}} * 100$$

$$a_{critical} = V_c * (x_{\max} - x_{\min})$$

$$V_c = \frac{1.63}{\sqrt{N}}, \quad N \geq 35$$

,

where critical value depends on the number of the data pairs *N*. As the KSI value is dependent on the size of the sample, the KSI measure may be used only for the relative comparison of fit of cumulative distribution of irradiance values.

For the accuracy enhancement of solar resource parameters in this study, a combination of two methods was used. First, systematic deviations due to influence of aerosols were partially removed. Afterwards, to improve the distribution of values, the fitting of cumulative frequency distribution curves of ground measurements and satellite data was used.

The site-adaptation procedure first identifies the sources of discrepancies by comparing the ground-measured data with Solargis model data, for the period of the overlap between both data sets approx. 24-25 months). Based on this analysis, correction coefficients to improve the fit between the measured and the model Solargis data are developed. In the second step, these coefficients are used for the adaptation of the full (24 years) time series.

The satellite data is available in 15-minute time step and the ground measurements in 1-minute time step. To partially remove the conceptual difference of point and satellite pixel measurements, prior to site adaptation, all the measures are calculated using aggregated data in the hourly time step.

The adaptation was based on measured DNI data from CHP1 instrument at UNZA Lusaka and RSR instrument for other stations. Measured GHI data from the secondary standard CMP10 instrument is used at all stations. GHI measured by the RSR was not used because of higher uncertainty of the outputs (Chapter 3.3).

More about the Solargis site adaptation is in [21], more general description can be found in [22].

4.3 Results of the model adaptation at six sites

The original Solargis data show a regional pattern of overestimation, compared to the ground measurements, for both GHI and DNI. The biggest difference between ground measurements and satellite data is found **at Mutanda station (GHI)**. In Mutanda, the mismatch between the measured and modelled GHI is 9.5% (Table 4.2). Such discrepancy is beyond usual uncertainty interval known for Solargis GHI data in this region (6% to 8% for GHI). The detailed inspection of the measurements and the satellite data indicates two possible sources (or their combination) of this difference:

- Performance of satellite models is in general lower for conditions with high occurrence of scattered and fast-changing clouds.
- Ground measurements for Mutanda site, but partly also for other sites, indicate some issues, mostly related to the occurrence of dew influence on measurements and the local shading. The high frequency variability (small scattered clouds) makes it difficult to distinguish the shading from surrounding objects from drop of solar irradiance due to clouds.

The model adaptation allowed removing a large part of the mismatch between the satellite-based data and the ground measurements. Tables 4.2 to 4.5 summarize the site-adaptation results for all solar meteorological stations in Zambia.

Table 4.2 Direct Normal Irradiance: bias and KSI before and after model site-adaptation

Meteo station	Original DNI data			DNI after site adaptation		
	Bias [kWh/m²]	Bias [%]	KSI [-]	Bias [kWh/m²]	Bias [%]	KSI [-]
UNZA Lusaka	44	10.5	213	0	0.0	79
Mount Makulu	42	9.9	200	0	0.0	74
Mochipapa	41	9.0	197	0	0.0	87
Longe	32	6.9	156	0	0.0	68
Misamfu	44	10.1	206	0	0.1	83
Mutanda	43	10.5	202	0	0.0	84
Mean	41	9.5	196	0	0.0	79
Standard deviation	5	1.4		0	0.0	

Table 4.3 Global Horizontal Irradiance: bias and KSI before and after model site-adaptation

Meteo station	Original GHI data			GHI after site adaptation		
	Bias	Bias	KSI	Bias	Bias	KSI
	[kWh/m²]	[%]	[-]	[kWh/m²]	[%]	[-]
UNZA Lusaka	32	6.8	156	0	0.0	24
Mount Makulu	30	6.4	148	0	0.1	26
Mochipapa	26	5.4	127	0	0.0	21
Longe	33	6.6	156	0	0.0	24
Misamfu	32	6.4	154	0	0.0	22
Mutanda	46	9.5	218	0	0.0	35
Mean	33	6.9	160	0	0.0	25
Standard deviation	7	1.4		0	0.0	

Table 4.4 Direct Normal Irradiance: RMSD before and after model site-adaptation

Meteo station	RMSD of original DNI data			RMSD of DNI after site adaptation		
	Hourly	Daily	Monthly	Hourly	Daily	Monthly
	[%]	[%]	[%]	[%]	[%]	[%]
UNZA Lusaka	32.3	18.2	14.6	30.0	13.7	5.8
Mount Makulu	34.8	19.5	14.9	33.0	15.9	7.0
Mochipapa	30.4	17.1	12.6	28.9	13.4	4.0
Longe	30.9	18.3	13.7	29.5	14.7	5.6
Misamfu	35.3	19.2	14.2	33.4	15.5	7.0
Mutanda	36.0	20.9	16.5	33.5	16.2	7.0
Mean	33.3	18.9	14.4	31.4	14.9	6.1

Table 4.5 Global Horizontal Irradiance: RMSD before and after model site-adaptation

Meteo station	RMSD of original GHI data			RMSD of GHI after site adaptation		
	Hourly	Daily	Monthly	Hourly	Daily	Monthly
	[%]	[%]	[%]	[%]	[%]	[%]
UNZA Lusaka	19.1	10.4	8.6	17.4	7.6	4.0
Mount Makulu	21.2	11.0	9.0	19.7	8.6	4.9
Mochipapa	18.4	9.1	7.1	17.2	7.1	3.5
Longe	18.4	10.3	8.7	16.8	7.7	4.4
Misamfu	19.8	9.9	7.9	18.3	7.4	4.0
Mutanda	21.8	12.6	11.2	18.9	7.9	4.5
Mean	19.8	10.6	8.8	18.1	7.7	4.2

As a result, at the level of individual meteorological sites in Zambia, the mean bias of the site-adapted values was reduced to zero. The values of RMSD and KSI accuracy parameters are also reduced, both for GHI and DNI.

The effect of the site adaptation is presented in a detail for all sites (Figures 4.2 to 4.7).

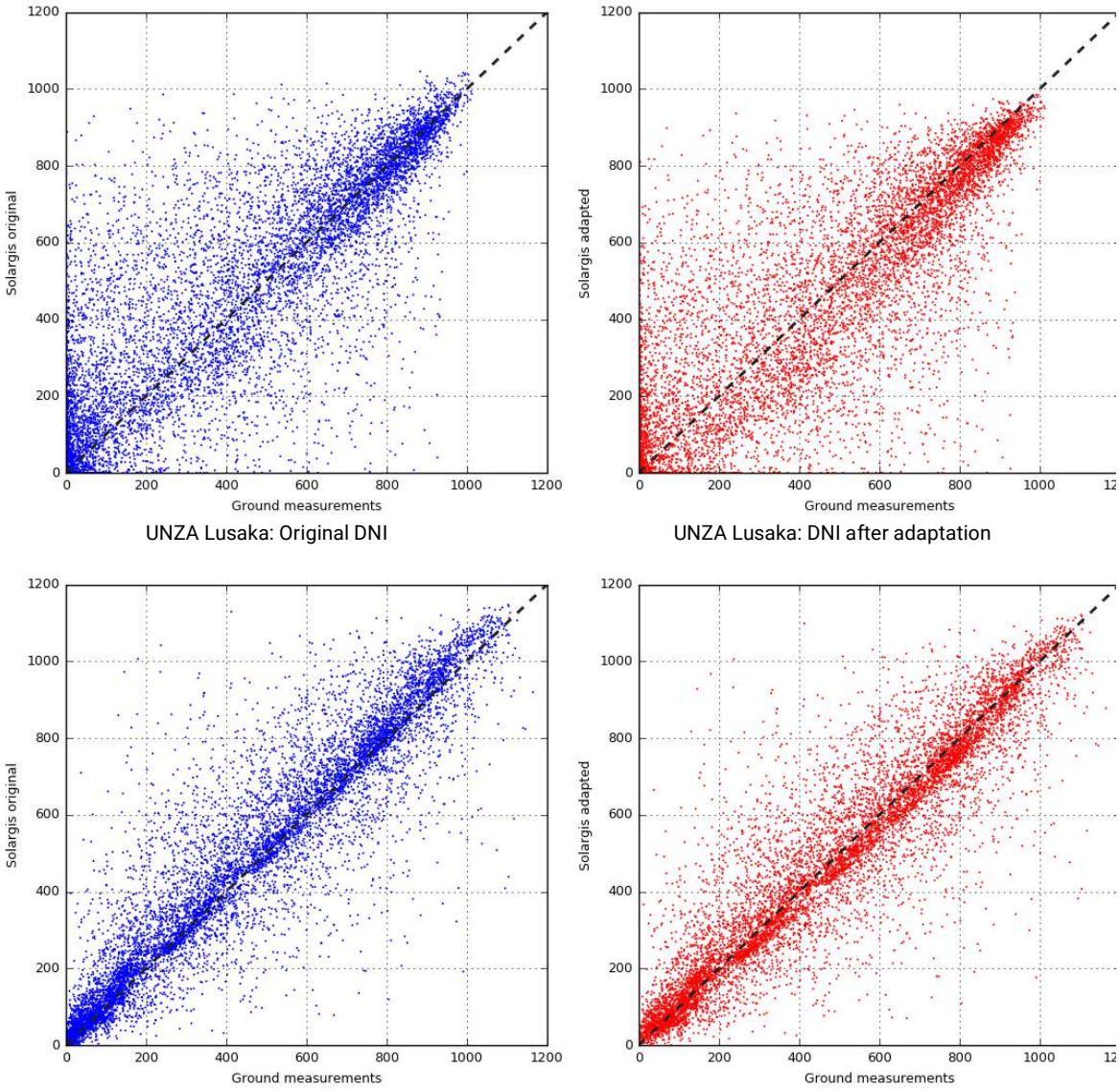

UNZA Lusaka: Original DNI

UNZA Lusaka: DNI after adaptation

UNZA Lusaka: Original GHI

UNZA Lusaka: GHI after adaptation

Figure 4.2: Correction of DNI and GHI hourly values for UNZA Lusaka.
Left: original Solargis data, right: site-adapted Solargis data.
The X-axis represents the measured data and the Y-axis represents the satellite-derived data.

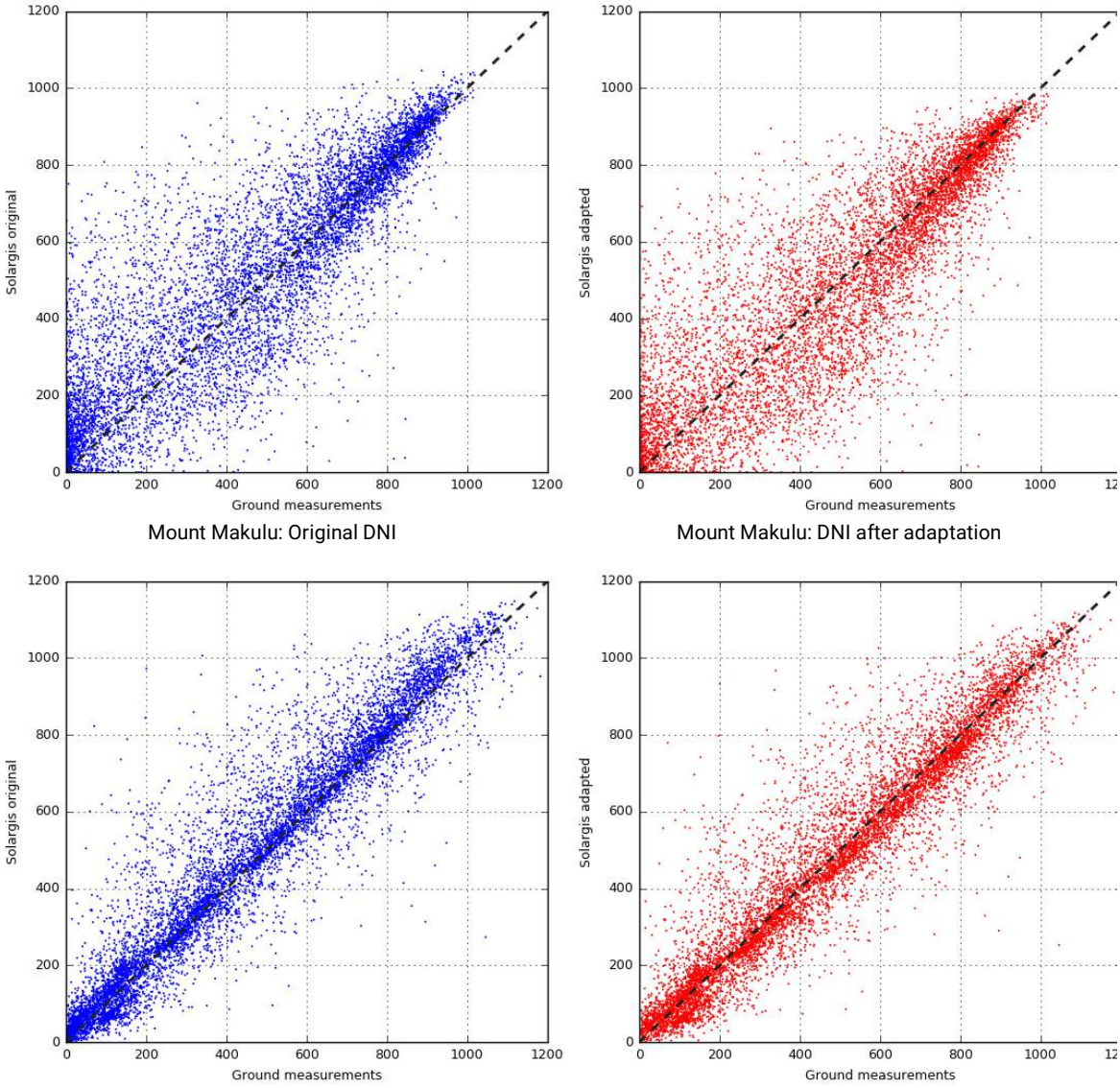

Mount Makulu: Original DNI

Mount Makulu: DNI after adaptation

Mount Makulu: Original GHI

Mount Makulu: GHI after adaptation

Figure 4.3: Correction of DNI and GHI hourly values for Mount Makulu
Left: original Solargis data, right: site-adapted Solargis data.
The X-axis represents the measured data and the Y-axis represents the satellite-derived data.

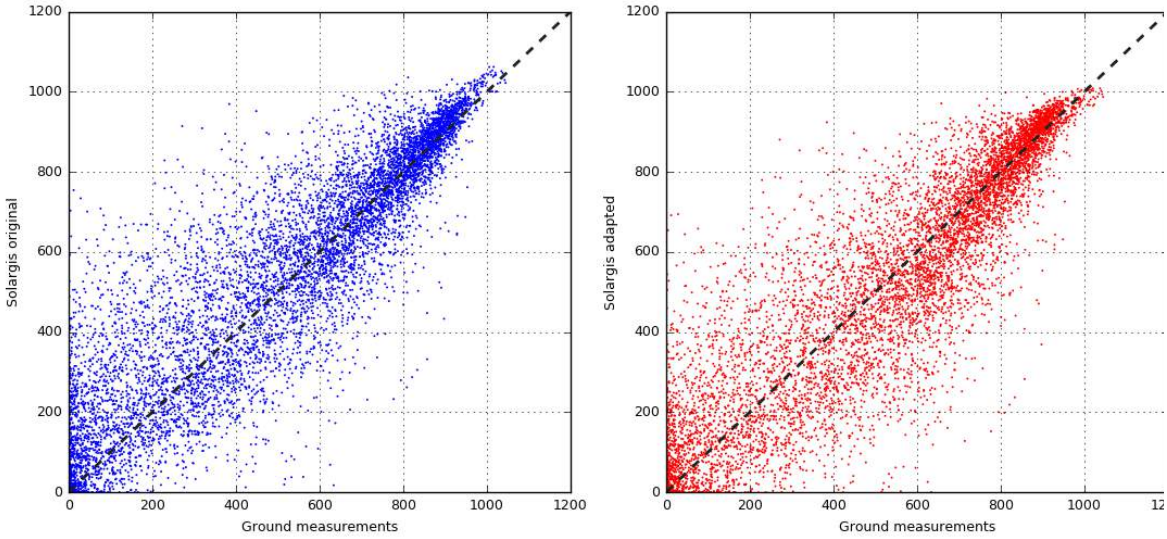

Mochipapa: Original DNI

Mochipapa: DNI after adaptation

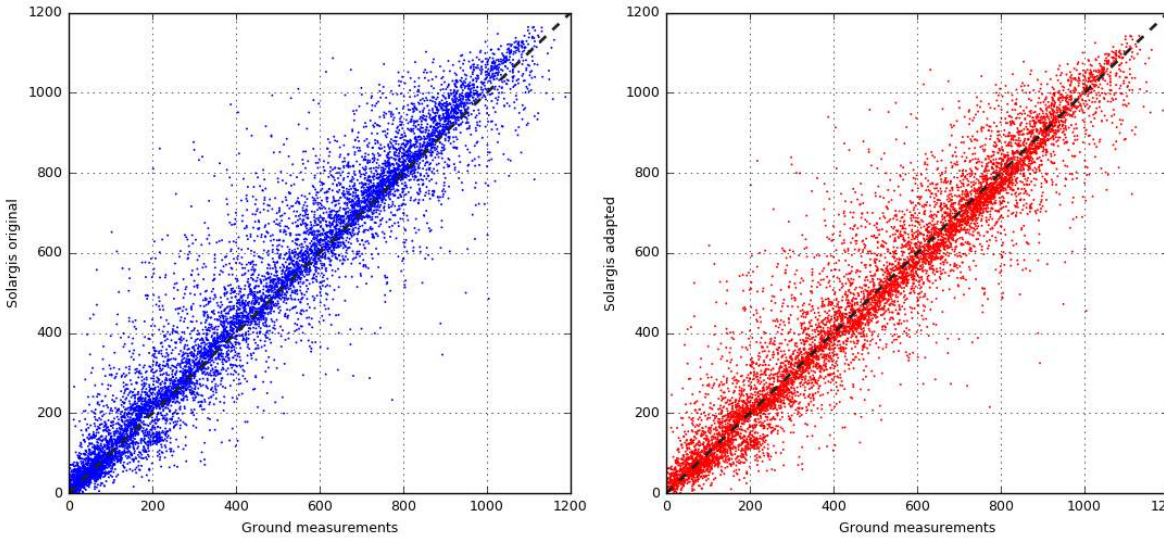

Mochipapa: Original GHI

Mochipapa: GHI after adaptation

Figure 4.4: Correction of DNI and GHI hourly values for Mochipapa.
Left: original Solargis data, right: site-adapted Solargis data.
The X-axis represents the measured data and the Y-axis represents the satellite-derived data.

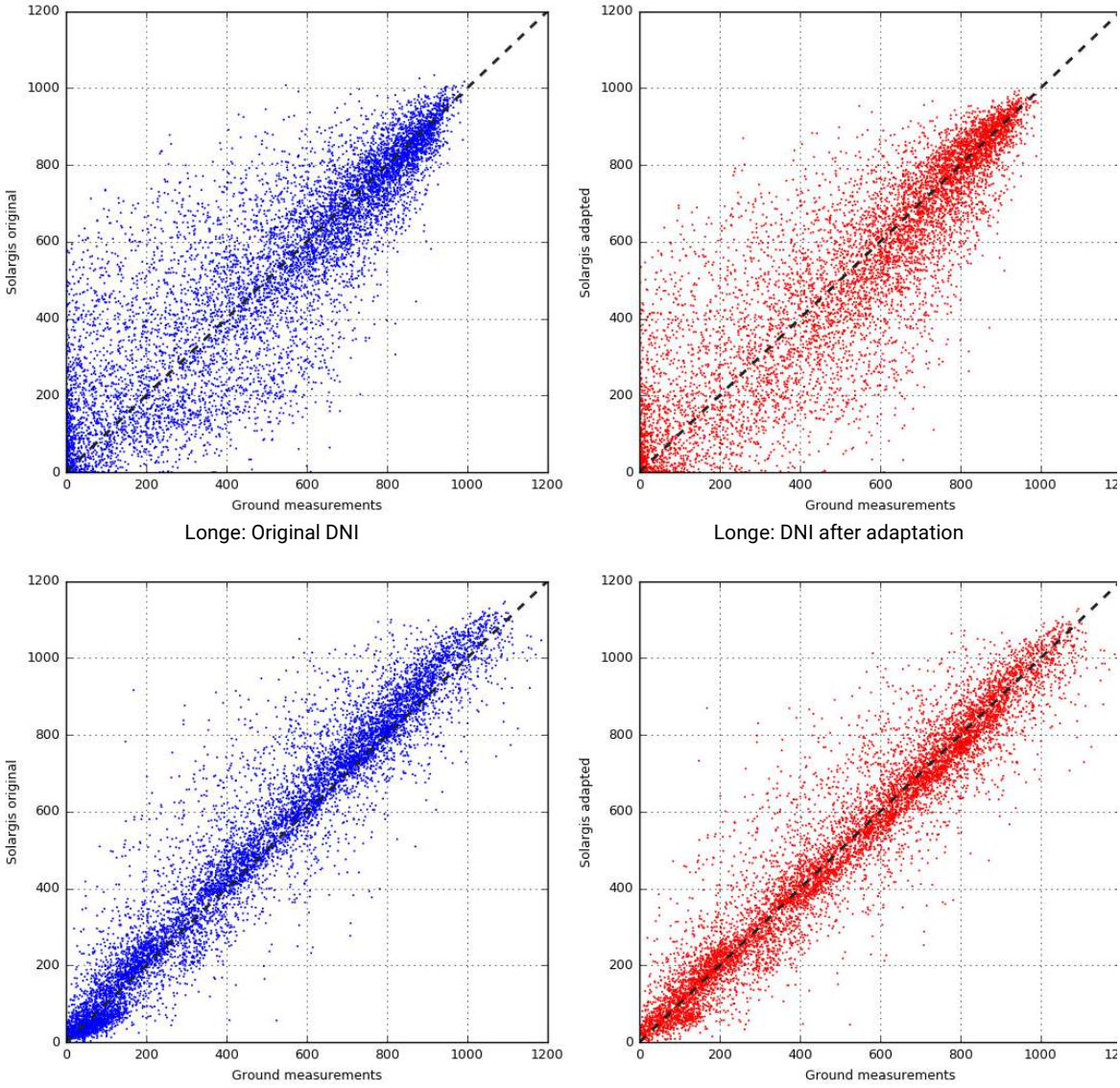

Longe: Original DNI

Longe: DNI after adaptation

Longe: Original GHI

Longe: GHI after adaptation

Figure 4.5: Correction of DNI and GHI hourly values for Longe.
Left: original Solargis data, right: site-adapted Solargis data.
The X-axis represents the measured data and the Y-axis represents the satellite-derived data.

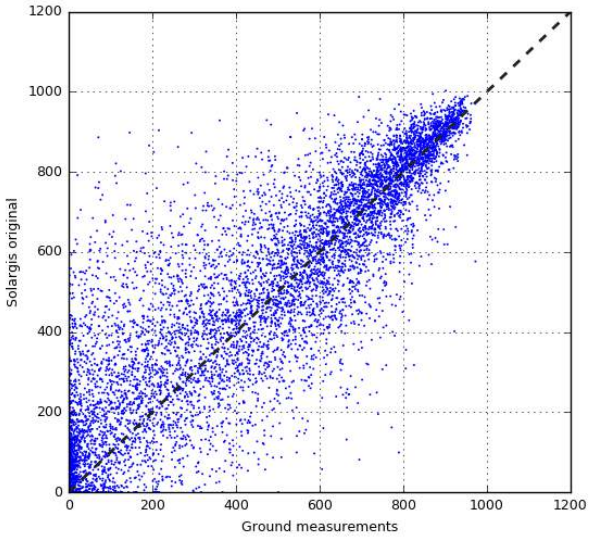

Misamfu: Original DNI

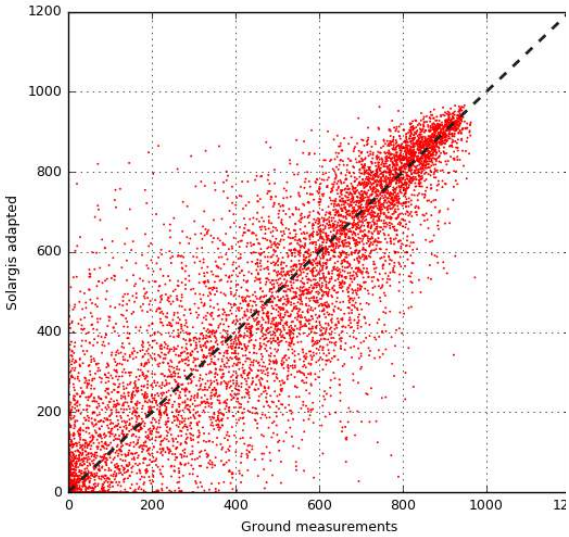

Misamfu: DNI after adaptation

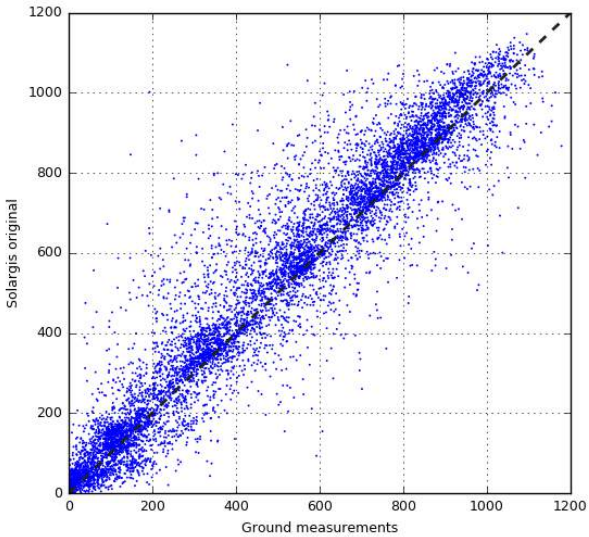

Misamfu: Original GHI

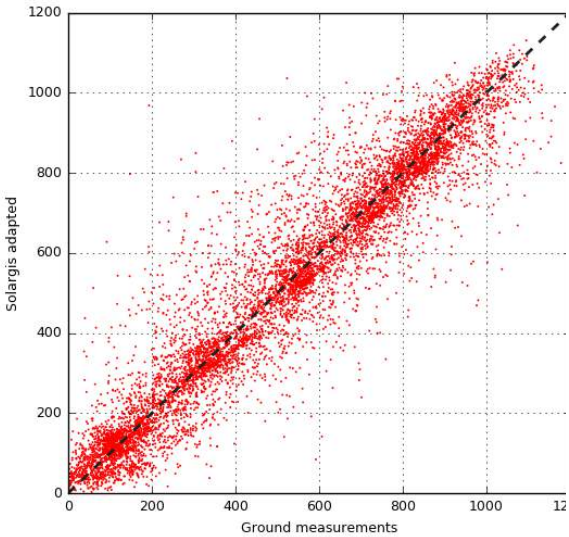

Misamfu: GHI after adaptation

Figure 4.6: Correction of DNI and GHI hourly values for Misamfu.
Left: original Solargis data, right: site-adapted Solargis data.
The X-axis represents the measured data and the Y-axis represents the satellite-derived data.

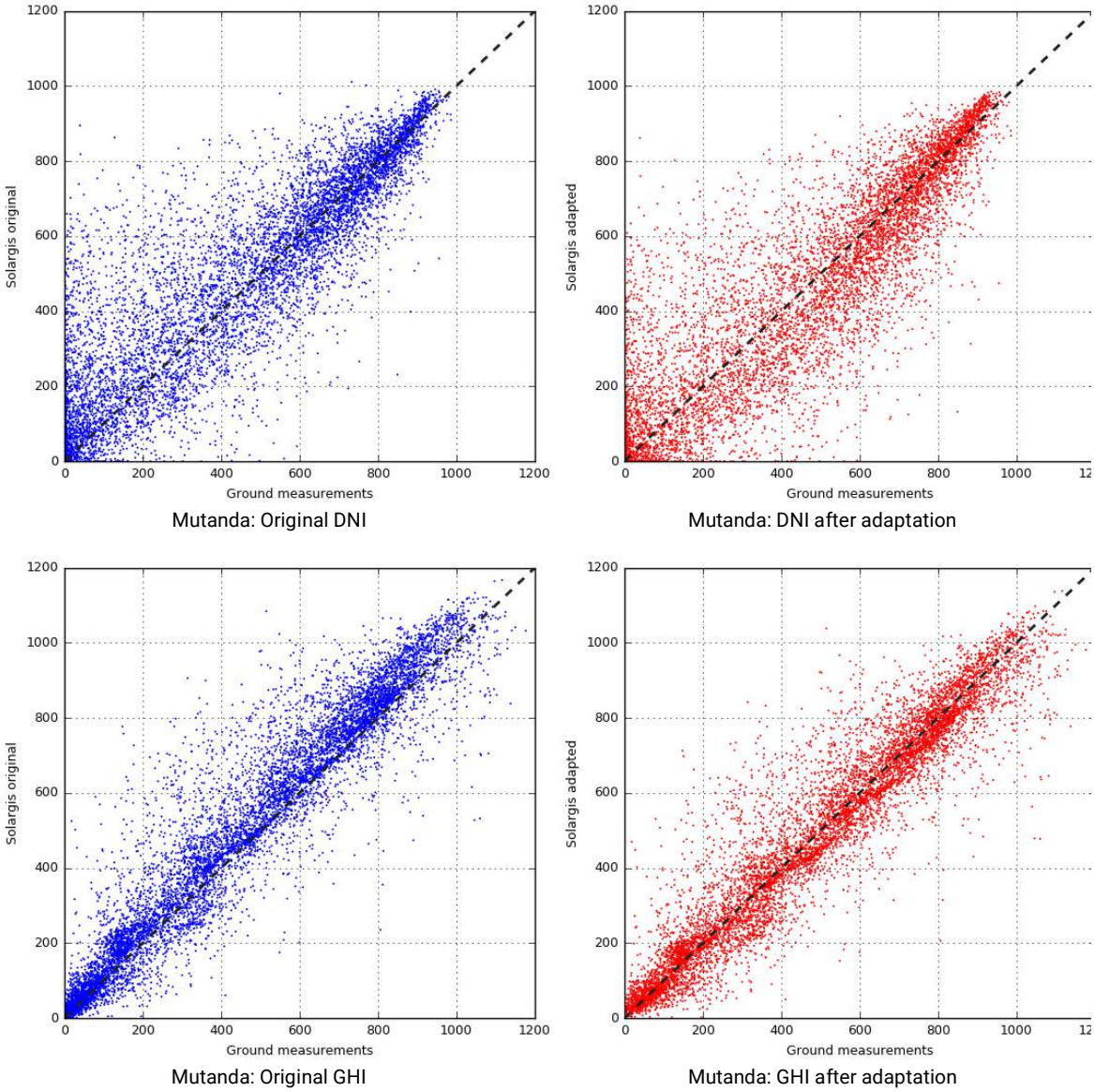

Mutanda: Original DNI | Mutanda: DNI after adaptation

Mutanda: Original GHI | Mutanda: GHI after adaptation

Figure 4.7: Correction of DNI and GHI hourly values for Mutanda.
Left: original Solargis data, right: site-adapted Solargis data.
The X-axis represents the measured data and the Y-axis represents the satellite-derived data.

The change of model GHI and DNI after site adaptation is presented on an example of UNZA Lusaka (Figure 4.8). Both the adapted GHI and DNI values are lower than the original values. The other sites show similar pattern (Table 4.6).

The site-adapted model values better represent the geographical variability of DNI and GHI solar resource, and they also improve the distribution and match of hourly values.

The measurements show that the Solargis model overestimates GHI and DNI in the region, and the results of site adaptation significantly improve the model performance. The results increase the confidence about the reliability of the measured and modelled solar resource data for Zambia.

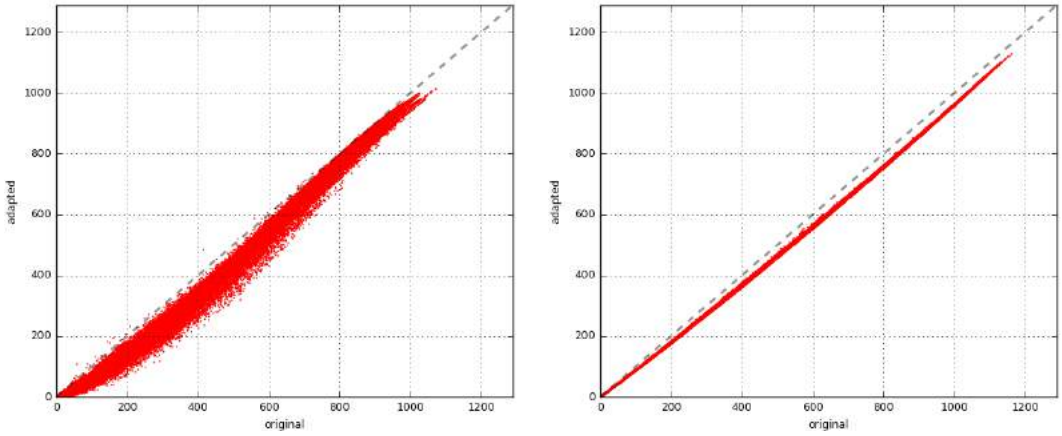

Figure 4.8: Comparison of Solargis original and site-adapted data for UNZA Lusaka site.
Left: DNI; Right: GHI; Data represent years 1994 to 2017.

Table 4.6 Comparison of long term average of yearly summaries of original and site-adapted values

Meteo station	DNI annual values			GHI annual values		
	Original	Site-adapted	Difference	Original	Site-adapted	Difference
	[kWh/m^2]	[kWh/m^2]	[%]	[kWh/m^2]	[kWh/m^2]	[%]
Lusaka UNZA	2030	1846	-9.0	2131	1996	-6.3
Mount Makulu	2033	1861	-8.5	2128	2001	-6.0
Mochipapa	2134	1969	-7.7	2150	2041	-5.1
Longe	2127	1995	-6.2	2212	2076	-6.2
Misamfu	1944	1763	-9.3	2190	2059	-6.0
Mutanda	1930	1755	-9.1	2165	1978	-8.7

5 METEOROLOGICAL MODEL DATA

5.1 Meteorological model

For the territory of Zambia, the last 24 years of the Solargis model-based meteorological data is derived from the meteorological models CFSR and CFSv2, with original characteristics specified in Table 5.1.

Table 5.1 Source of Solargis meteorological data: models CFSR and CFSv2 and their characteristics.

	Climate Forecast System Reanalysis (CFSR)	Climate Forecast System (CFSv2)
Period	1994 to 2010	2011 to the present time
Original spatial resolution	30 x 35 km	19 x 22 km
Original time resolution	1 hour	1 hour

Table 5.2 shows meteorological parameters available in Solargis, their specifications and it also indicates, which of them have been delivered within this study. The original spatial resolution of the models is enhanced to 1 km for air temperature and relative humidity by spatial disaggregation and use of the Digital Elevation Model SRTM-3. The spatial resolution (spatial representation) of other parameters is unchanged.

Table 5.2 Solargis meteorological parameters delivered within this project

Meteorological parameter	Acronym	Unit	Time resolution	Spatial representation	Data delivered	Data validated
Air temperature at 2 metres (dry bulb temperature)	TEMP	°C	60 minute	1 km	Yes	Yes
Relative humidity at 2 metres	RH	%	60 minute	Original model	Yes	Yes
Wind speed at 10 metres	WS	m/s^2	60 minute	Original model	Yes	Yes
Wind direction at 10 metres	WD	°	60 minute	Original model	Yes	Yes
Atmospheric pressure	AP	hPa	60 minute	1 km	Yes	Yes
Precipitable water	PWAT		60 minute	Original model	Yes	No

Important note: meteorological parameters are derived from the numerical weather model outputs and these models have lower spatial and temporal resolution. Thus, they do not represent the same accuracy as the solar resource data. Especially wind speed data has higher uncertainty, and it provides only overview information for solar energy projects. Thus, the **local microclimate at the meteorological stations may deviate from the values derived from the Solargis meteorological database.**

5.2 Validation of meteorological data

The validation procedure was carried out to compare the modelled data with ground-measurements from the 6 meteorological stations installed within the ESMAP project: Lusaka, Mount Makulu, Mochipapa, Longe, Misamfu and Mutanda. In general, the data from the meteorological model outputs represent larger area, and it is not capable to represent accurately the local microclimate.

5.2.1 Air temperature at 2 metres

Air temperature is derived from the CSFR and CSFv2 meteorological models and recalculated at the spatial resolution of 1 km (Table 5.3 and Figures 5.1 to 5.6). Considering spatial and time interpolation, the deviation of the modelled values to the ground observations for hourly values can occasionally reach several degrees of Celsius.

Figures 5.1 to 5.6 show graphical representation of the model values accuracy at the meteorological stations. In general, the model matches the ground measurements quite well. The main issue identified is underestimation or overestimation of night-time temperature by the model. Day-time temperature is represented with higher accuracy compared to night-time.

Table 5.3 Air temperature at 2 m: accuracy indicators of the model outputs [°C].

Meteorological station	CFSv2 model							
	Bias mean	Bias min	Bias max	Bias nigh-time	Bias day-time	RMSD hourly	RMSD daily	RMSD monthly
Lusaka UNZA	-1.6	-1.7	-0.9	-1.9	-1.3	2.5	1.8	1.6
Mount Makulu	-1.7	-1.6	-1.3	-1.8	-1.7	2.7	2.0	1.8
Mochipapa	-1.1	-0.6	-0.9	-1.0	-1.3	2.2	1.5	1.2
Longe	0.2	1.3	-0.4	1.0	-0.7	2.5	1.4	0.9
Misamfu	-1.7	-0.8	-2.0	-1.0	-2.3	2.7	2.0	1.8
Mutanda	0.8	2.8	-1.2	2.2	-0.6	3.4	2.2	1.9

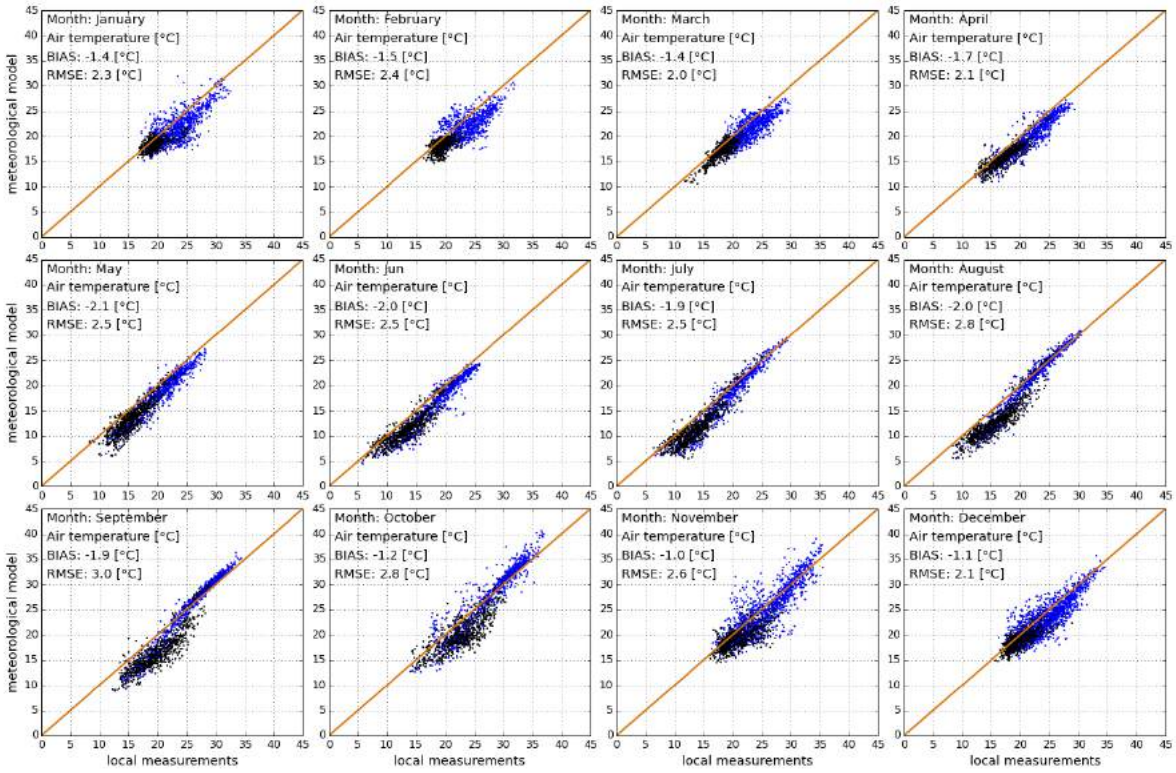

Figure 5.1: Scatterplots of air temperature at 2 m at Lusaka UNZA meteorological station.
Measured values (horizontal axis) and meteorological model values (vertical axis)
Blue: day-time, Black: night-time measurements

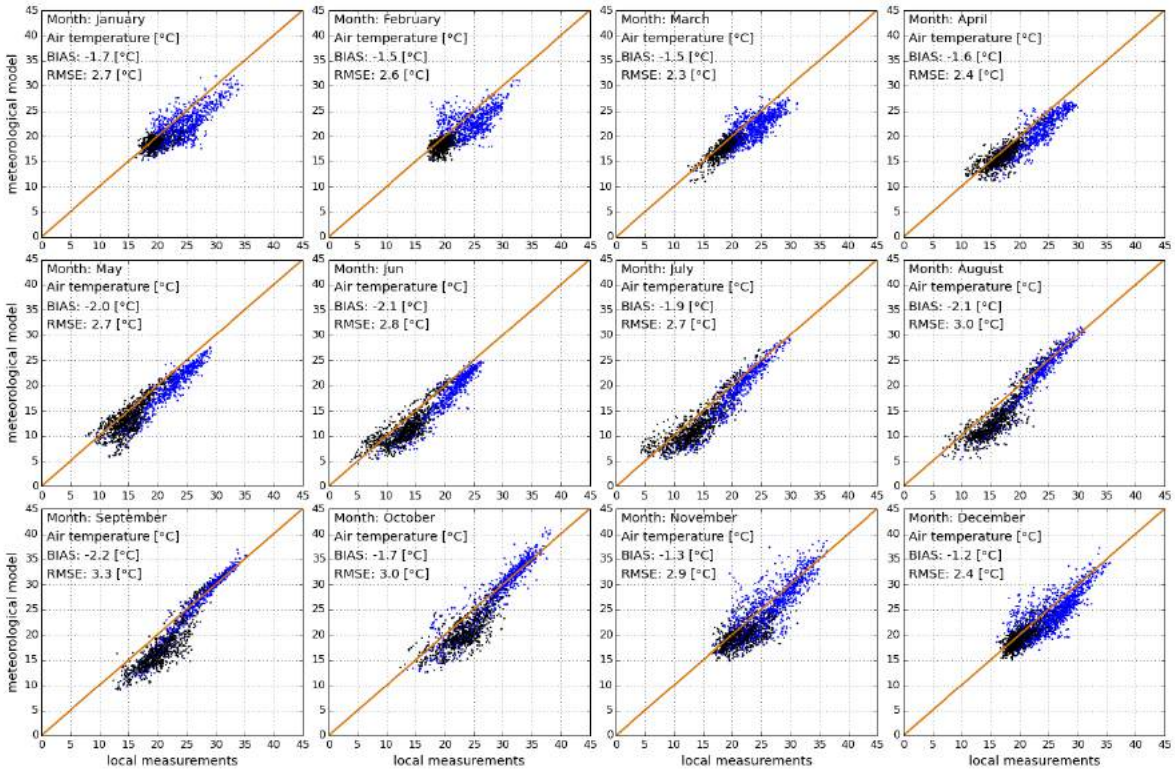

Figure 5.2: Scatterplots of air temperature at 2 m at Mount Makulu meteorological station.
Measured values (horizontal axis) and meteorological model values (vertical axis)
Blue: day-time, Black: night-time measurements

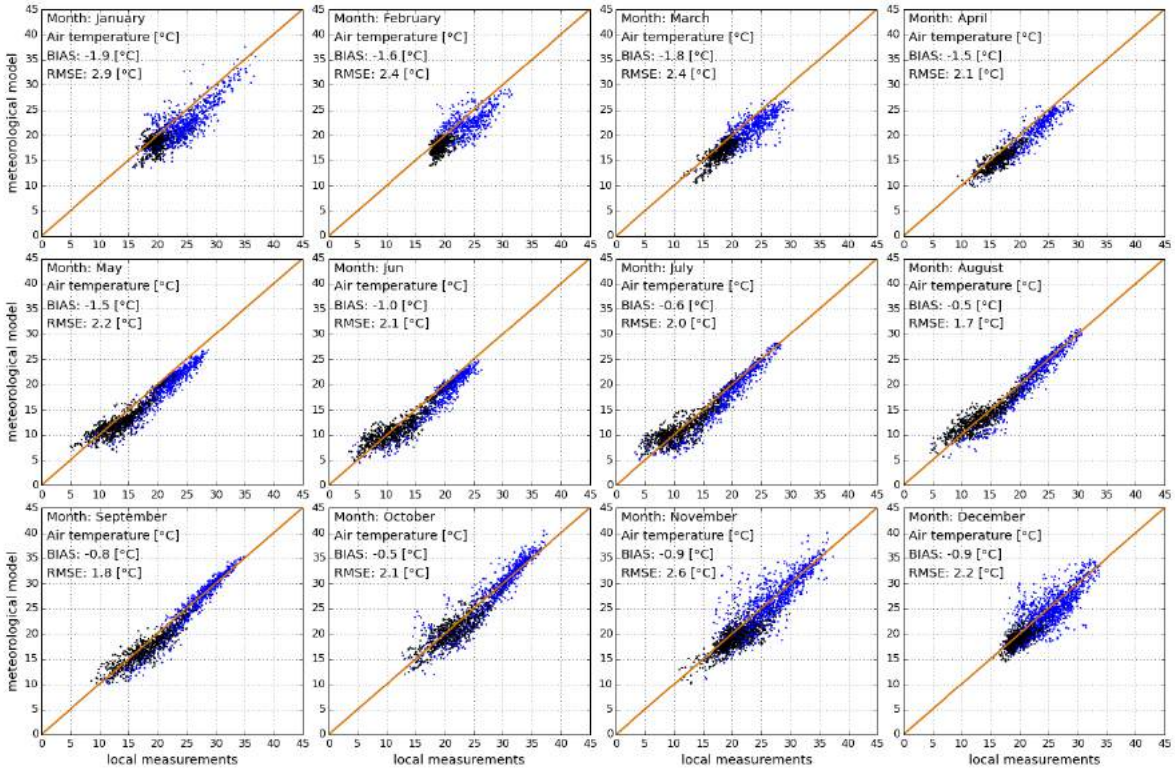

Figure 5.3: Scatterplots of air temperature at 2 m at Mochipapa meteorological station.
Measured values (horizontal axis) and meteorological model values (vertical axis)
Blue: day-time, Black: night-time measurements

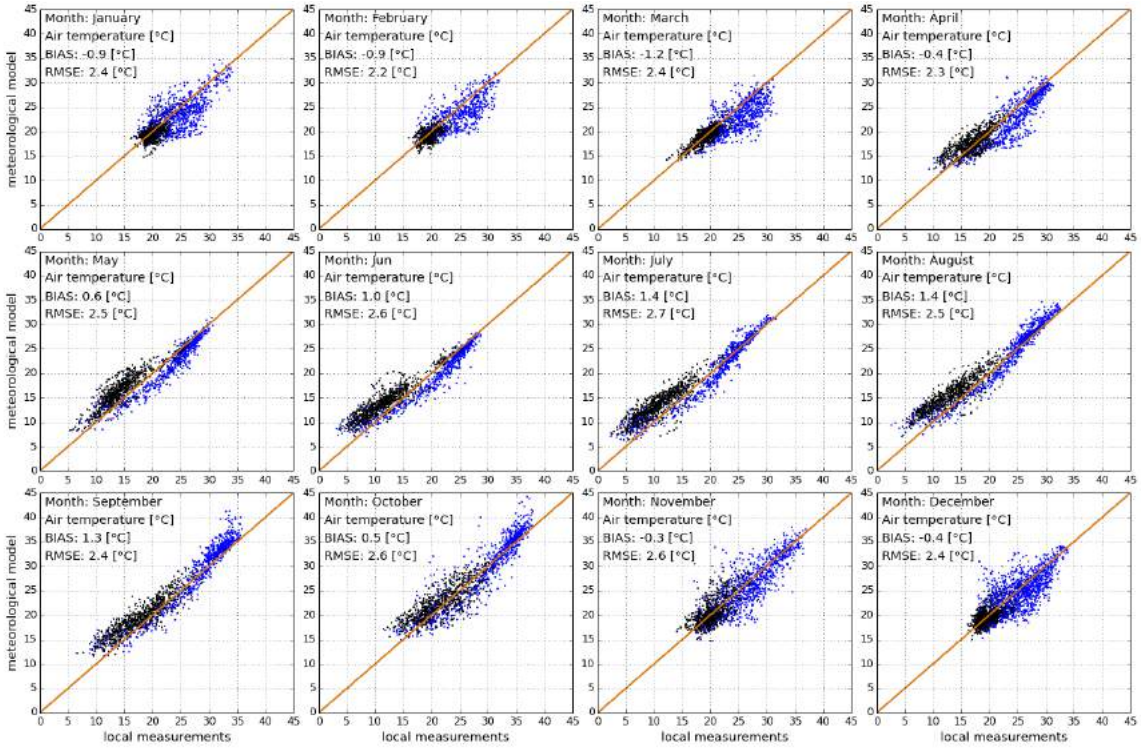

Figure 5.4: Scatterplots of air temperature at 2 m at Longe meteorological station.
Measured values (horizontal axis) and meteorological model values (vertical axis)
Blue: day-time, Black: night-time measurements

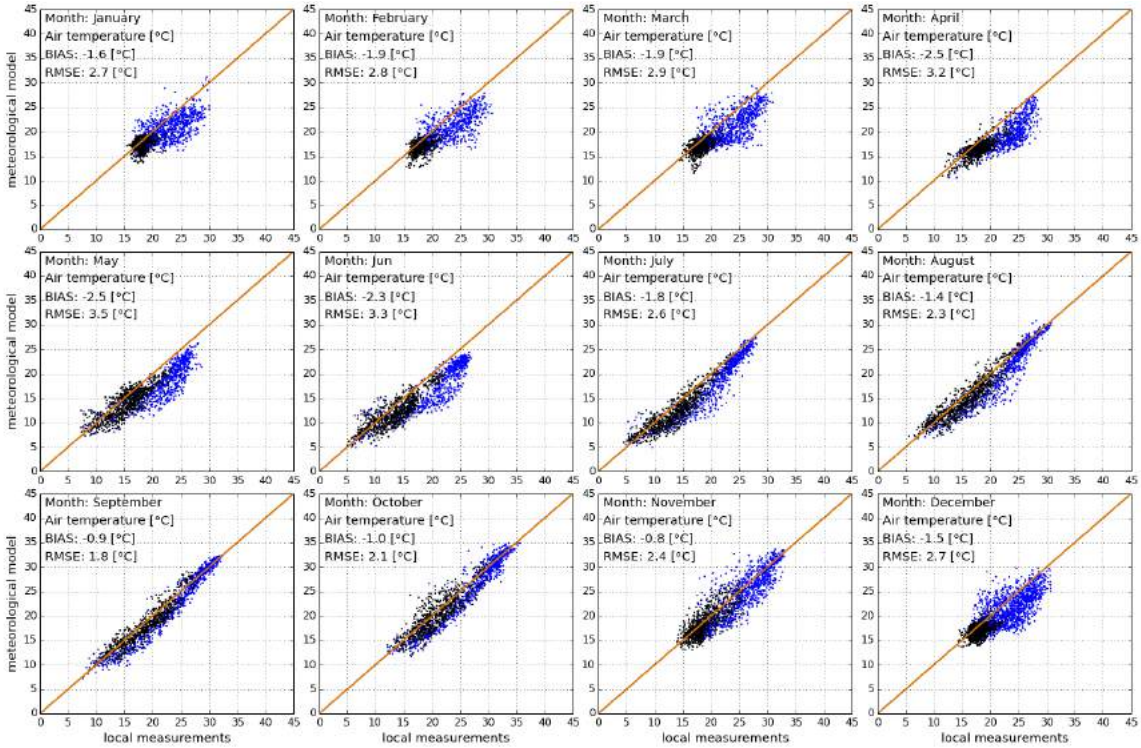

Figure 5.5: Scatterplots of air temperature at 2 m at Misamfu meteorological station.
Measured values (horizontal axis) and meteorological model values (vertical axis)
Blue: day-time, Black: night-time measurements

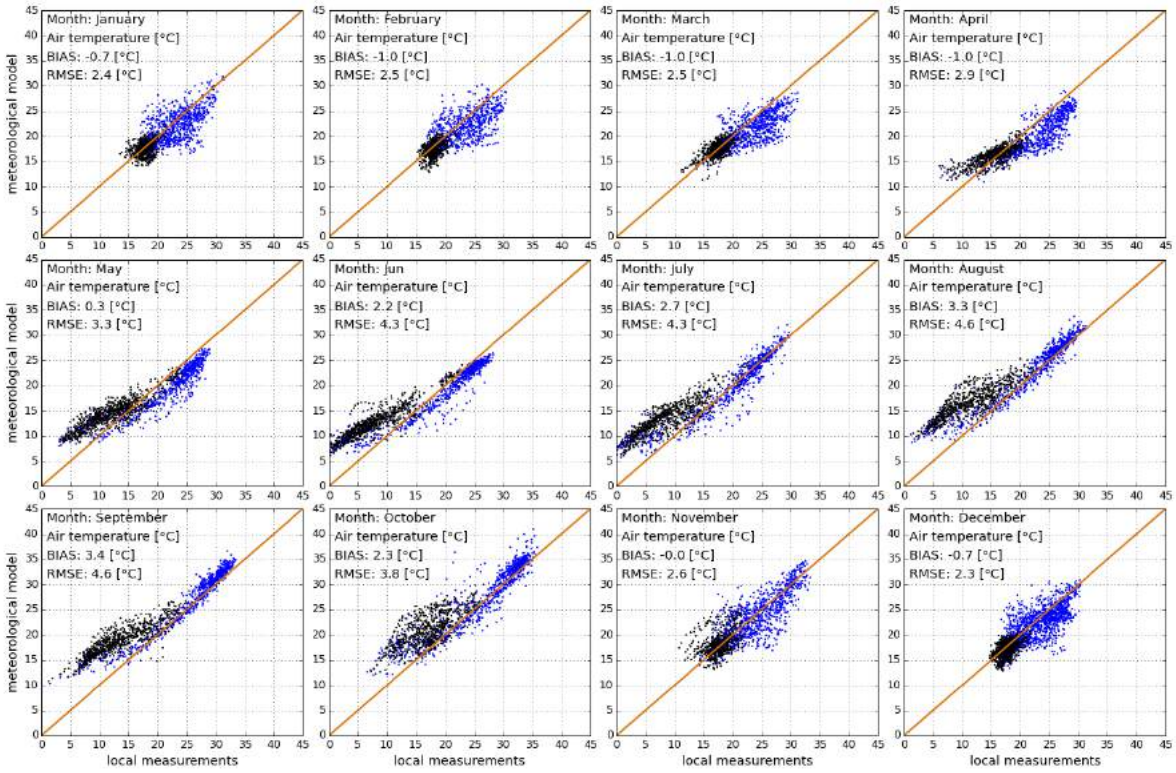

Figure 5.6: Scatterplots of air temperature at 2 m at Mutanda meteorological station.
Measured values (horizontal axis) and meteorological model values (vertical axis)
Blue: day-time, Black: night-time measurements

5.2.2 Relative humidity

Relative humidity is calculated from the specific humidity, atmospheric pressure and the air temperature. The comparison of the model values with ground measurements at all 6 meteorological stations is shown in Table 5.4 and Figures 5.7 to 5.12. In general, the model matches the ground measurements quite well, representing both daily and yearly profiles.

Table 5.4 Relative humidity: accuracy indicators of the model outputs [%].

Meteorological station	CFSv2 model							
	Bias mean	Bias min	Bias max	Bias nigh-time	Bias day-time	RMSD hourly	RMSD daily	RMSD monthly
Lusaka	-1	0	-2	-1	-1	10	6	2
Mount Makulu	0	0	-1	-1	0	10	6	2
Mochipapa	-3	1	-6	-5	-1	11	7	4
Longe	-9	-3	-12	-14	-4	16	12	11
Misamfu	1	3	-2	-2	4	11	6	4
Mutanda	-9	1	-15	-16	-2	19	14	13

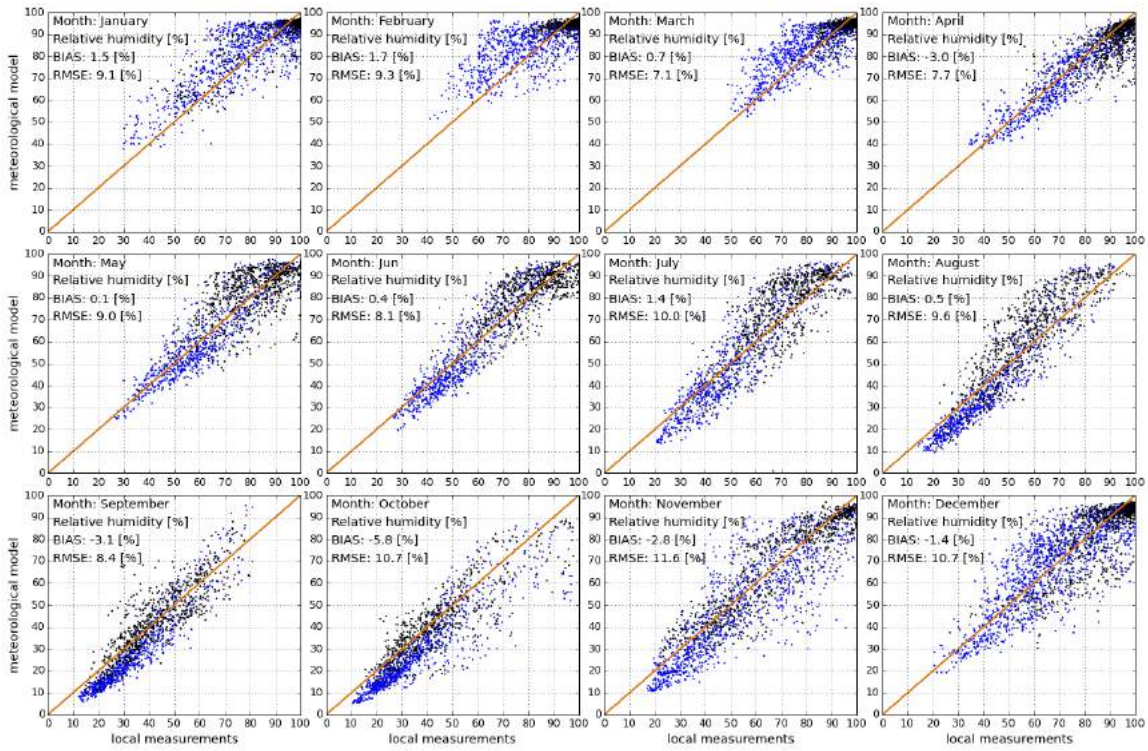

Figure 5.7: Scatterplots of relative humidity at 2 m at Lusaka UNZA meteorological station.
Measured values (horizontal axis) and meteorological model values (vertical axis).
Blue: day-time, black: night-time measurements.

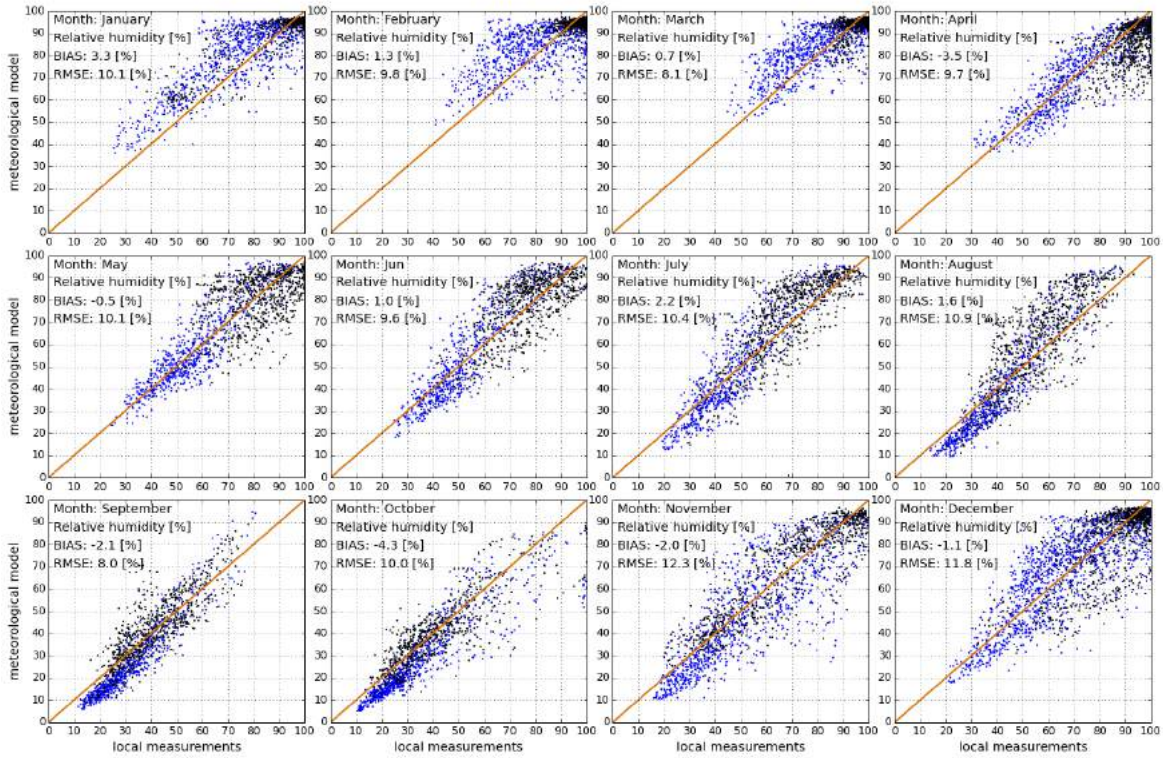

Figure 5.8: Scatterplots of relative humidity at 2 m at Mount Makulu meteorological station.
Measured values (horizontal axis) and meteorological model values (vertical axis).
Blue: day-time, black: night-time measurements.

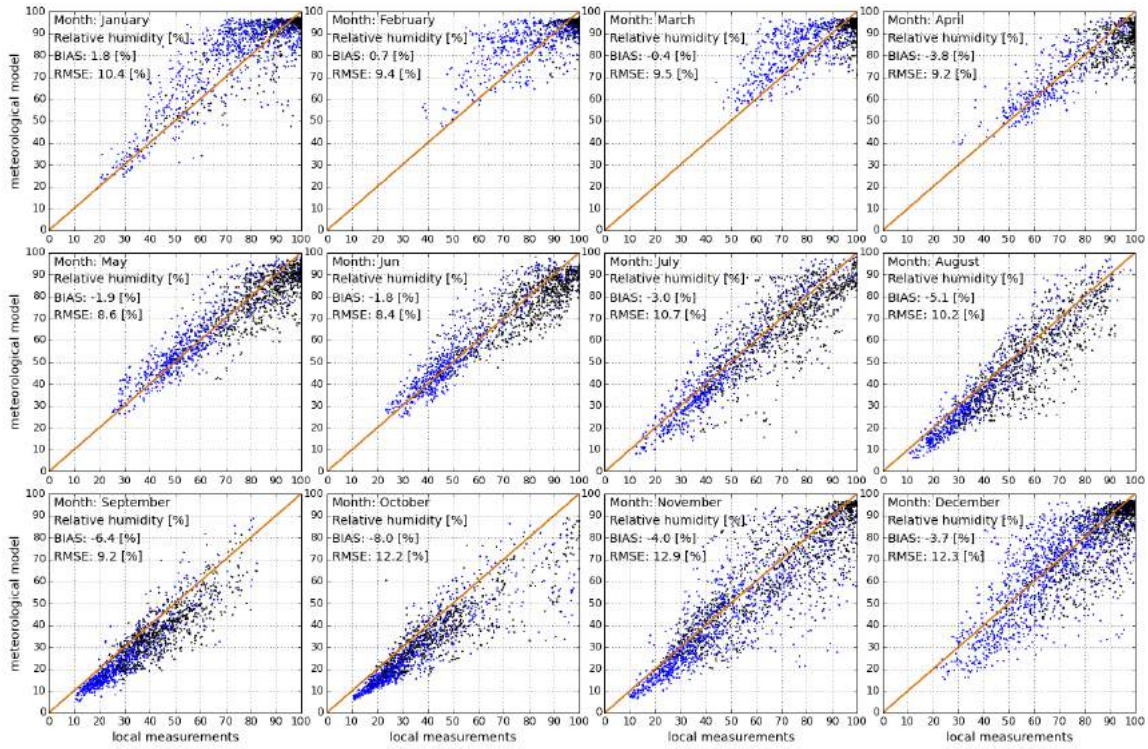

Figure 5.9: Scatterplots of relative humidity at 2 m at Mochipapa meteorological station.
Measured values (horizontal axis) and meteorological model values (vertical axis).
Blue: day-time, black: night-time measurements.

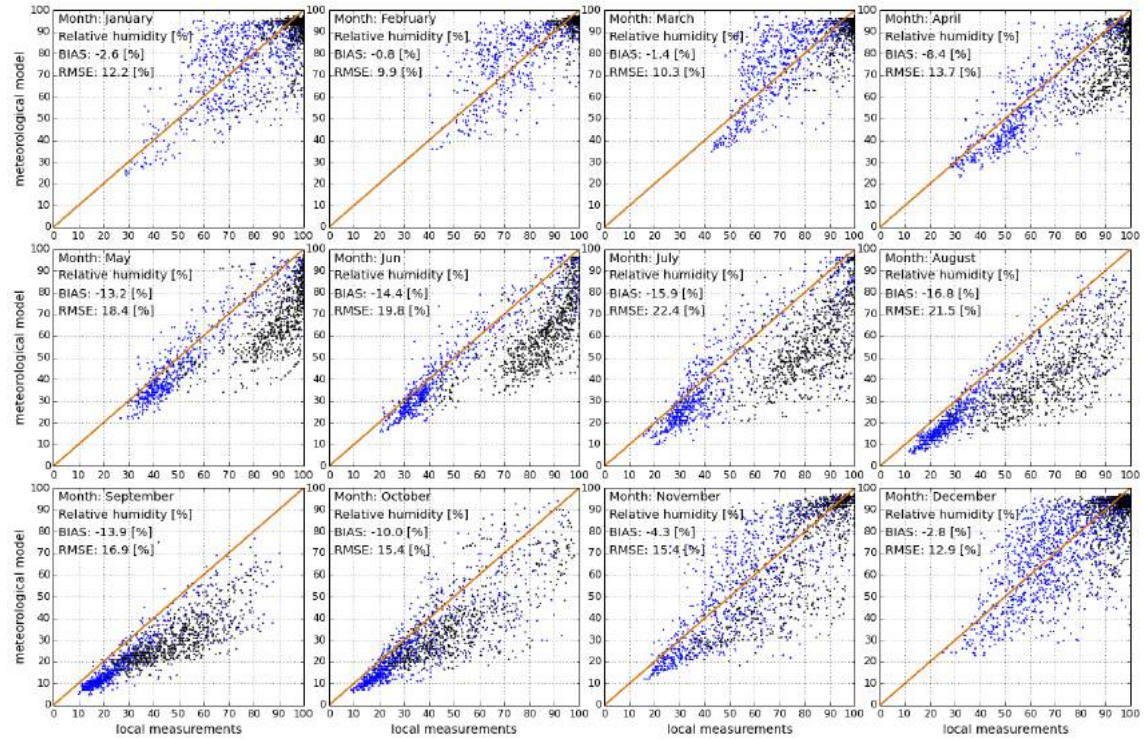

Figure 5.10: Scatterplots of relative humidity at 2 m at Longe meteorological station.
Measured values (horizontal axis) and meteorological model values (vertical axis).
Blue: day-time, black: night-time measurements.

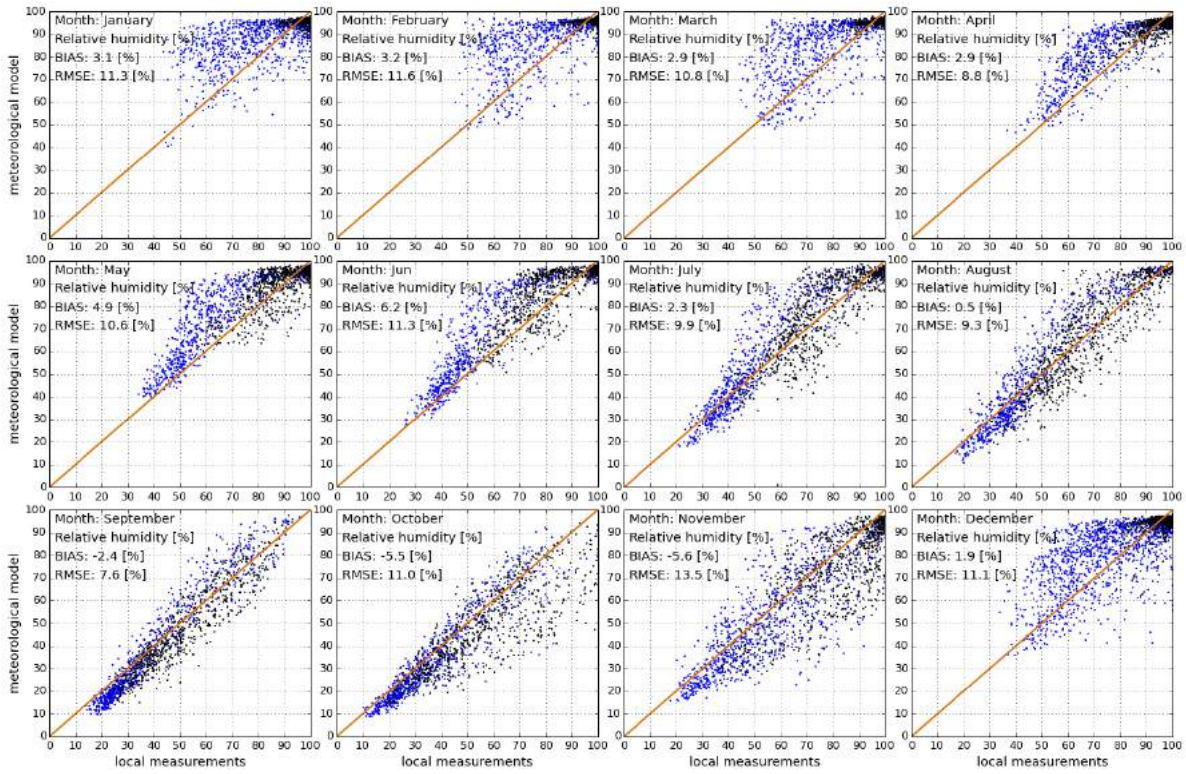

Figure 5.11: Scatterplots of relative humidity at 2 m at Misamfu meteorological station.
Measured values (horizontal axis) and meteorological model values (vertical axis).
Blue: day-time, black: night-time measurements.

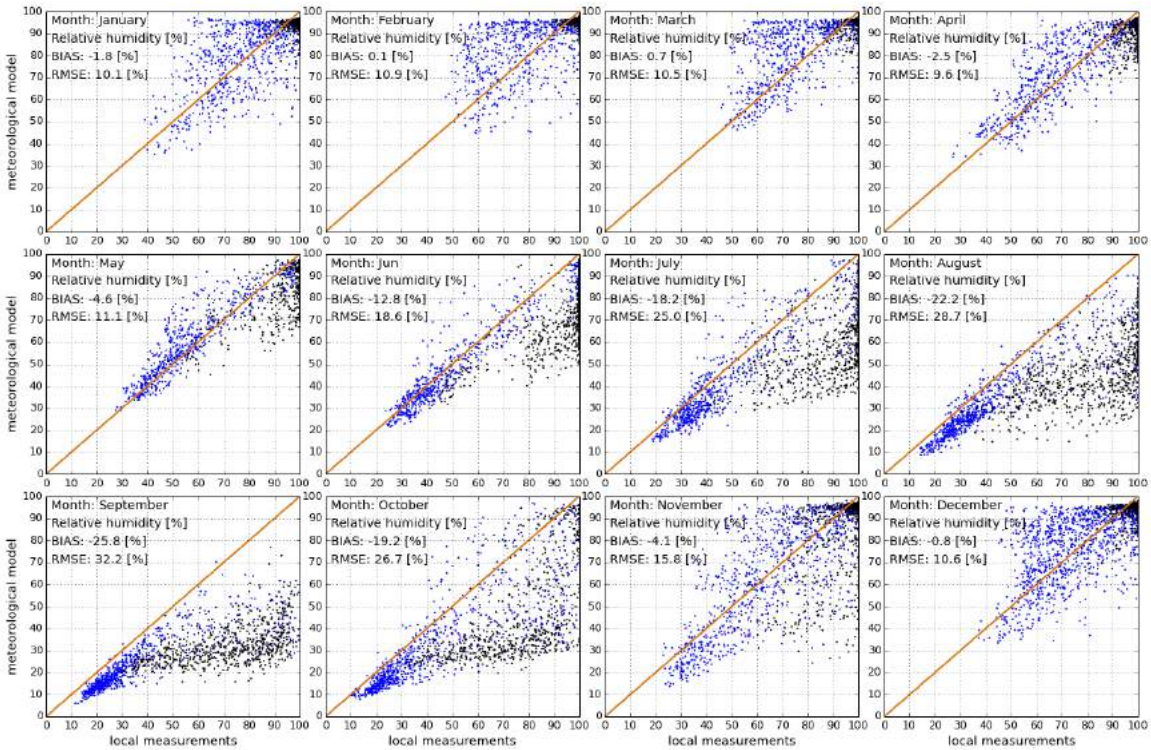

Figure 5.12: Scatterplots of relative humidity at 2 m at Mutanda meteorological station.
Measured values (horizontal axis) and meteorological model values (vertical axis).
Blue: day-time, black: night-time measurements.

5.2.3 Wind speed and wind direction at 10 metres

Wind speed and direction values delivered within Solargis data represent the height at 10 meters and they are calculated from the CFSR and CFSv2 models, from 10 m wind u- and v- components. The spatial resolution is kept the same, as in the original data. Wind measurements take place **at the height of 10 metres (Lusaka) and 3 metres (other stations), while the model data represent values at height of 10 m above ground**.

Comparison of the modelled wind speed with ground measurements is shown in Table 5.5 and Figures 5.13 to 5.18. The model values underestimate the wind conditions measured at the meteorological stations. Similar to relative humidity, the data representation for wind speed and wind direction strongly depends on the local conditions; therefore the model values are only indicative and better characterize a larger region rather than the local microclimate. The important source of systematic difference is different height of the installed wind sensor at Tier 2 stations (3 metres above ground), compared to the model assumptions (10 metres above ground).

Table 5.5 Wind speed: accuracy indicators of the model outputs [m/s].

Meteorological station	CFSR and CFSv2 models							
	Bias mean	Bias min	Bias max	Bias nigh-time	Bias day-time	RMSD hourly	RMSD daily	RMSD monthly
Lusaka UNZA	-0.1	0.2	-0.2	0.1	-0.2	1.0	0.5	0.3
Mount Makulu	1.8	1.4	2.2	1.7	1.8	2.1	1.9	1.9
Mochipapa	1.4	1.3	0.9	1.8	1.0	1.9	1.6	1.5
Longe	1.7	1.5	1.3	2.2	1.3	2.0	1.9	1.8
Misamfu	1.1	1.1	0.7	1.4	0.8	1.4	1.2	1.2
Mutanda	1.7	1.4	1.2	1.9	1.4	1.9	1.8	1.7

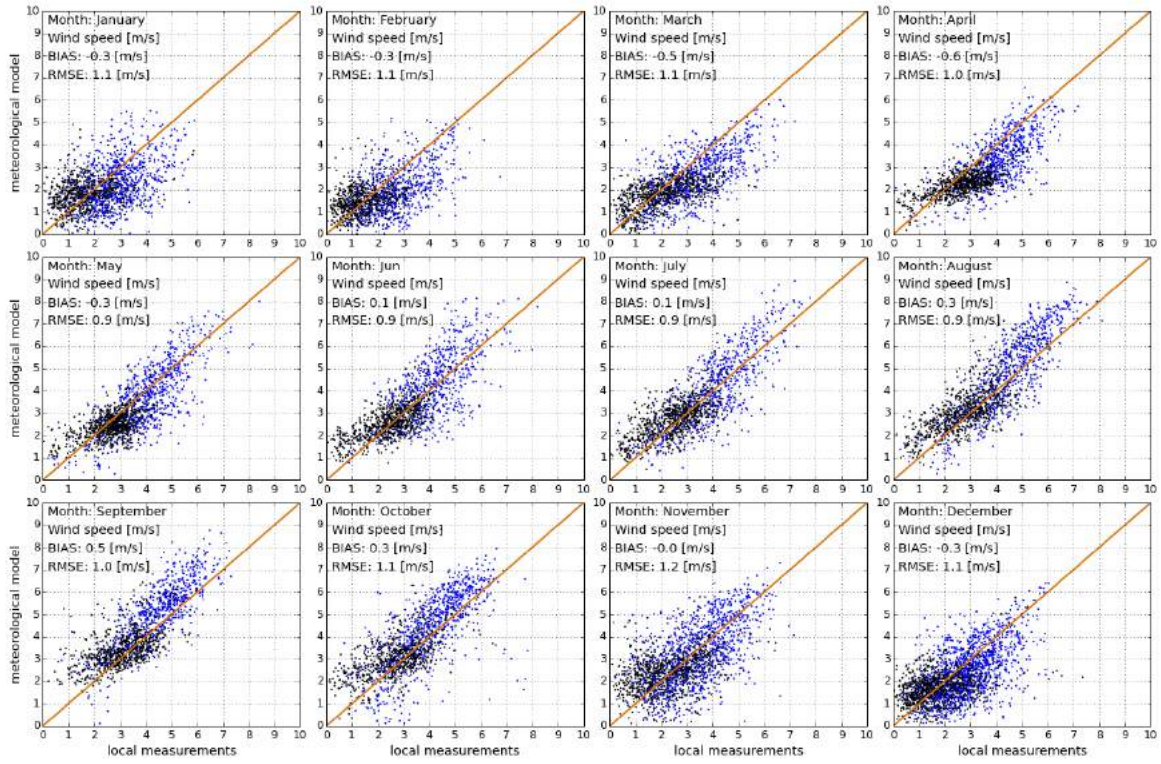

Figure 5.13: Scatterplots of wind speed at Lusaka UNZA meteorological station.
Measured values (horizontal axis) and meteorological model values (vertical axis).
Blue: day-time, black: night-time. (observations and model data at 10 m)

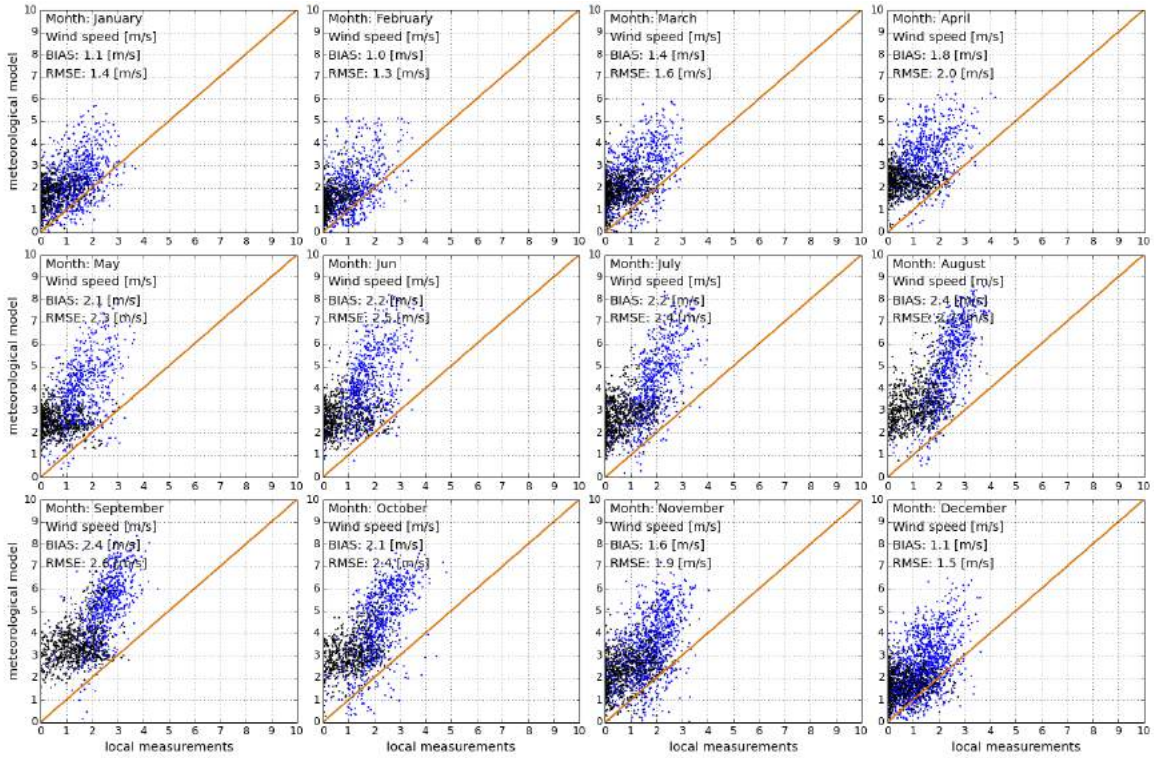

Figure 5.14: Scatterplots of wind speed at Mount Makulu meteorological station.
Measured values (horizontal axis) and meteorological model values (vertical axis).
Blue: day-time, black: night-time. (observations at 3 m height and model data at 10 m)

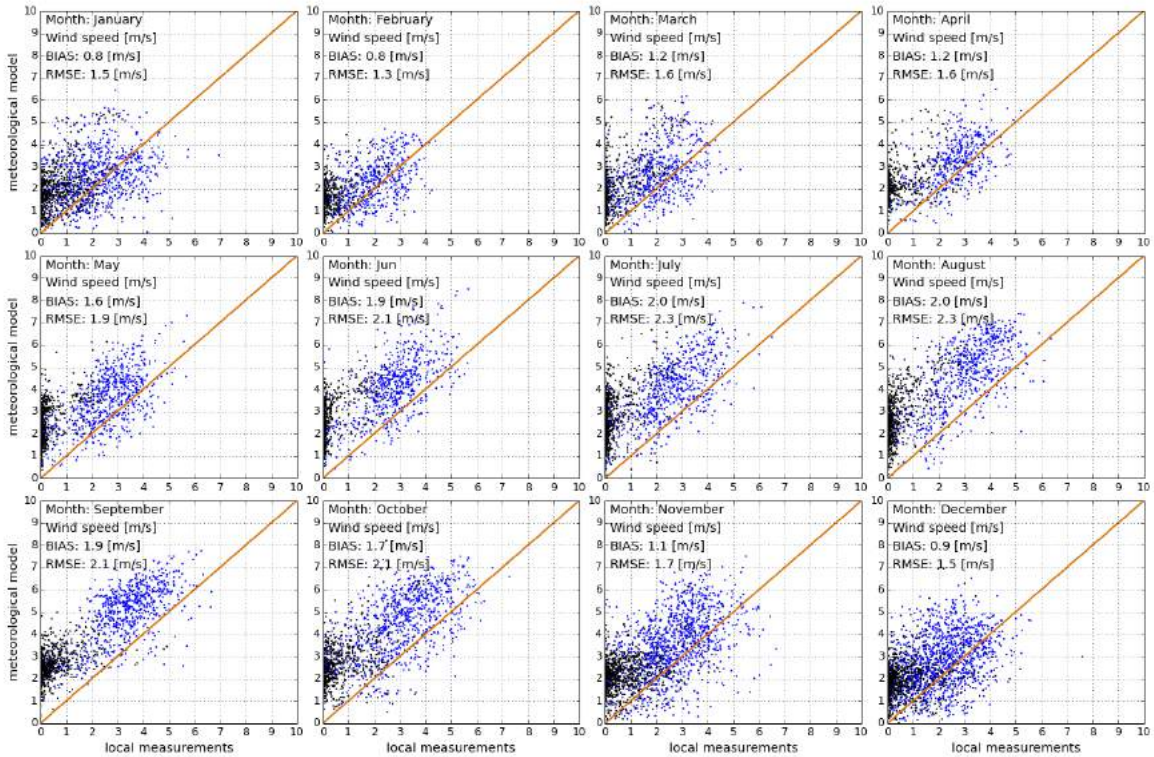

Figure 5.15: Scatterplots of wind speed at Mochipapa meteorological station.
Measured values (horizontal axis) and meteorological model values (vertical axis).
Blue: day-time, black: night-time. (observations at 3 m height and model data at 10 m)

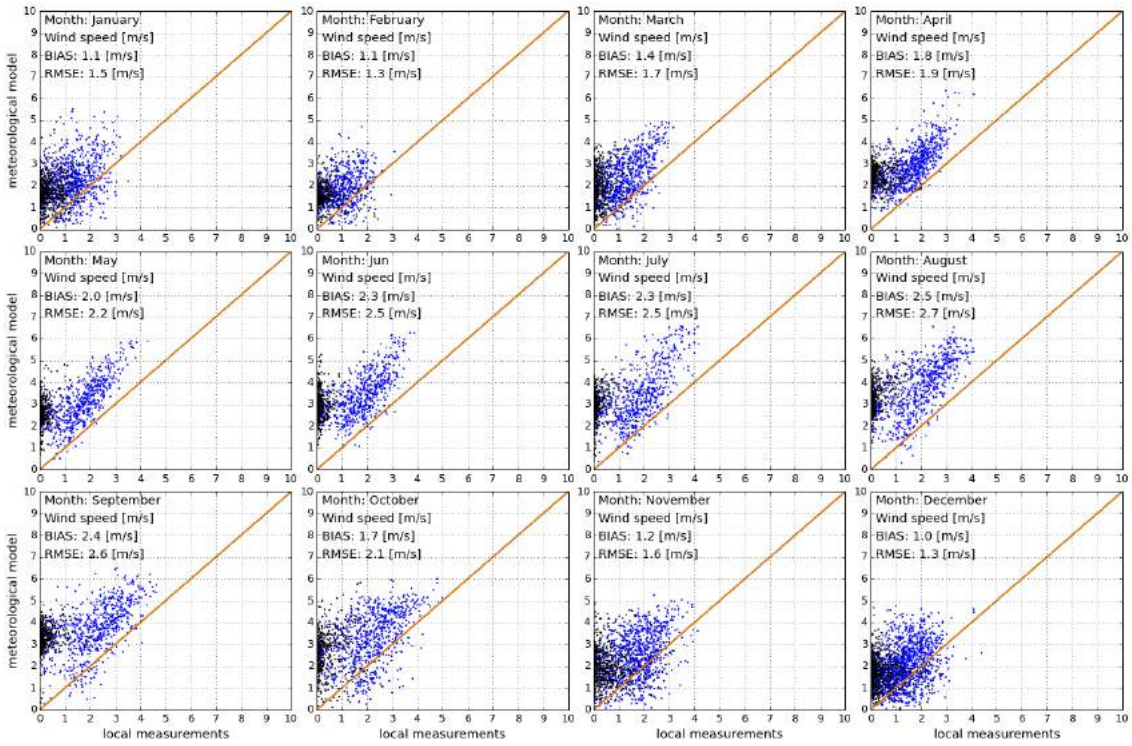

Figure 5.16: Scatterplots of wind speed at Longe meteorological station.
Measured values (horizontal axis) and meteorological model values (vertical axis).
Blue: day-time, black: night-time. (observations at 3 m height and model data at 10 m)

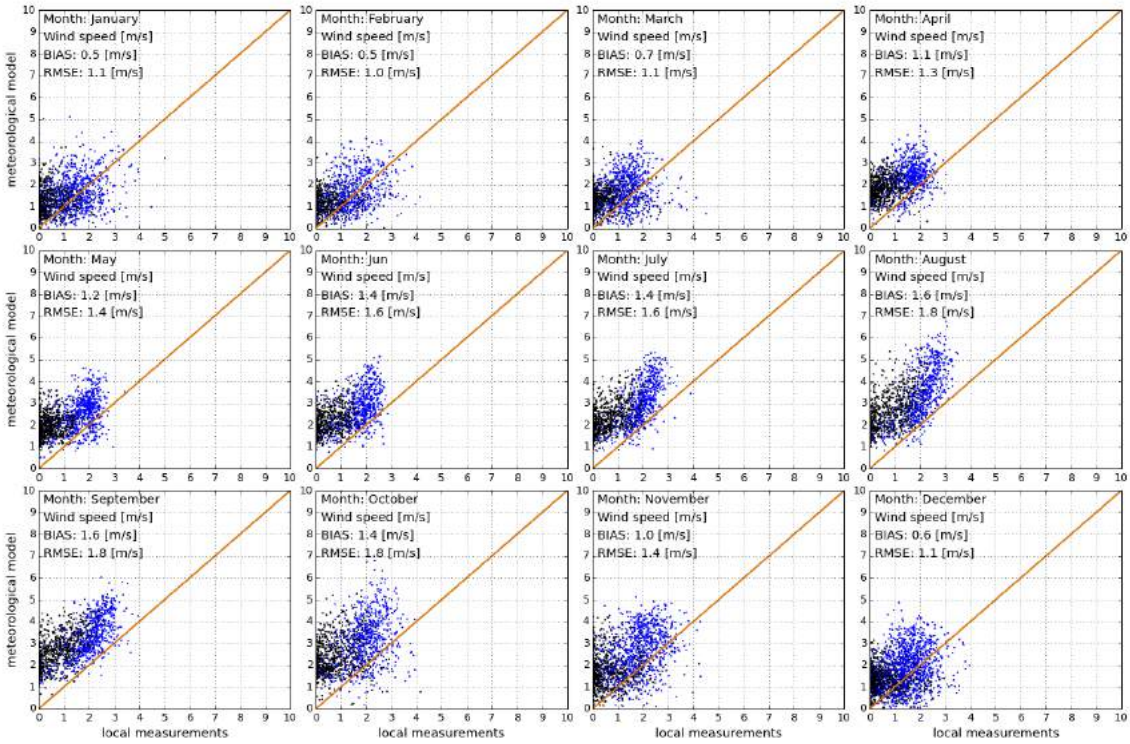

Figure 5.17: Scatterplots of wind speed at Misamfu meteorological station.
Measured values (horizontal axis) and meteorological model values (vertical axis).
Blue: day-time, black: night-time. (observations at 3 m height and model data at 10 m)

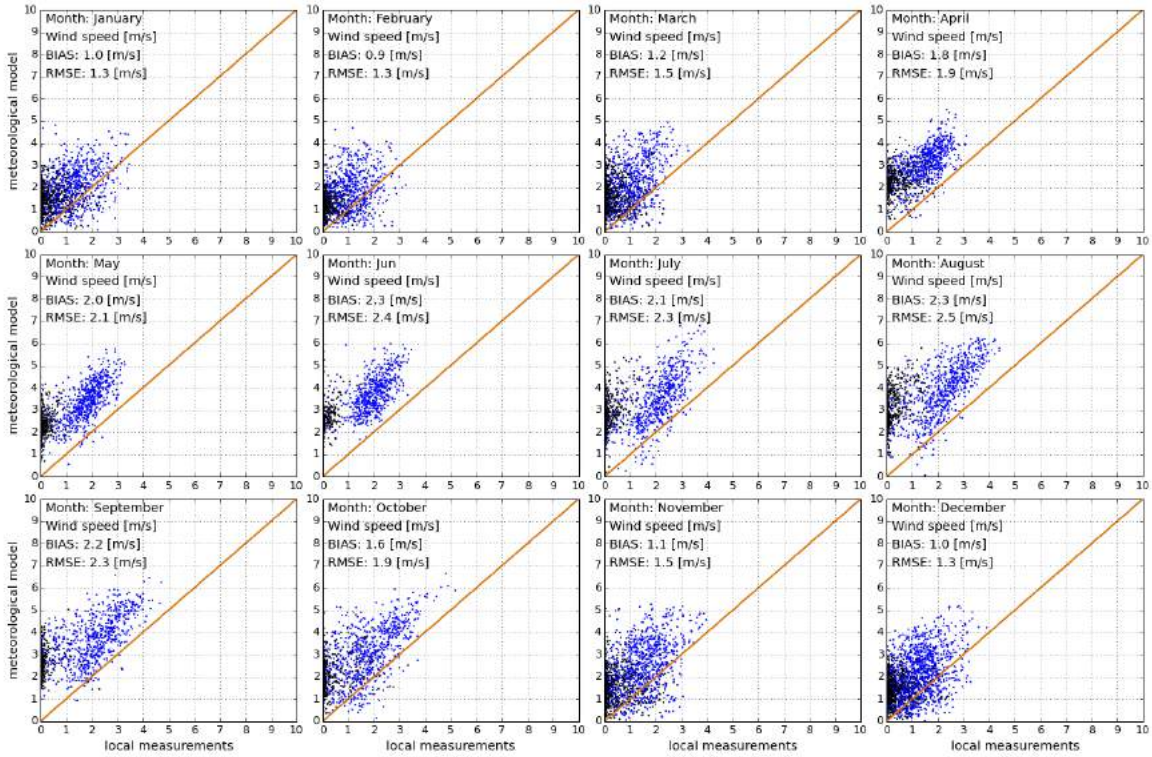

Figure 5.18: Scatterplots of wind speed at Mutanda meteorological station.
Measured values (horizontal axis) and meteorological model values (vertical axis).
Blue: day-time, black: night-time. (observations at 3 m height and model data at 10 m)

5.3 Uncertainty of meteorological model data

The meteorological parameters are derived from two very similar numerical meteorological models covering periods from 1994 to 2010 (CFSR model) and 2011 to 2017 (CFSv2). Considering the comparison results, the uncertainty of the estimate for the main meteorological parameters is summarised in Table 5.6. The uncertainty is expressed for 80% occurrence.

It was found that the modelled air temperature fits reasonably well the measured data though (logically) due to the spatial resolution there are some issues like underestimation of night-time temperature. Similar to air temperature, the model relative humidity fits well the measured data representing both daily and yearly amplitude.

Wind speed data, obtained from the meteorological model, represents an area of larger region, in comparison to the point measurements collected at the meteorological sites. The model values represent wind conditions at 10 metres height above ground, while the measurements represent 3 metres height.

Atmospheric pressure from the models fits well the measured data with a very small bias for all meteorological stations not exceeding 3 hPa.

Table 5.6 Expected uncertainty of modelled meteorological parameters at the project sites.

	Unit	Annual	Monthly	Hourly
Air temperature at 2 m	°C	±2.0	±2.0	±3.5
Relative humidity at 2 m	%	±10	±10	±15
Average wind speed at 10 m	m/s	±1.5	±1.5	±2.0
Atmospheric pressure	hPa	±3	±3	±3

6 SOLAR RESOURCE: UNCERTAINTY OF LONG-TERM ESTIMATES

6.1 Uncertainty of solar resource yearly estimate

The **uncertainty of site-adapted satellite-based GHI and DNI** is determined by the uncertainty of the model and of the ground measurements [7], more specifically it depends on:

1. Parameterization and adaptation of **numerical models integrated in Solargis** for the given data inputs and their ability to generate accurate results for various geographical and time-variable conditions:
    - Data inputs into Solargis model (accuracy of satellite data, aerosols and water vapour and Digital Terrain Model).
    - Clear-sky model and its capability to properly characterize various states of the atmosphere
    - Simulation accuracy of the satellite model and cloud transmittance algorithms, being able to properly distinguish different types of desert surface, clouds, fog, but also snow and ice.
    - Diffuse and direct decomposition models
    - Site adaptation methods.
2. Uncertainty of the **ground-measurements**, which is determined by:
    - Accuracy of the instruments
    - Maintenance practices, including sensor cleaning, calibration
    - Data post-processing and quality control procedures.

Solargis model uncertainty is compared to the high-quality data measured by the meteorological instruments. Representativeness of such data comparison (satellite and ground-measured) is determined by the precision of the measuring instruments, the maintenance and operational practices, and by quality control of the measured data – in other words, by the measurement accuracy achieved at each meteorological station.

Accuracy statistics, such as bias and RMSD (Chapter 4.3) characterize accuracy of the Solargis model in the given validation points, relative to the ground measurements. The validation statistics is affected by local geography and by quality and reliability of the ground-measured data. Therefore, the validation statistics only indicates performance of the model in the region.

From the user's perspective, the information about the model uncertainty has probabilistic nature. It generalizes the validation accuracy and it has to be considered at different confidence levels. The expert estimate of the calculation uncertainty in this report assumes 80% probability of occurrence of values.

The solar model uncertainty is discussed in Chapters 4 and 6.1. The main findings are summarized in Table 6.1. The site-adaptation procedure reduced uncertainty of estimate of all parameters. Chapter 6.3 evaluates combined uncertainty, in which also interannual variability is included (Chapter 6.2).

The physical reduction of the model uncertainty was significant already after site adaptation using ground measurements after first year, and it was further reduced after second year of measurement campaign (Table 6.1). In addition, the site adaptation increases confidence in the model data values.

Table 6.1 Uncertainty of the model estimates for original and site-adapted annual long-term values (Considers 80% probability of occurrence)

Uncertainty of long-term annual values	Acronym	Uncertainty of the original Solargis model	Uncertainty of the Solargis model after site adaptation	
			After 1st year	After 2nd year
Global Horizontal Irradiation	GHI	±7.5% (up to ±10.0%*)	±4.5%	±4.0%
Direct Normal Irradiance	DNI	±12.0% (up to ±18.0%*)	±6.0%	±5.5%

* in complex microclimate

6.2 Uncertainty due to interannual variability of solar radiation

Weather changes in cycles and has also stochastic nature. Therefore, annual solar radiation in each year can deviate from the long-term average in the range of few percent. The estimation of the interannual variability below shows the magnitude of this change. The uncertainty of GHI and DNI prediction is highest if only one single year is considered, but when averaged for a longer period, weather oscillations even out and approximate to the long-term average.

In this report, the **interannual variability** is calculated from the unbiased standard deviation *stdev* of GHI and DNI over **24 years**, considering, in the long-term, the normal distribution of the annual sums for *n* years, where x_i is any particular year and $\bar{x}$is longterm yearly average. Due to the limited number of years of available data, for the calculation we apply simplified assumption of normal distribution of yearly values:

$$stdev = \sqrt{\frac{1}{n-1}\sum_{i=1}^{n}(x_i - \bar{x})^2}$$

Tables 6.2 and 6.3 show GHI and DNI values that are to be exceeded at P90 for a consecutive number of years. The variability (var_n) for a number of years (n) is calculated from the unbiased standard deviation (*stdev*):

$$var_n = \frac{stdev}{\sqrt{n}}$$

The uncertainty, which characterises 80% probability of *occurrence* (U_{var}), is calculated from the variability (var_n), multiplying it with 1.28155:

$$uncert = 1.28155\ var$$

The lower boundary (negative value) of uncertainty represents 90% probability of *exceedance*, and it is used for calculating the P90 value.

Table 6.2 Annual GHI that should be exceeded with 90% probability in the period of 1 to 10 (25) years

Lusaka UNZA | Years	**1**	**2**	**3**	**4**	**5**	**6**	**7**	**8**	**9**	**10**	**25**
Variability [±%]	3.6	2.5	2.1	1.8	1.6	1.5	1.3	1.3	1.2	1.1	0.7
Uncertainty P90 [±%]	4.6	3.2	2.6	2.3	2.0	1.9	1.7	1.6	1.5	1.4	0.9
Minimum GHI P90	**1905**	**1932**	**1943**	**1950**	**1955**	**1959**	**1961**	**1964**	**1966**	**1967**	**1978**
Mount Makulu | Years	**1**	**2**	**3**	**4**	**5**	**6**	**7**	**8**	**9**	**10**	**25**
Variability [±%]	3.3	2.3	1.9	1.7	1.5	1.4	1.3	1.2	1.1	1.0	0.7
Uncertainty P90 [±%]	4.2	3.0	2.5	2.1	1.9	1.7	1.6	1.5	1.4	1.3	0.8
Minimum GHI P90	**1916**	**1941**	**1952**	**1959**	**1963**	**1967**	**1969**	**1971**	**1973**	**1974**	**1984**
Mochipapa | Years	**1**	**2**	**3**	**4**	**5**	**6**	**7**	**8**	**9**	**10**	**25**
Variability [±%]	3.0	2.1	1.7	1.5	1.3	1.2	1.1	1.1	1.0	0.9	0.6
Uncertainty P90 [±%]	3.8	2.7	2.2	1.9	1.7	1.6	1.5	1.4	1.3	1.2	0.8
Minimum GHI P90	**1963**	**1986**	**1996**	**2002**	**2006**	**2009**	**2011**	**2013**	**2015**	**2016**	**2025**
Longe | Years	**1**	**2**	**3**	**4**	**5**	**6**	**7**	**8**	**9**	**10**	**25**
Variability [±%]	2.7	1.9	1.6	1.3	1.2	1.1	1.0	1.0	0.9	0.9	0.5
Uncertainty P90 [±%]	3.4	2.4	2.0	1.7	1.5	1.4	1.3	1.2	1.1	1.1	0.7
Minimum GHI P90	**2004**	**2025**	**2034**	**2040**	**2044**	**2046**	**2049**	**2050**	**2052**	**2053**	**2061**
Misamfu | Years	**1**	**2**	**3**	**4**	**5**	**6**	**7**	**8**	**9**	**10**	**25**
Variability [±%]	2.8	2.0	1.6	1.4	1.3	1.2	1.1	1.0	0.9	0.9	0.6
Uncertainty P90 [±%]	3.6	2.6	2.1	1.8	1.6	1.5	1.4	1.3	1.2	1.1	0.7
Minimum GHI P90	**1984**	**2006**	**2016**	**2021**	**2025**	**2028**	**2031**	**2032**	**2034**	**2035**	**2044**
Mutanda | Years	**1**	**2**	**3**	**4**	**5**	**6**	**7**	**8**	**9**	**10**	**25**
Variability [±%]	2.7	1.9	1.5	1.3	1.2	1.1	1.0	0.9	0.9	0.8	0.5
Uncertainty P90 [±%]	3.4	2.4	2.0	1.7	1.5	1.4	1.3	1.2	1.1	1.1	0.7
Minimum GHI P90	**1910**	**1930**	**1939**	**1944**	**1947**	**1950**	**1952**	**1954**	**1955**	**1956**	**1964**

Table 6.3 Annual DNI that should be exceeded with 90% probability in the period of 1 to 10 (25) years.

Lusaka UNZA | Years	**1**	**2**	**3**	**4**	**5**	**6**	**7**	**8**	**9**	**10**	**25**
Variability [±%]	8.7	6.2	5.0	4.4	3.9	3.6	3.3	3.1	2.9	2.8	1.7
Uncertainty P90 [±%]	11.2	7.9	6.5	5.6	5.0	4.6	4.2	4.0	3.7	3.5	2.2
Minimum DNI P90	**1639**	**1700**	**1727**	**1743**	**1754**	**1762**	**1768**	**1773**	**1777**	**1781**	**1805**

Mount Makulu | Years	**1**	**2**	**3**	**4**	**5**	**6**	**7**	**8**	**9**	**10**	**25**
Variability [±%]	8.0	5.6	4.6	4.0	3.6	3.3	3.0	2.8	2.7	2.5	1.6
Uncertainty P90 [±%]	10.2	7.2	5.9	5.1	4.6	4.2	3.9	3.6	3.4	3.2	2.0
Minimum DNI P90	**1670**	**1726**	**1751**	**1765**	**1775**	**1783**	**1789**	**1793**	**1797**	**1800**	**1822**

Mochipapa | Years	**1**	**2**	**3**	**4**	**5**	**6**	**7**	**8**	**9**	**10**	**25**
Variability [±%]	7.6	5.4	4.4	3.8	3.4	3.1	2.9	2.7	2.5	2.4	1.5
Uncertainty P90 [±%]	9.8	6.9	5.7	4.9	4.4	4.0	3.7	3.5	3.3	3.1	2.0
Minimum DNI P90	**1777**	**1833**	**1858**	**1873**	**1883**	**1891**	**1897**	**1901**	**1905**	**1908**	**1931**

Longe | Years	**1**	**2**	**3**	**4**	**5**	**6**	**7**	**8**	**9**	**10**	**25**
Variability [±%]	6.5	4.6	3.7	3.2	2.9	2.6	2.4	2.3	2.2	2.0	1.3
Uncertainty P90 [±%]	8.3	5.9	4.8	4.1	3.7	3.4	3.1	2.9	2.8	2.6	1.7
Minimum DNI P90	**1830**	**1878**	**1899**	**1912**	**1921**	**1927**	**1932**	**1936**	**1940**	**1943**	**1962**

Misamfu | Years	**1**	**2**	**3**	**4**	**5**	**6**	**7**	**8**	**9**	**10**	**25**
Variability [±%]	6.5	4.6	3.7	3.2	2.9	2.6	2.4	2.3	2.2	2.0	1.3
Uncertainty P90 [±%]	8.3	5.8	4.8	4.1	3.7	3.4	3.1	2.9	2.8	2.6	1.7
Minimum DNI P90	**1617**	**1660**	**1679**	**1690**	**1698**	**1703**	**1708**	**1711**	**1714**	**1717**	**1734**

Mutanda | Years	**1**	**2**	**3**	**4**	**5**	**6**	**7**	**8**	**9**	**10**	**25**
Variability [±%]	6.3	4.5	3.6	3.2	2.8	2.6	2.4	2.2	2.1	2.0	1.3
Uncertainty P90 [±%]	8.1	5.7	4.7	4.0	3.6	3.3	3.1	2.9	2.7	2.6	1.6
Minimum DNI P90	**1613**	**1655**	**1673**	**1684**	**1692**	**1697**	**1701**	**1705**	**1708**	**1710**	**1727**

We can interpret the above Table 6.2 and 6.3 on the example of **Lusaka UNZA** site:

i. GHI interannual variability at P90 of 4.6% has to be considered for any single year at Lusaka UNZA site. In other words, assuming that the long-term average is 1996 kWh/m^2, it is expected (with 90% probability) that annual GHI exceeds, at any single year, the value of 1905 kWh/m^2.

ii. Within a period of three consecutive years, it is expected at P90 that annual average of GHI exceeds value of 1943 kWh/m^2;

iii. For a period of 25 years, it is expected at 90% probability that due to interannual variability the estimate of the long-term annual DNI average will deviate within the range of ±2.2% in Lusaka UNZA. Thus, assuming that the estimate of the long-term average is 1846 kWh/m^2, it can be expected at P90 that *due to variability of weather*, it should be at least 1805 kWh/m^2.

It is to be underlined that prediction of the future irradiation is based on the analysis of the recent historical data (period 1994 to 2017). Future weather changes may include man-induced or natural events such as volcano eruptions, which may have impact on this prediction.

Based on the existing scientific knowledge [23, 24], an effect of **extreme volcano eruptions**, with an emission of large amount of stratospheric aerosols, can be estimated on the example of Pinatubo event in 1991 (the second largest volcano eruption in 20th century). It can be expected that in such a case, the annual DNI in the affected year can decrease by approx. 16% or more, compared to the long-term average, still influencing another two consecutive years. In the same way, the volcano eruption of the comparable size may reduce long-term average estimate of DNI by about 4%. The decrease of GHI is much lower; the annual value in the particular year of eruption could be reduced by about 2% compared to the long-term average.

6.3 Combined uncertainty

In this Chapter, the combined uncertainty of the annual GHI and DNI values is quantified. Taking into account uncertainties of both types of data (satellite and ground measured), the combined effect of two components of the uncertainty of the site-adapted GHI and DNI values has to be considered.

1. **Uncertainty of the estimate** (U_{est}) of the annual solar resource values, which is ±4.0% for GHI and ±5.5% for DNI (Chapter 6.1);
2. **Interannual variability** (U_{var}) in any particular year, due to changing weather. In six Zambian sites, it varies from ±3.4% to ±4.6% for GHI and from ±8.1% to ±11.2% for DNI. The uncertainty due to weather variability decreases over the time with square root of the number of years (Chapter 6.2).

The two above-mentioned uncertainties combine in U_c (see Glossary), which represents a conservative expectation of the minimum GHI and DNI assuming various number of years N (Tables 6.4 and 6.5). Considering a simplified assumption of normal distribution of the annual values, probability of exceedance can be calculated at different confidence levels. GHI and DNI minimum annual values expected for combined uncertainty in any single year are shown on Figure 6.2 and 6.3.

Table 6.4 Combined probability of exceedance of annual GHI for uncertainty of the estimate ±4.0%.

Nr. of years	Uncertainty of estimate	Interanual variability	Combined uncertainty	Expected minimum | **Lusaka UNZA** [kWh/m^2]								
N	[±%]	N years [±%]	P90 [±%]	P01	P05	P10	P25	P50	P75	P90	P95	P99
1	4.0	4.6	6.1	2216	2151	2117	2060	1996	1932	1875	1840	1776
5	4.0	2.0	4.5	2159	2111	2086	2043	1996	1949	1906	1881	1833
10	4.0	1.4	4.3	2150	2105	2081	2041	1996	1951	1911	1887	1842
25	4.0	0.9	4.1	2145	2101	2078	2039	1996	1953	1914	1891	1847

Nr. of years	Uncertainty of estimate	Interanual variability	Combined uncertainty	Expected minimum | **Mount Makulu** [kWh/m^2]								
N	[±%]	N years [±%]	P90 [±%]	P01	P05	P10	P25	P50	P75	P90	P95	P99
1	4.0	4.2	5.8	2213	2151	2118	2063	2001	1940	1885	1852	1789
5	4.0	1.9	4.4	2162	2115	2090	2048	2001	1955	1913	1888	1841
10	4.0	1.3	4.2	2155	2110	2086	2046	2001	1957	1917	1893	1848
25	4.0	0.8	4.1	2150	2106	2083	2044	2001	1958	1920	1896	1853

Nr. of years	Uncertainty of estimate	Interanual variability	Combined uncertainty	Expected minimum | **Mochipapa** [kWh/m^2]								
N	[±%]	N years [±%]	P90 [±%]	P01	P05	P10	P25	P50	P75	P90	P95	P99
1	4.0	3.8	5.5	2246	2186	2154	2101	2041	1981	1928	1896	1836
5	4.0	1.7	4.4	2202	2155	2130	2088	2041	1994	1952	1927	1880
10	4.0	1.2	4.2	2196	2151	2126	2086	2041	1996	1956	1932	1886
25	4.0	0.8	4.1	2192	2148	2124	2085	2041	1997	1958	1934	1890

Nr. of years	Uncertainty of estimate	Interanual variability	Combined uncertainty	Expected minimum | **Longe** [kWh/m^2]								
N	[±%]	N years [±%]	P90 [±%]	P01	P05	P10	P25	P50	P75	P90	P95	P99
1	4.0	3.4	5.3	2275	2216	2185	2133	2076	2018	1966	1935	1877
5	4.0	1.5	4.3	2237	2190	2165	2123	2076	2029	1987	1961	1914
10	4.0	1.1	4.1	2232	2186	2162	2121	2076	2030	1990	1965	1919
25	4.0	0.7	4.1	2229	2184	2160	2120	2076	2031	1991	1968	1923

Nr. of years	Uncertainty of estimate	Interanual variability	Combined uncertainty	Expected minimum | **Misamfu** [kWh/m^2]								
N	[±%]	N years [±%]	P90 [±%]	P01	P05	P10	P25	P50	P75	P90	P95	P99
1	4.0	3.6	5.4	2260	2201	2170	2117	2059	2000	1948	1916	1857
5	4.0	1.6	4.3	2220	2173	2148	2106	2059	2012	1970	1945	1897
10	4.0	1.1	4.2	2214	2169	2144	2104	2059	2014	1973	1949	1903
25	4.0	0.7	4.1	2211	2166	2142	2103	2059	2015	1975	1951	1907

Nr. of years	Uncertainty of estimate	Interanual variability	Combined uncertainty	Expected minimum | **Mutanda** [kWh/m^2]								
N	[±%]	N years [±%]	P90 [±%]	P01	P05	P10	P25	P50	P75	P90	P95	P99
1	4.0	3.4	5.3	2167	2112	2082	2033	1978	1923	1874	1844	1789
5	4.0	1.5	4.3	2132	2087	2063	2022	1978	1933	1893	1869	1824
10	4.0	1.1	4.1	2127	2083	2060	2021	1978	1935	1896	1873	1829
25	4.0	0.7	4.1	2123	2081	2058	2020	1978	1936	1898	1875	1832

Table 6.5 Combined probability of exceedance of annual DNI for uncertainty of the estimate ±5.5%.

Nr. of years	Uncertainty of estimate	Interanual variability	Combined uncertainty	Expected minimum | **Lusaka UNZA** [kWh/m^2]								
N	[±%]	N years [±%]	P90 [±%]	P01	P05	P10	P25	P50	P75	P90	P95	P99
1	5.5	11.2	12.5	2263	2141	2076	1967	1846	1725	1616	1551	1428
5	5.5	5.0	7.4	2095	2022	1983	1918	1846	1774	1709	1670	1597
10	5.5	3.5	6.5	2065	2001	1967	1909	1846	1782	1725	1691	1627
25	5.5	2.2	5.9	2045	1987	1955	1904	1846	1788	1736	1705	1647

Nr. of years	Uncertainty of estimate	Interanual variability	Combined uncertainty	Expected minimum | **Mount Makulu** [kWh/m^2]								
N	[±%]	N years [±%]	P90 [±%]	P01	P05	P10	P25	P50	P75	P90	P95	P99
1	5.5	10.2	11.6	2253	2138	2077	1974	1861	1747	1644	1583	1468
5	5.5	4.6	7.2	2102	2032	1994	1931	1861	1791	1727	1690	1619
10	5.5	3.2	6.4	2076	2013	1979	1923	1861	1798	1742	1708	1645
25	5.5	2.0	5.9	2059	2001	1970	1918	1861	1803	1751	1720	1662

Nr. of years	Uncertainty of estimate	Interanual variability	Combined uncertainty	Expected minimum | **Mochipapa** [kWh/m^2]								
N	[±%]	N years [±%]	P90 [±%]	P01	P05	P10	P25	P50	P75	P90	P95	P99
1	5.5	9.8	11.2	2371	2253	2191	2086	1969	1853	1748	1686	1568
5	5.5	4.4	7.0	2221	2147	2108	2042	1969	1897	1831	1792	1718
10	5.5	3.1	6.3	2195	2129	2094	2035	1969	1904	1845	1810	1744
25	5.5	2.0	5.8	2178	2117	2084	2030	1969	1909	1854	1822	1761

Nr. of years	Uncertainty of estimate	Interanual variability	Combined uncertainty	Expected minimum | **Longe** [kWh/m^2]								
N	[±%]	N years [±%]	P90 [±%]	P01	P05	P10	P25	P50	P75	P90	P95	P99
1	5.5	8.3	10.0	2355	2250	2193	2099	1995	1890	1796	1740	1635
5	5.5	3.7	6.6	2235	2165	2127	2065	1995	1925	1863	1825	1755
10	5.5	2.6	6.1	2216	2151	2116	2059	1995	1931	1873	1839	1774
25	5.5	1.7	5.7	2203	2142	2110	2055	1995	1935	1880	1848	1787

Nr. of years	Uncertainty of estimate	Interanual variability	Combined uncertainty	Expected minimum | **Misamfu** [kWh/m^2]								
N	[±%]	N years [±%]	P90 [±%]	P01	P05	P10	P25	P50	P75	P90	P95	P99
1	5.5	8.3	9.9	2080	1987	1938	1855	1763	1671	1588	1538	1445
5	5.5	3.7	6.6	1975	1913	1880	1824	1763	1701	1646	1613	1551
10	5.5	2.6	6.1	1958	1901	1870	1819	1763	1706	1655	1625	1568
25	5.5	1.7	5.7	1947	1893	1864	1816	1763	1709	1662	1633	1579

Nr. of years	Uncertainty of estimate	Interanual variability	Combined uncertainty	Expected minimum | **Mutanda** [kWh/m^2]								
N	[±%]	N years [±%]	P90 [±%]	P01	P05	P10	P25	P50	P75	P90	P95	P99
1	5.5	8.1	9.8	2066	1975	1927	1845	1755	1665	1583	1535	1444
5	5.5	3.6	6.6	1965	1903	1871	1816	1755	1694	1640	1607	1545
10	5.5	2.6	6.1	1948	1892	1861	1811	1755	1699	1649	1618	1562
25	5.5	1.6	5.7	1938	1884	1856	1808	1755	1702	1654	1626	1572

This analysis is based on the data representing a history of year 1994 to 2017, and on the expert extrapolation of the related weather variability. This report may not reflect possible man-induced climate change or occurrence of extreme events such as large volcano eruptions in the future (see the last paragraph in Chapter 6.2).

Graphical visualisation of Tables 6.4 and 6.5 on the example of Lusaka UNZA site is shown in Figures 6.1 and 6.2, where the expected probabilities of exceedance (different Pxx scenarios) are drawn on the cumulative distribution curve showing yearly GHI and DNI values.

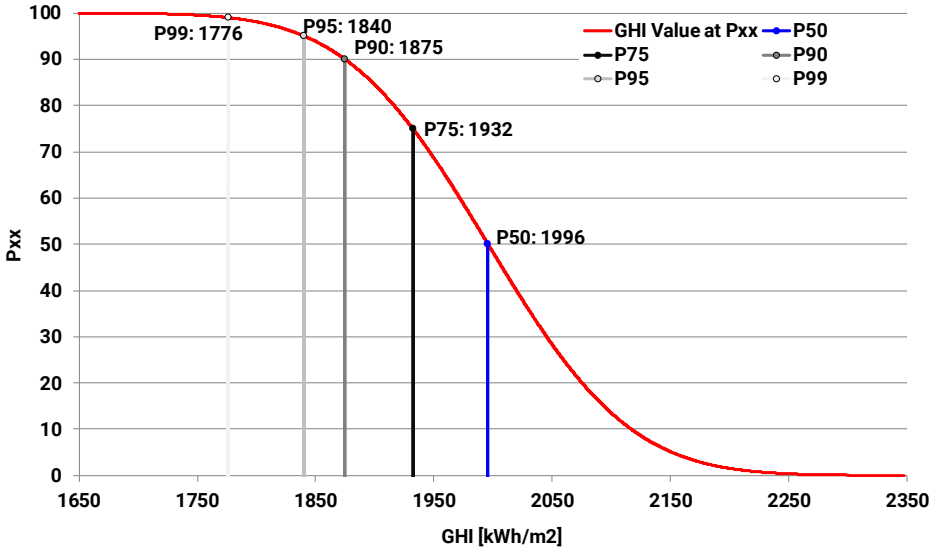

Figure 6.1: Expected Pxx values for GHI at Lusaka UNZA site

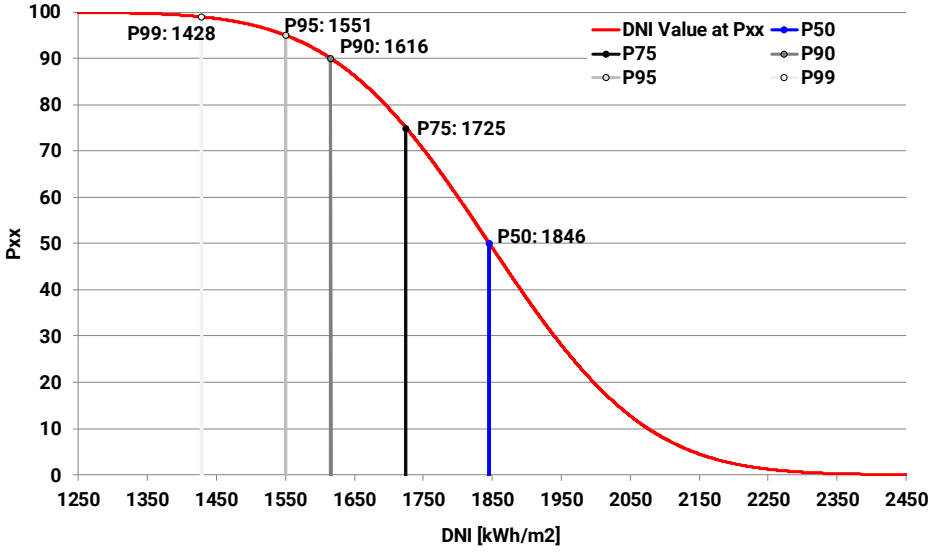

Figure 6.2: Expected Pxx values for DNI at Lusaka UNZA site

7 TIME SERIES AND TYPICAL METEOROLOGICAL YEAR DATA

7.1 Delivered data sets

This report is accompanied by data sets delivered individually for position of each of six solar meteorological stations in Zambia. The data include (Tables 7.1 and 7.2):

- Solar and meteorological measurements, after second level quality assessment (first level was delivered by GeoSUN Africa) representing minimum of 24 months of the measuring campaign;
- Time series, representing last 24+ years;
- Typical Meteorological Year data, representing last 24 years.

The data is delivered in formats ready to use in energy simulation software. This report provides detailed insight of the methodologies and results.

Table 7.1 Delivered data characteristics

Feature	Time coverage	Primary time step	Delivered files
Ground measurements (GeoSUN Africa)	Nov 2015 to Dec 2017	1 minute	Quality controlled measurements 1- minute time step
Model data original model (Solargis)	Jan 1994 to Dec 2017	15 minutes	Time series – hourly Time series – monthly Time series – yearly
Model data site adapted model (Solargis)	Jan 1994 to Dec 2017	15 minutes	Time series – hourly Time series – monthly Time series – yearly
Model data site adapted model (Solargis)	Jan 1994 to Dec 2017	hourly	Typical Meteorological Year P50 Typical Meteorological Year P90

Table 7.2 Parameters in the delivered site-adapted time series and TMY data (hourly time step)

Parameter	Acronym	Unit	Time series	TMY P50	TMY P90
Global horizontal irradiance	GHI	W/m^2	X	X	X
Direct normal irradiance	DNI	W/m^2	X	X	X
Diffuse horizontal irradiance	DIF	W/m^2	X	X	X
Global tilted irradiance (at optimum angle)	GTI	W/m^2	X	-	-
Solar azimuth	SA	°	X	X	X
Solar elevation	SE	°	X	X	X
Air temperature at 2 metres	TEMP	°C	X	X	X
Wind speed at 10 metres	WS	m/s	X	X	X
Wind direction at 10 metres	WD	°	X	X	X
Relative humidity	RH	%	X	X	X
Air Pressure	AP	hPa	X	X	X
Precipitable Water	PWAT	kg/m^2	X	X	X

7.2 TMY method

The Typical Meteorological Year (TMY) data sets are delivered, together with Solargis time series data and this report. TMY contains hourly data derived from the time series covering complete 24 years (1994 to 2017). The data history of 24 years is compressed into one year (Figure 7.1 to 7.4) following two criteria:

- Minimum difference between statistical characteristics (annual average, monthly averages) of TMY and long-term time series. This criterion is given about 80% weighting.
- Maximum similarity of monthly Cumulative Distribution Functions (CDF) of TMY and full-time series, so that occurrence of typical hourly values is well represented for each month. This criterion is given about 20% weighting.

TMY P50 data set is constructed on the monthly basis. For each month, the long-term average monthly value and cumulative distribution for each parameter is calculated: Direct Normal Irradiance (DNI), Global Horizontal Irradiance (GHI), Diffuse Horizontal Irradiance (DIF) and Air Temperature (TEMP). Following the monthly data for each individual year from the set of 24 years are compared to the long-term parameters. The monthly data from the year, which resembles the long-term parameters more closely, is selected. The procedure is repeated for all 12 months, and the TMY is constructed by concatenating the selected months into one artificial (but representative) year.

The method for calculation **P90** data set is based on the TMY P50 method. It has been modified in a way of how a candidate month is selected. The search for set of twelve candidates is repeated in iteration until a condition of minimization of difference between annual P90 value and annual average of new TMY is reached (instead of minimization of differences in monthly means and CDFs, as applied in P50 case). Once the selection converges to minimum difference, the TMY is created by concatenation of selected months. The P90 annual values are calculated for each confidence limit – from the combined uncertainty of estimate and inter-annual variability, which can occur in any year (Chapter 6.3).

To derive TMY that fits specific needs of the selected energy application the different weights are given to individual parameters – thus highlighting important properties. In solar energy applications, the higher importance is given to GHI and DNI. In assembling TMY P50, the values of DNI, GHI, DIF and TEMP are only considered, where the weights are set as follows: 0.9 is given to DNI, 0.3 to GHI, 0.02 to diffuse horizontal irradiance, and 0.07 to air temperature (divided by the total of 1.29).

To derive solar resource parameters with the **hourly time step**, the original satellite data with time resolution of 15-minutes are aggregated by time integration. The meteorological parameters are available in the original 1-hourly time step. The TMY datasets were constructed from solar radiation and meteorological data (Chapters 4 and 5). Time zone was adjusted to Central Africa Time CAT (UTC +02:00).

More about the Solargis TMY method in [25].

7.3 Results

Two data sets are derived from the Solargis historical time series for the six sites: P50 and P90. In graphs and tables below we show the values for the example of Lusaka UNZA meteorological site.

Important note: Due to the inherent features of the underlying methods, monthly values in TMY data set in Tables 7.3 to 7.6 do not fit to the values generated from full time series (Figures 7.1 to 7.4).

Table 7.3 Monthly and yearly long-term GHI averages as calculated from time series and from TMY representing P50, and P90 cases at Lusaka UNZA site

Global Horizontal Irradiation [kWh/m²]	1	2	3	4	5	6	7	8	9	10	11	12	Year
Time series (24 years)	161	144	159	156	158	140	150	175	193	206	183	172	**1996**
TMY for P50 case	163	145	155	157	156	139	150	176	193	207	182	173	**1996**
TMY for P90 case	130	103	145	153	157	139	149	172	189	203	181	154	**1875**

Table 7.4 Monthly and yearly long-term DNI averages as calculated from time series and from TMY representing P50, and P90 cases at Lusaka UNZA site

Direct Normal Irradiation [kWh/m²]	1	2	3	4	5	6	7	8	9	10	11	12	Year
Time series (24 years)	94	89	115	158	204	188	191	194	181	177	141	113	**1846**
TMY for P50 case	92	89	112	162	202	188	191	192	183	179	144	111	**1846**
TMY for P90 case	56	32	78	155	202	186	180	182	176	162	128	81	**1616**

Table 7.5 Monthly and yearly long-term DIF averages as calculated from time series and from TMY representing P50, and P90 cases at Lusaka UNZA site

Diffused Horizontal Irradiation [kWh/m²]	1	2	3	4	5	6	7	8	9	10	11	12	Year
Time series (24 years)	88	75	75	52	35	32	36	47	60	70	74	84	**729**
TMY for P50 case	90	74	74	52	34	32	36	48	60	70	71	86	**728**
TMY for P90 case	85	76	83	51	32	31	40	49	59	75	79	90	**751**

Table 7.6 Monthly and yearly long-term TEMP averages as calculated from time series and from TMY representing P50, and P90 cases at Lusaka UNZA site

Air temperature [°C]	1	2	3	4	5	6	7	8	9	10	11	12	Year
Time series (24 years)	19.9	19.5	19.1	17.9	15.9	14.0	13.6	16.4	20.2	22.6	22.8	20.8	**18.6**
TMY for P50 case	19.3	19.3	20.2	17.0	15.5	13.3	15.0	16.6	20.2	22.3	23.6	21.7	**18.7**
TMY for P90 case	18.3	18.3	18.1	16.2	15.9	13.4	12.8	15.8	19.5	23.1	22.6	20.6	**17.9**

As an example of interpretation of the tables above, the TMY P50 and P90 data can be described as follows:

1. **P50 TMY** data set represents, for each month, the average climate conditions and the most representative cumulative distribution function, therefore extreme situations (e.g. extremely cloudy weather) are not represented in this dataset. The long-term annual summary of GHI and DNI are considered as the most critical parameters to consider, and in this data set P50 **GHI value is 1996 kWh/m²** and **DNI value is 1846 kWh/m².**
2. **P90 TMY** data set represents for each month the climate conditions, which after summarization GHI and DNI for the whole year results in the value *equal or close to P90* derived by the analysis of uncertainty of the estimate and of the interannual variability for any single year (Chapter 6.3). Thus, TMY for P90 represents generally a conservative estimate, i.e. a year with the long-term value of **GHI of 1875 kWh/m²** and **DNI of 1616 kWh/m²**.

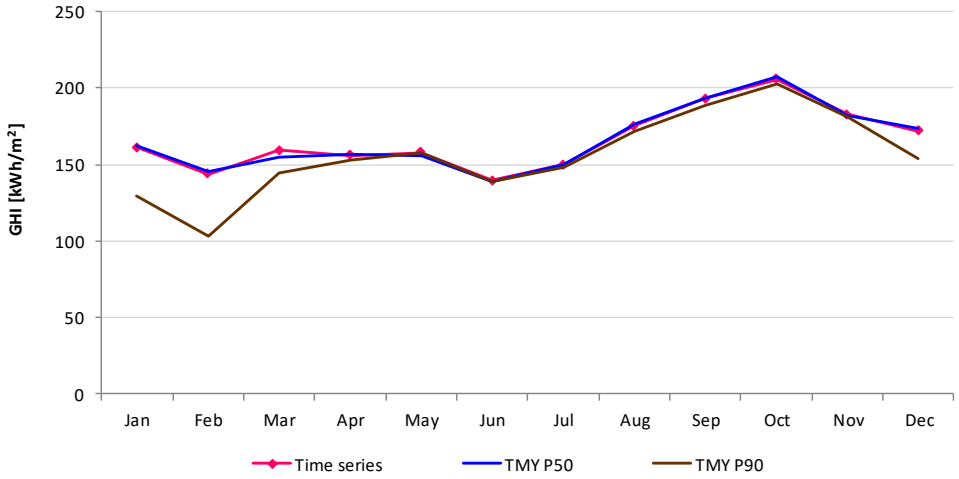

Figure 7.1: GHI monthly values derived from time series and TMY P50 and P90 at Lusaka UNZA site.

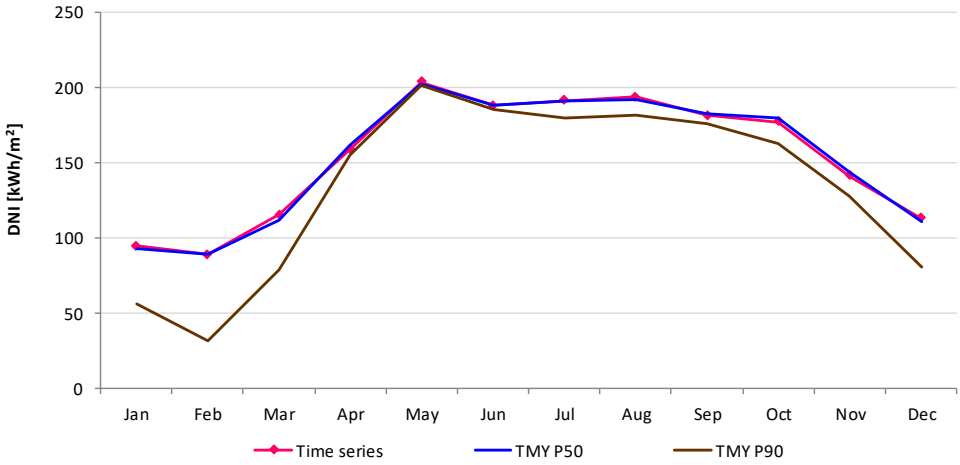

Figure 7.2: DNI monthly values derived from time series and TMY P50 and P90 at Lusaka UNZA site.

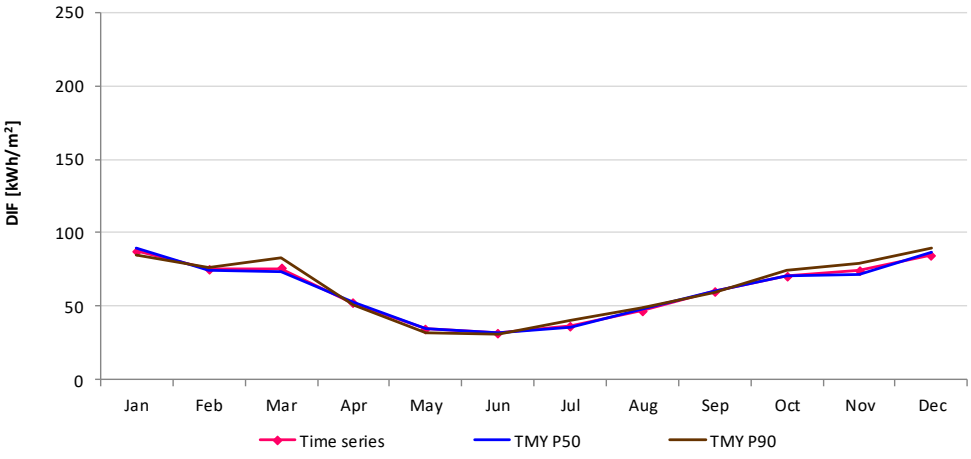

Figure 7.3: DIF monthly values derived from time series and TMY P50 and P90 at Lusaka UNZA site.

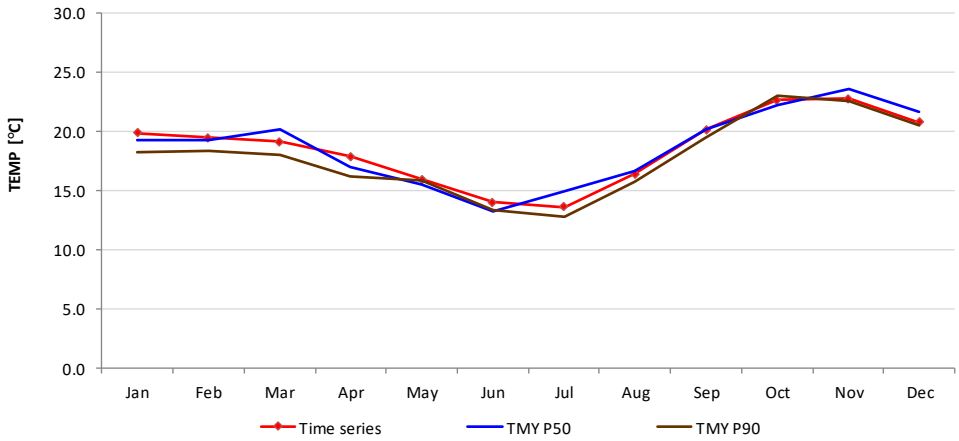

Figure 7.4: TEMP monthly values derived from time series and TMY P50 and P90 at Lusaka UNZA site

It is important to note that the data reduction in the TMY data set is not possible without loss of information contained in the original multiyear time series. Therefore, **time series data are considered as the most accurate reference suitable for the statistical analysis of solar resource and meteorological parameters of the site.**

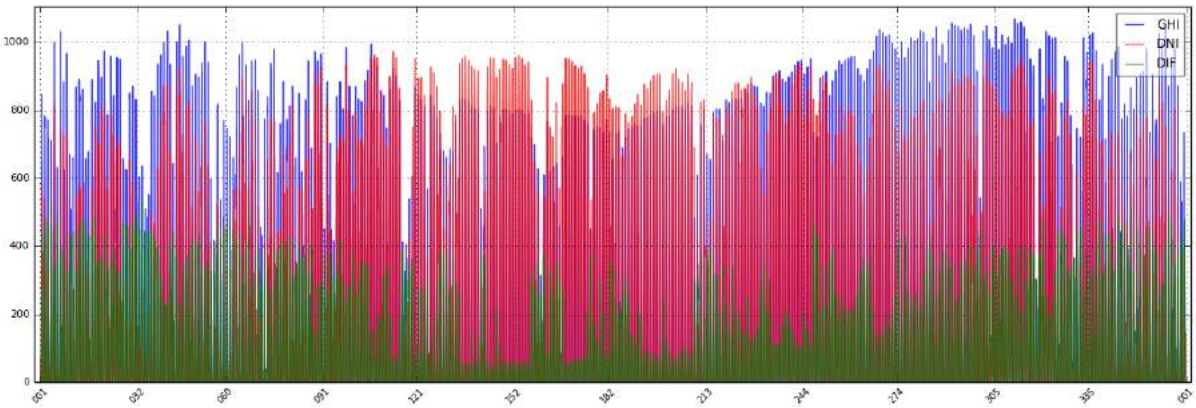

Figure 7.5: Seasonal profile of GHI, DNI and DIF for Typical Meteorological Year P50 Lusaka UNZA site: X-axis – day of the year; Y-axis – solar irradiance W/m^2

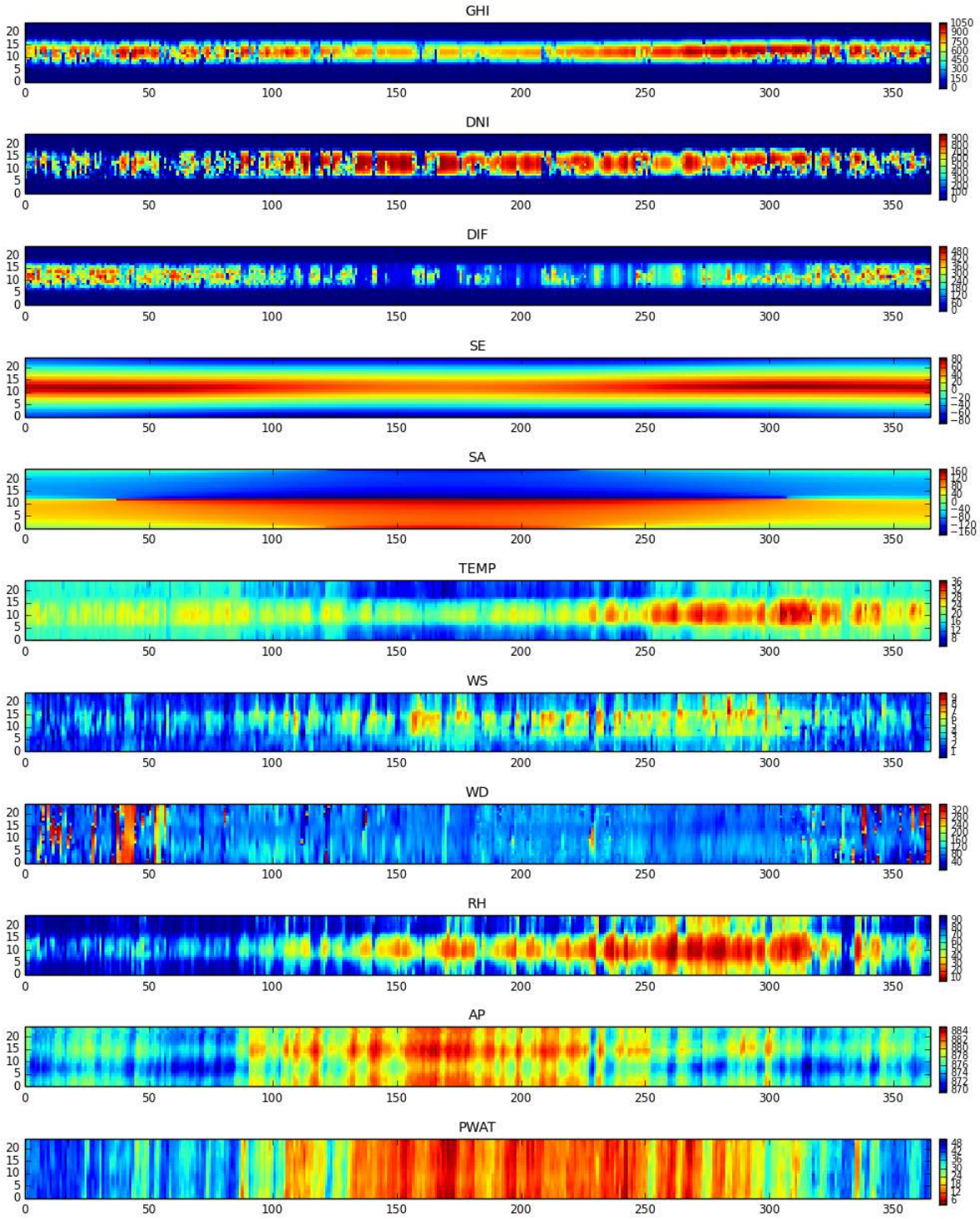

Figure 7.6: Snapshot of Typical Meteorological Year for P50 for Lusaka UNZA site

8 CONCLUSIONS

This report accompanies delivery of measured solar resource and meteorological data for six sites where solar meteorological stations have been installed during November 2015 and operated for a period of 25 months until December 2017. The measured data is a result of systematic work on (i) setting up a network of solar meteorological stations with high-standard equipment and on (ii) implementation of rigorous practices in operation and maintenance of solar equipment.

Well-linked to this infrastructure is satellite-based solar radiation model Solargis, which has proven quality and reliability of time series and derived site-specific data products. The measured data is used in site-adaptation of the Solargis model. As a result, reliable Solargis historical time series and TMY data is computed for six specific sites, and provided in formats ready to use in standard photovoltaic energy simulation software. The site adapted Solargis data prepared for six sites is also part of the delivery.

Role of solar measuring stations in maintaining sustainable solar data infrastructure

Receiving data from a number of high quality measuring stations enables an improved understanding of the geographical and temporal variability of solar resource in Zambia and a wider region. Even though the model adaptation reduced its uncertainty, it is important to maintain the operation of the solar meteorological stations, with special focus on the following cases:

- For new sites, relevant to any larger solar power project, it is important to set-up and operate a solar meteorological station to reduce uncertainty to an achievable minimum of the site-specific **long-term estimates.**
- For existing six sites in Zambia, the meteorological stations together with satellite data make it possible to maintain high quality and bankability of solar resource and meteorological data for sustainable **performance assessment** of solar power plants in the region.
- Keeping solar measuring stations is of strategic importance to maintain quality of satellite models and of solar power **forecasts** in future.

Reduced uncertainty of Solargis model

The uncertainty of the Solargis model for site-specific estimates has been reduced from the original range of ±12% to ±18% for **DNI** yearly values to approximately ±5.5% for accuracy-enhanced values. For site-specific yearly **GHI** estimates, the uncertainty reduction is seen from the original range of ±7.5% to ±10% to approximately ±4.0% for the accuracy-enhanced values.

Besides reducing systematic deviation (bias), the model adaptation for sites also results in the improvement of other data quality indicators such as reducing random deviation (measurable by Root Mean Square Deviation) and by improving the probability distribution of hourly values (measurable by Kolmogorov-Smirnoff Index). Higher-quality DNI and GHI data have substantial benefits in energy simulation, which can in turn be used for more reliable financial predictions.

ANNEX 1: SITE RELATED DATA STATISTICS

Yearly summaries of solar and meteorological parameters

Statistics for site-adapted Solargis model yearly values representing 24 years (1994 to 2017).

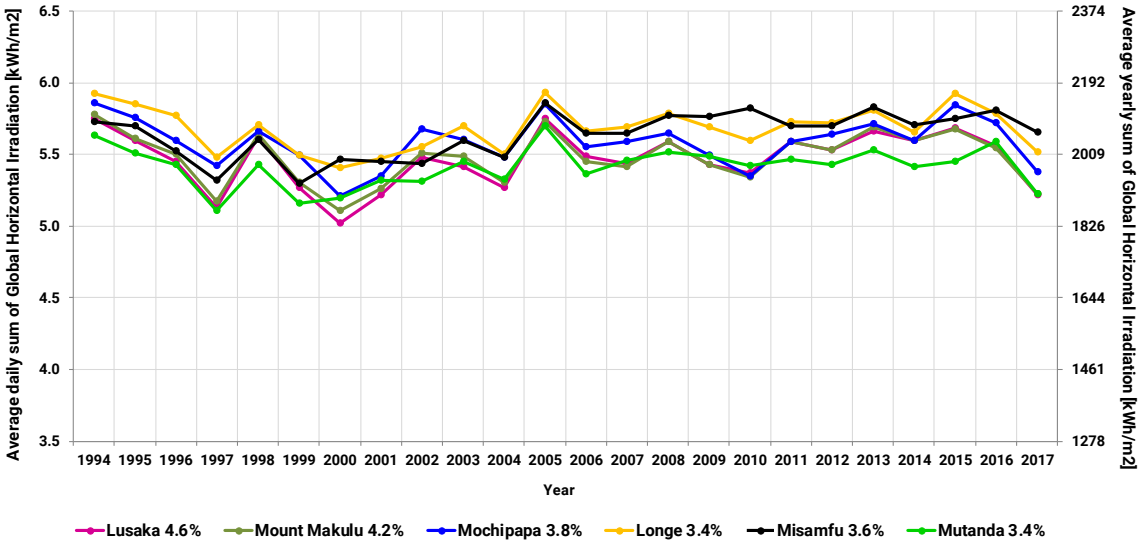

Figure I: Interannual variability of site-adapted yearly GHI [kWh/m^2].
Annual average (*avg*, solid line) and standard deviation (value behind the names of sites).

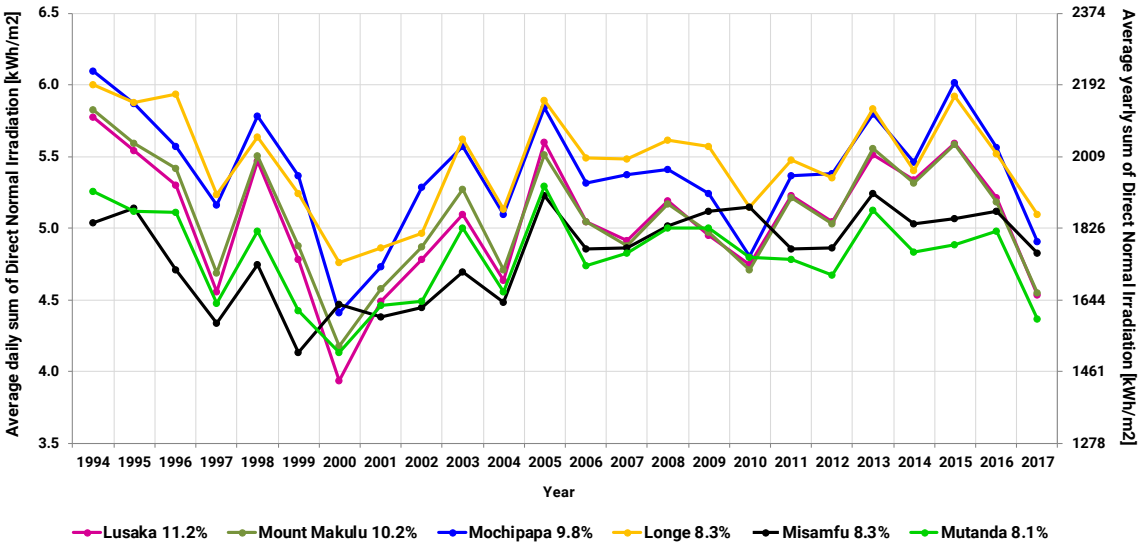

Figure II: Interannual variability of site-adapted yearly DNI [kWh/m^2].
Annual average (*avg*, solid line) and standard deviation (value behind the names of sites).

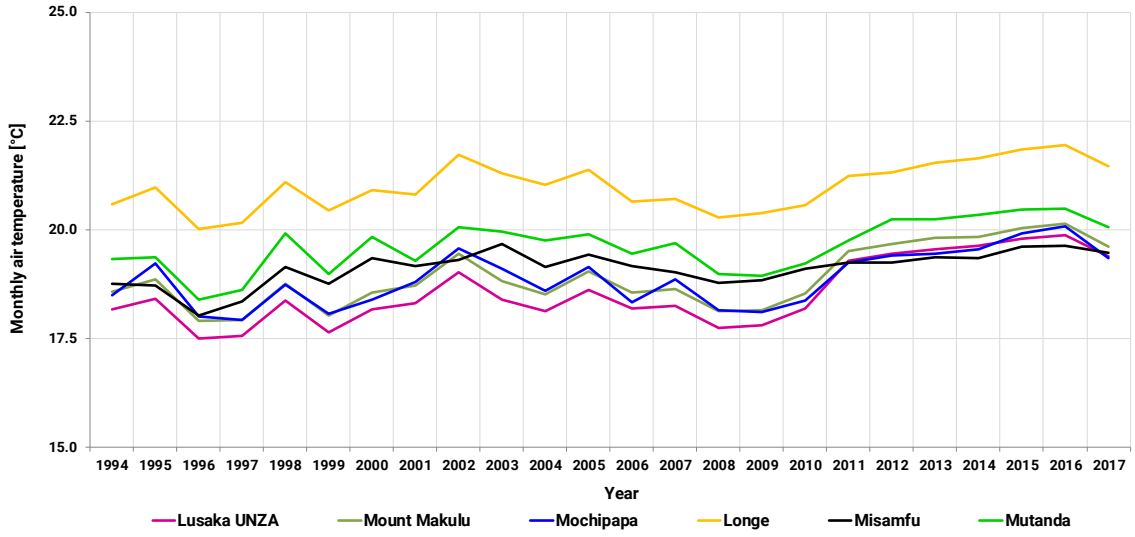

Figure III: Interannual variability of yearly TEMP [°C].
Annual average (*avg*, solid line).

Monthly summaries of solar and meteorological parameters

The graphs compare monthly site-adapted time series from Solargis model compared to long-term averages for a historical period 1994 to 2017.

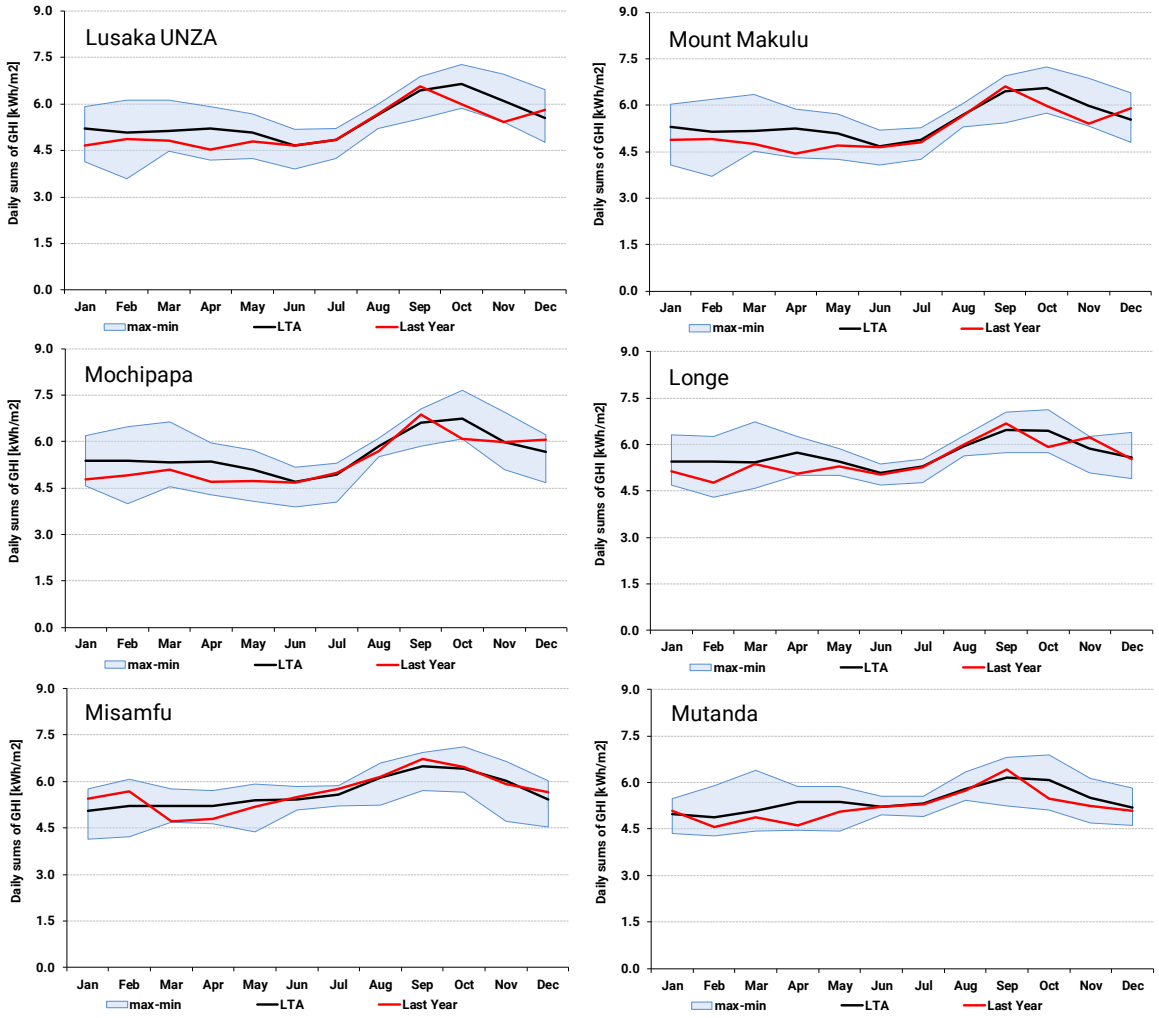

Figure IV: GHI monthly averages [kWh/m^2].
Monthly average shown as solid line; min/max monthly values as boundary lines; last 12 months in red.

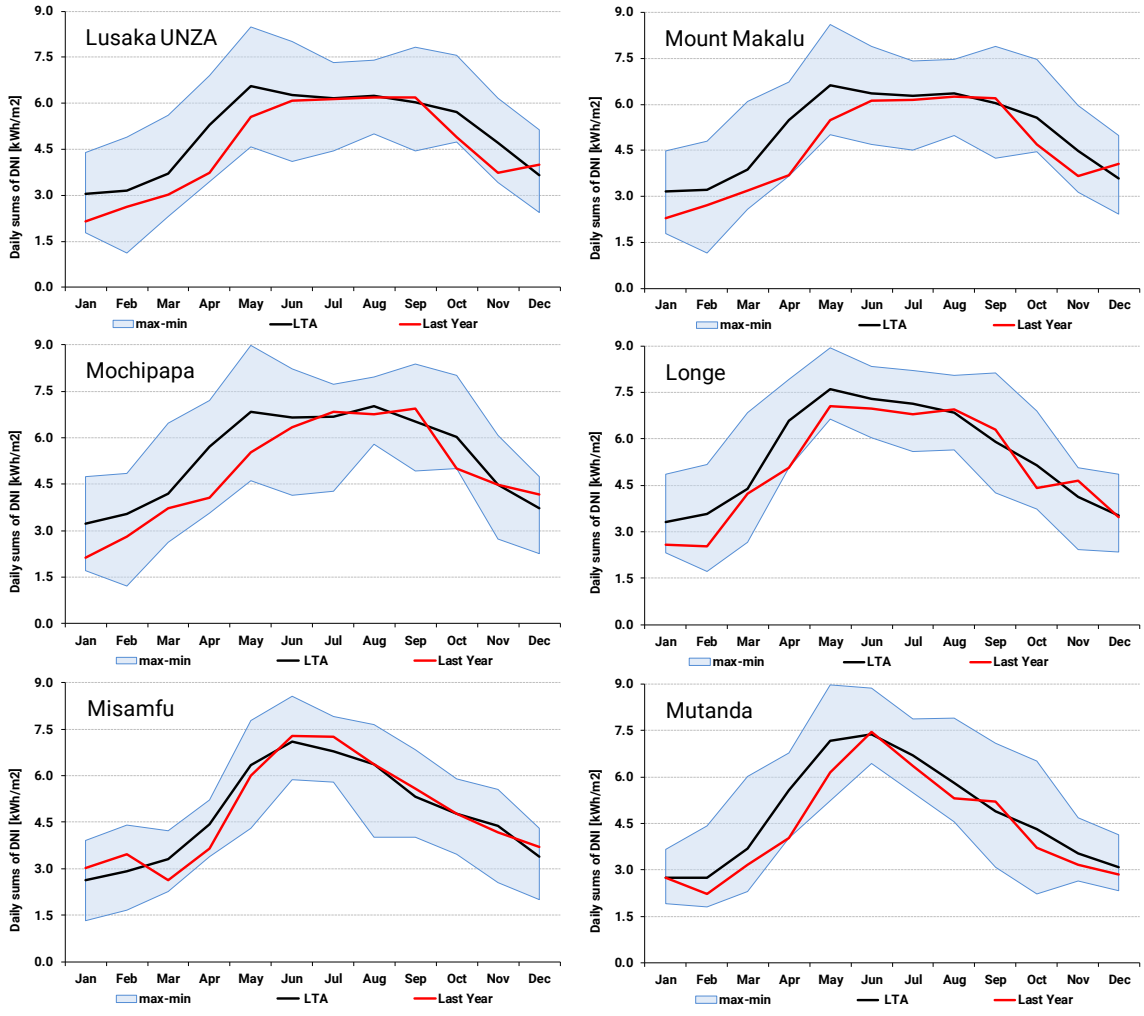

Figure V: DNI monthly averages [kWh/m^2].
Monthly average shown as solid line; min/max monthly values as boundary lines; last 12 months shown in red.

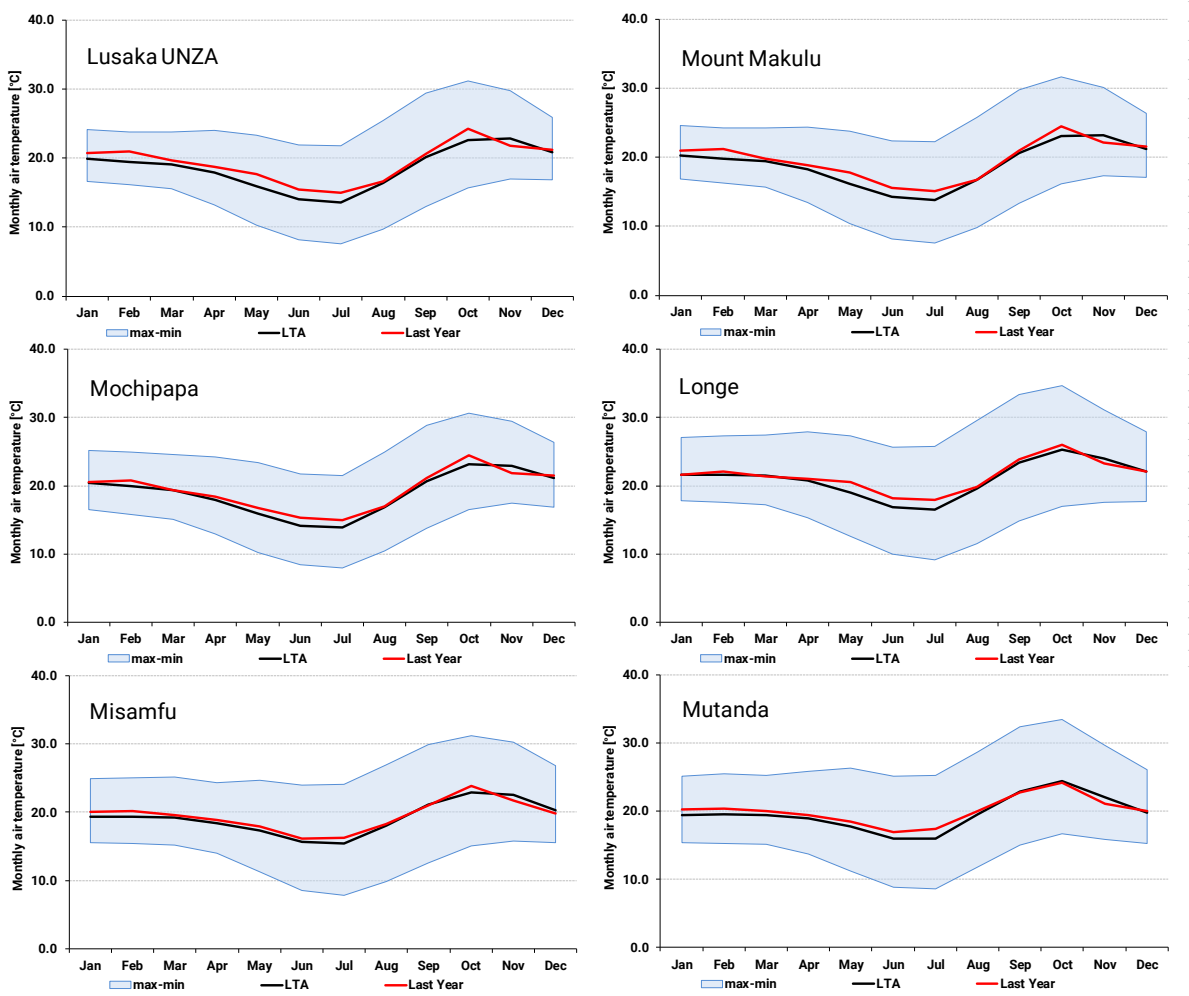

Figure VI: TEMP monthly averages [°C].
Monthly average shown as solid line; min/max monthly values as boundary lines; last 12 months shown in red.

Frequency of occurrence of GHI and DNI daily model values for a period 1994 to 2017

The histograms below show occurrence statistics of daily values derived from the satellite-based site-adapted time series – GHI and DNI parameters. The time covered in the graphs below is 24 complete calendar years (1994 to 2017). The occurrence is calculated separately for each month.

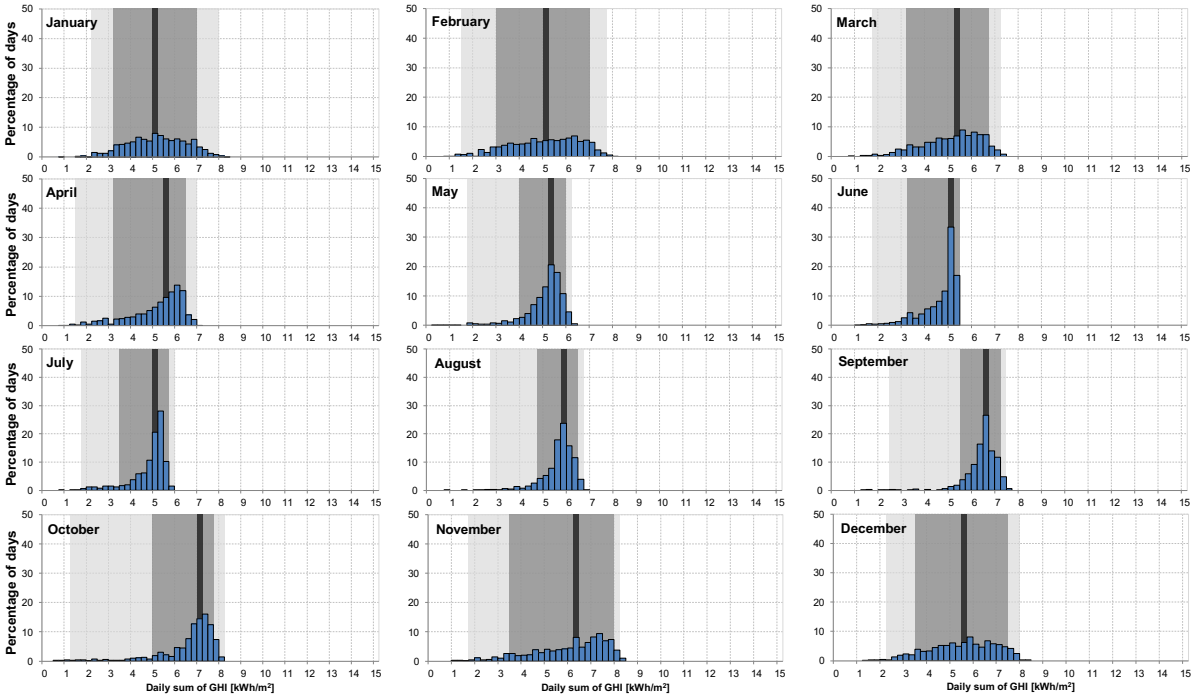

Figure VII: Histograms of daily summaries of Global Horizontal Irradiation in Lusaka UNZA.

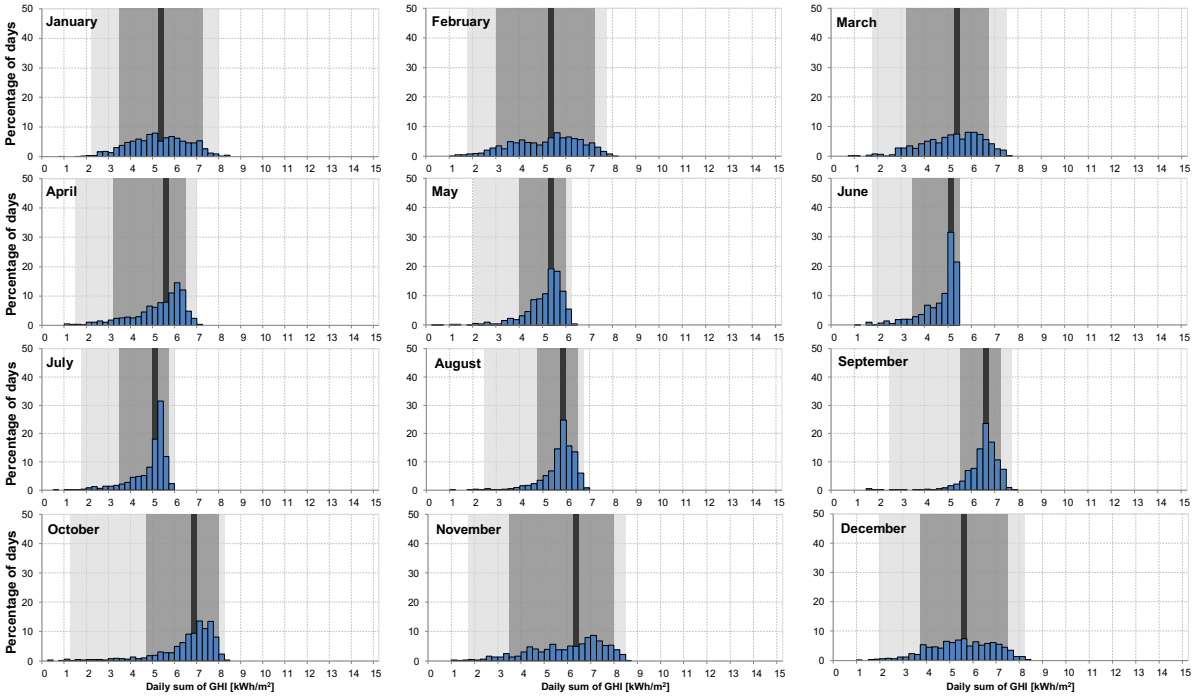

Figure VIII: Histograms of daily summaries of Global Horizontal Irradiation in Mount Makulu.

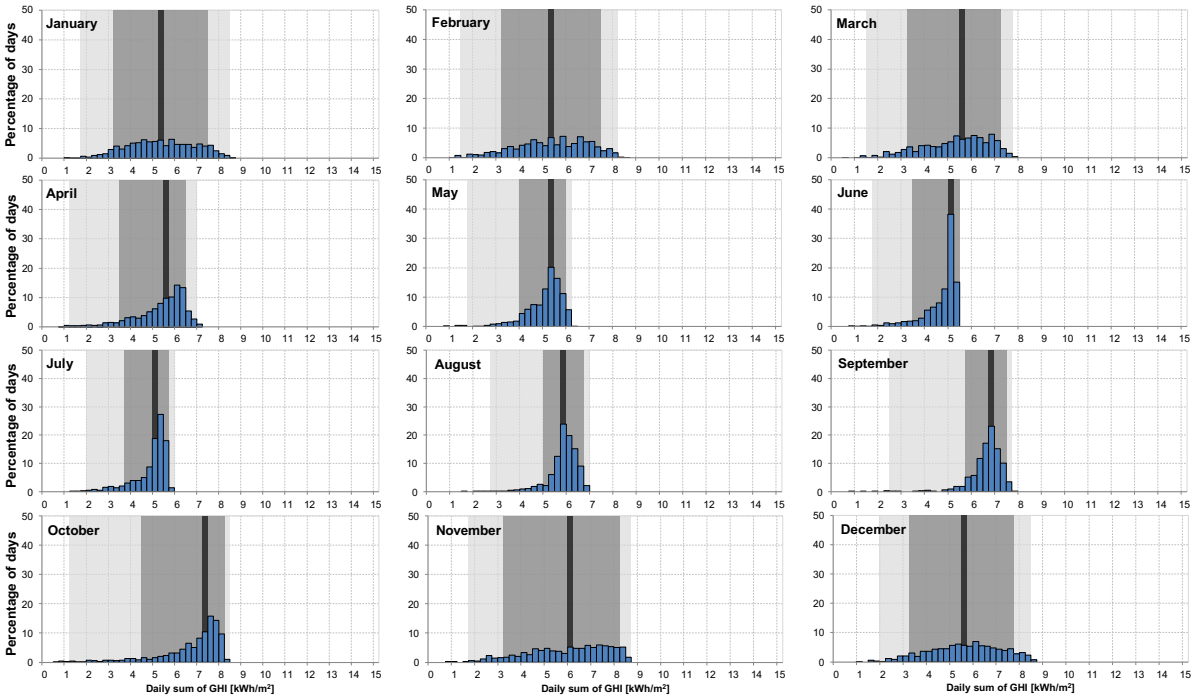

Figure IX: Histograms of daily summaries of Global Horizontal Irradiation in Mochipapa.

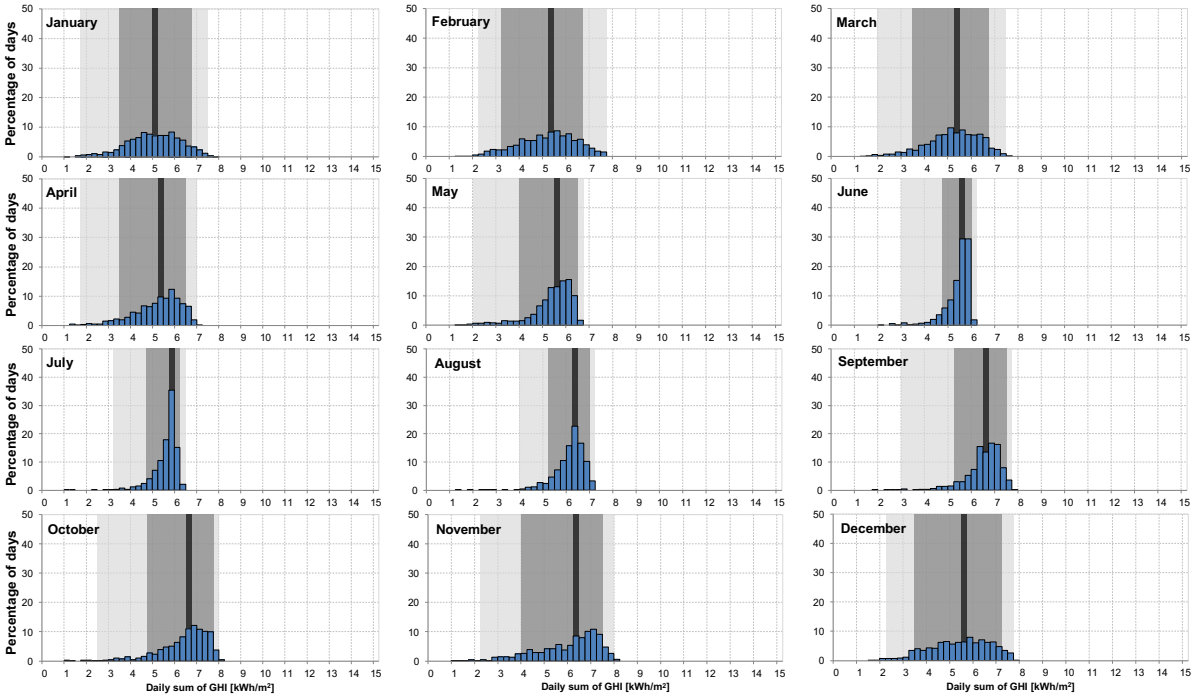

Figure X: Histograms of daily summaries of Global Horizontal Irradiation in Longe.

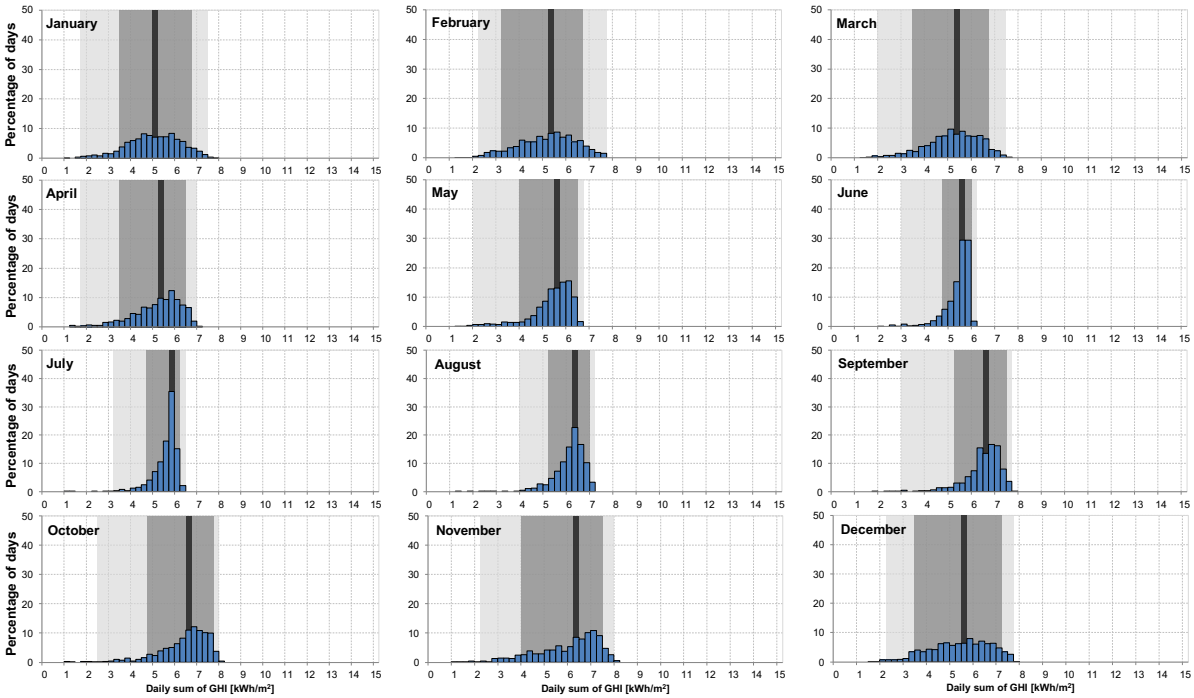

Figure XI: Histograms of daily summaries of Global Horizontal Irradiation in Misamfu.

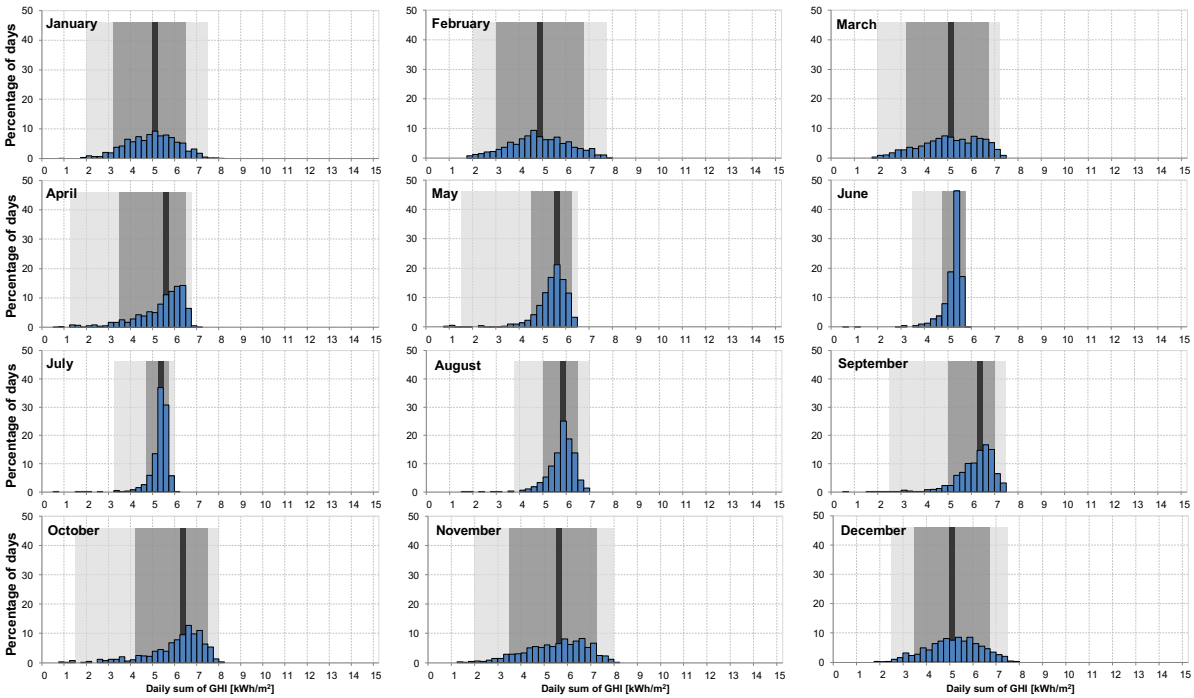

Figure XII: Histograms of daily summaries of Global Horizontal Irradiation in Mutanda.

Figures VII to XII show histograms of **daily GHI** summaries for each month as calculated from Solargis time series representing the years 1994 to 2017. The distribution of daily values is not symmetric: median is drawn by the vertical line, and percentiles P_{10}, P_{25}, and P_{75}, and P_{90} are displayed with dark grey and light grey colour bands, respectively. The percentiles P_{10} and P_{90} show 80% occurrence of daily values within each month and percentiles P_{25} and P_{75} show 50% occurrence.

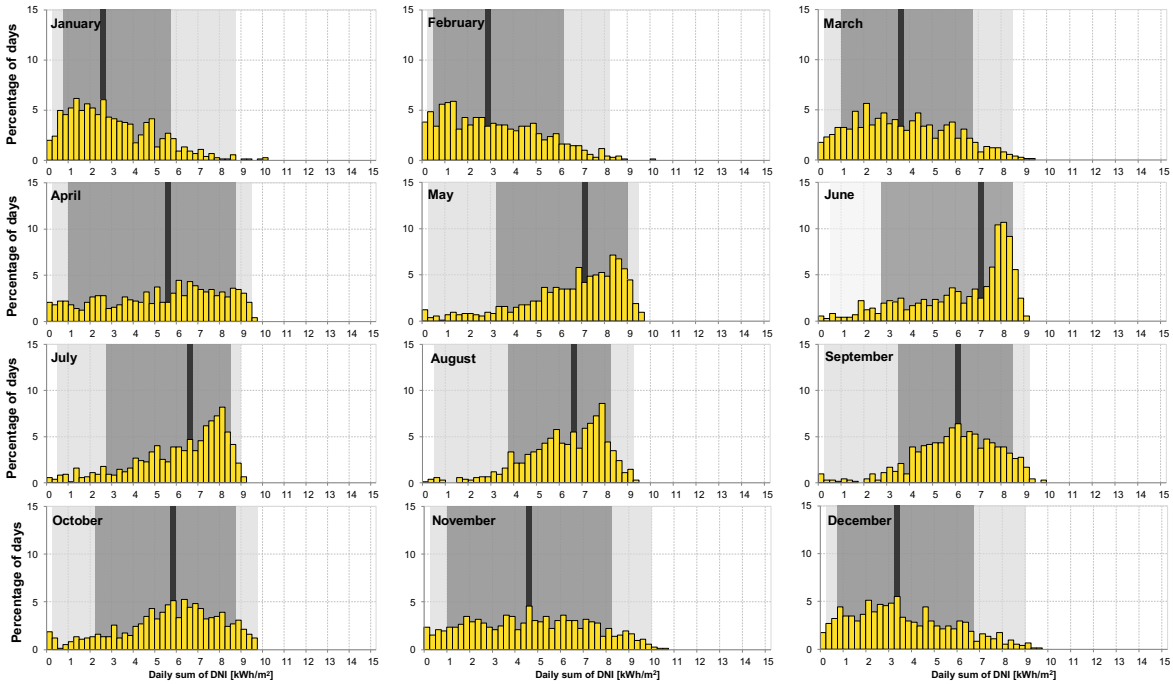

Figure XIII: Histograms of daily summaries of Direct Normal Irradiation in Lusaka UNZA.

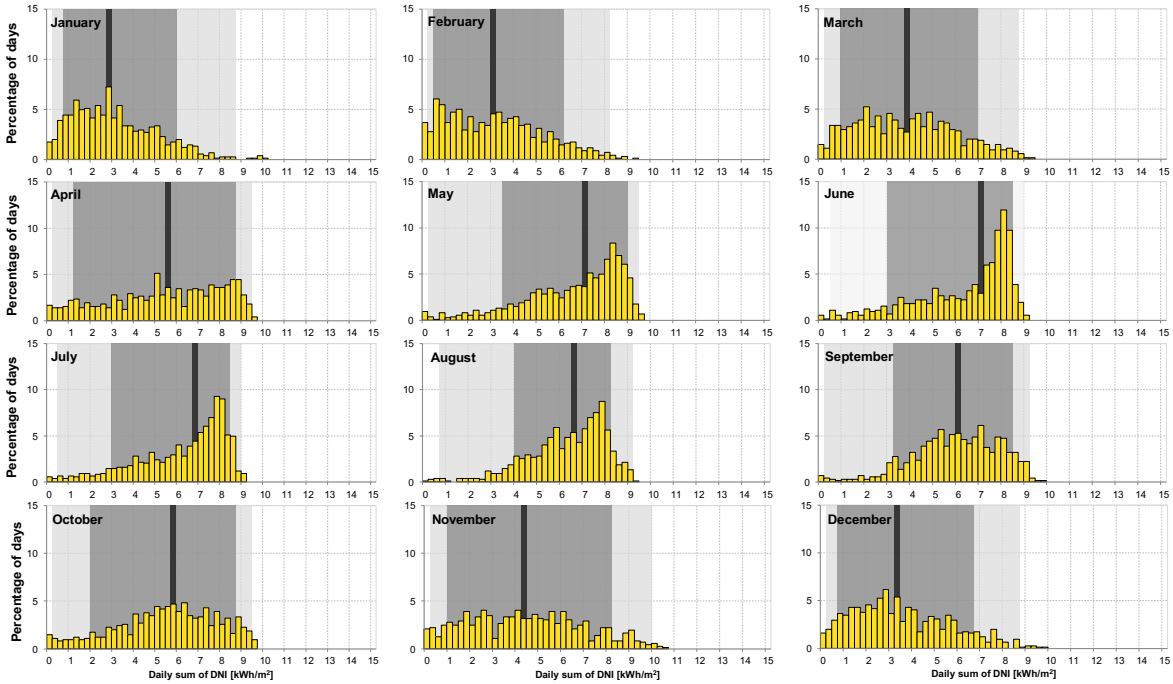

Figure XIV: Histograms of daily summaries of Direct Normal Irradiation in Mount Makulu.

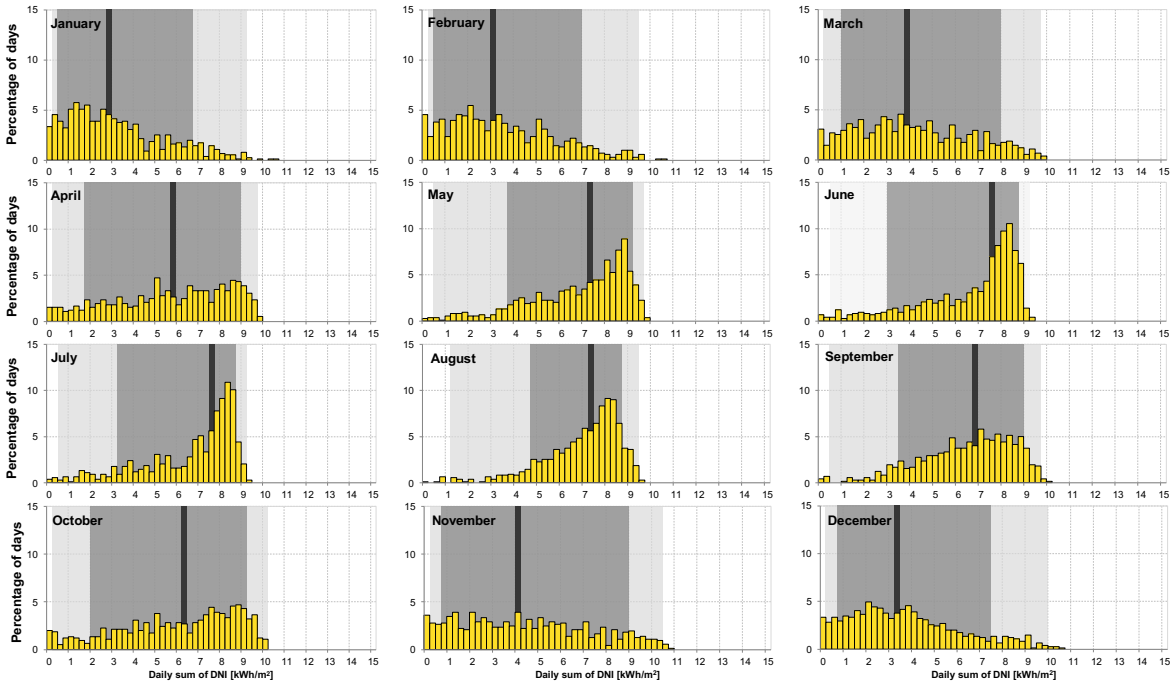

Figure XV: Histograms of daily summaries of Direct Normal Irradiation in Mochipapa.

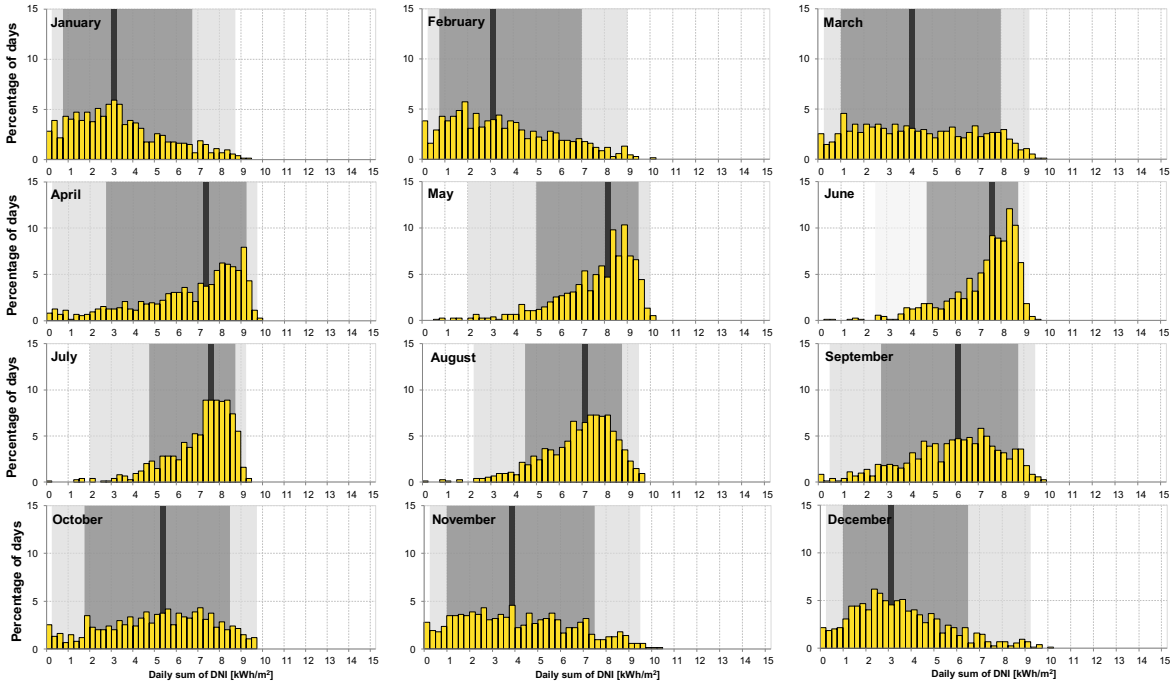

Figure XVI: Histograms of daily summaries of Direct Normal Irradiation in Longe.

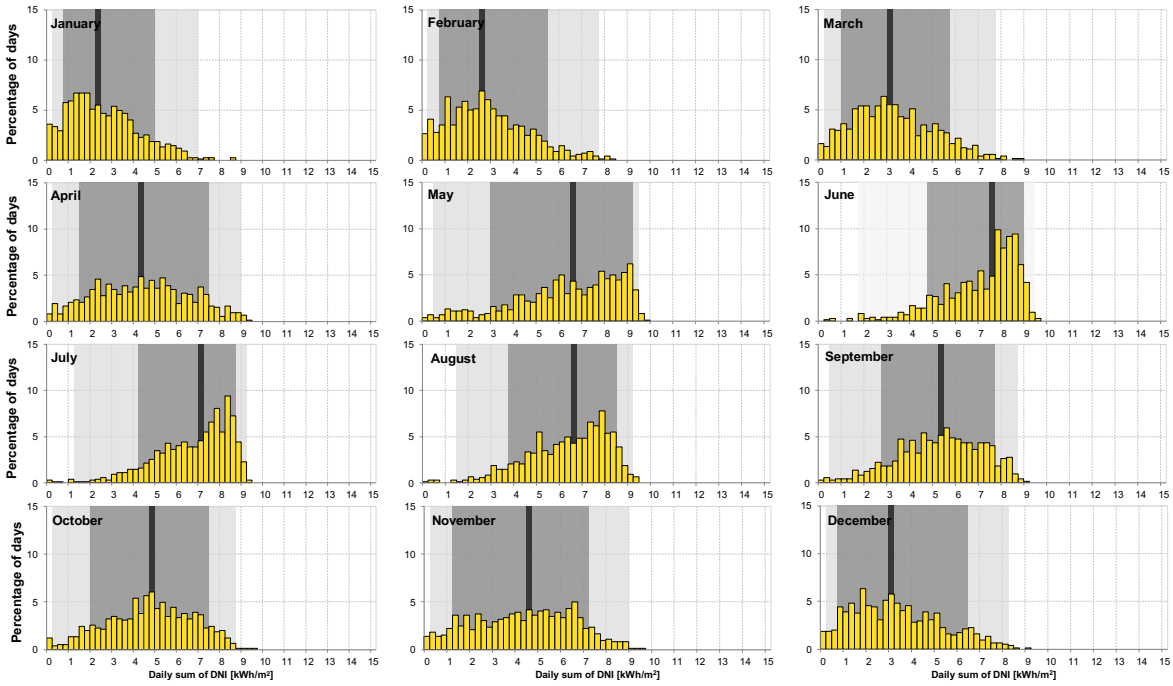

Figure XVII: Histograms of daily summaries of Direct Normal Irradiation in Misamfu.

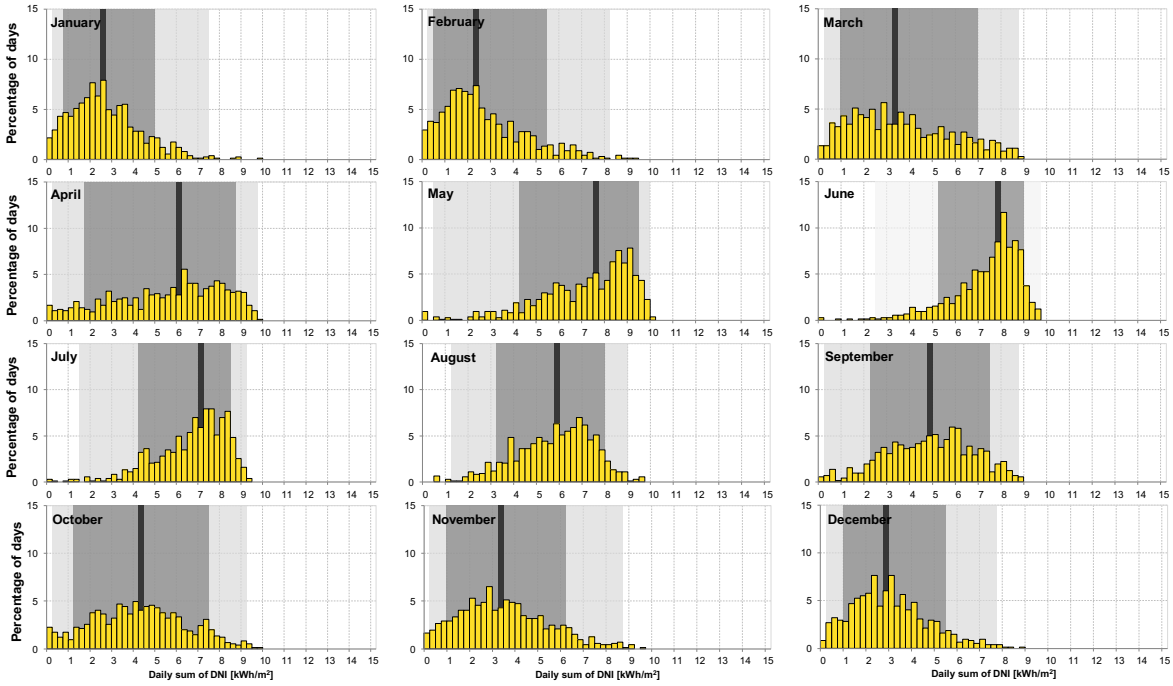

Figure XVIII: Histograms of daily summaries of Direct Normal Irradiation in Mutanda.

Figures XIII to XVIII show histograms of **daily DNI** summaries for each month as calculated from Solargis time series representing the years 1994 to 2017. The distribution of daily values is not symmetric: median is drawn by the vertical line, and percentiles P_{10}, P_{25}, and P_{75}, and P_{90} are displayed with dark grey and light grey colour bands, respectively. The percentiles P_{10} and P_{90} show 80% occurrence of daily values within each month and percentiles P_{25} and P_{75} show 50% occurrence.

Frequency of occurrence of GHI and DNI 15-minute model values for a period 1994 to 2017

The histograms below show occurrence statistics of 15-minute values derived from the satellite-based site-adapted time series – GHI and DNI parameters. The time covered in the graphs below is 24 complete calendar years (1994 to 2017). The occurrence is calculated separately for each month.

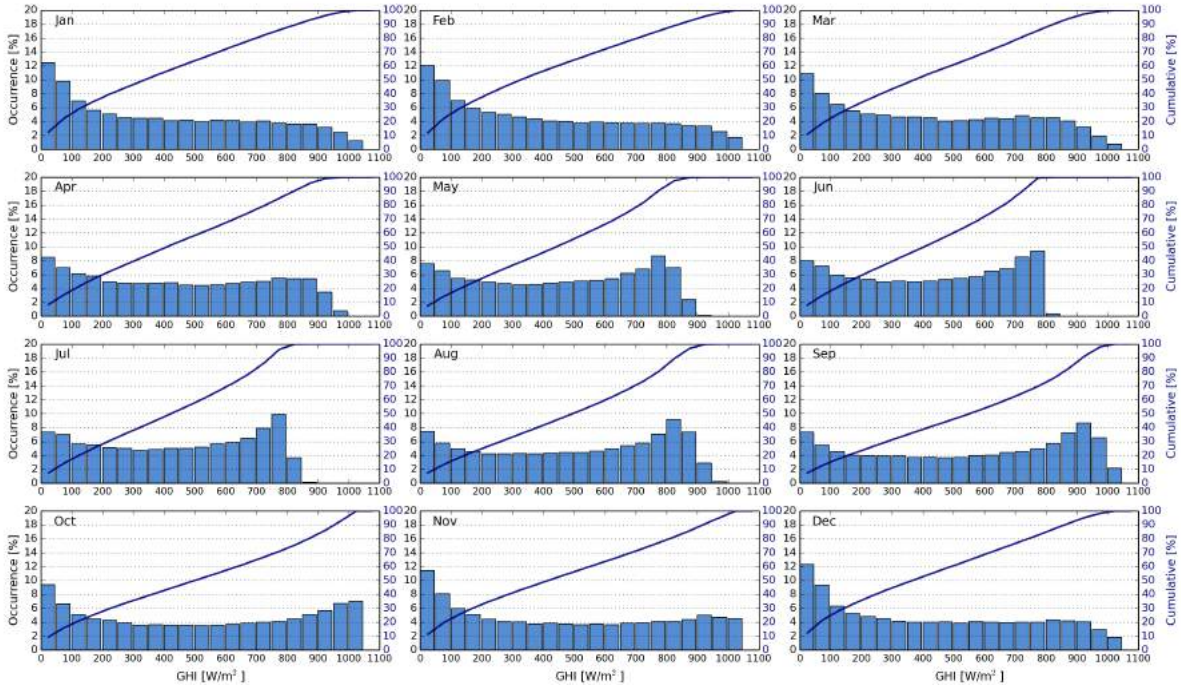

Figure XIX: Histograms and cumulative distribution function of 15-minute GHI in Lusaka UNZA

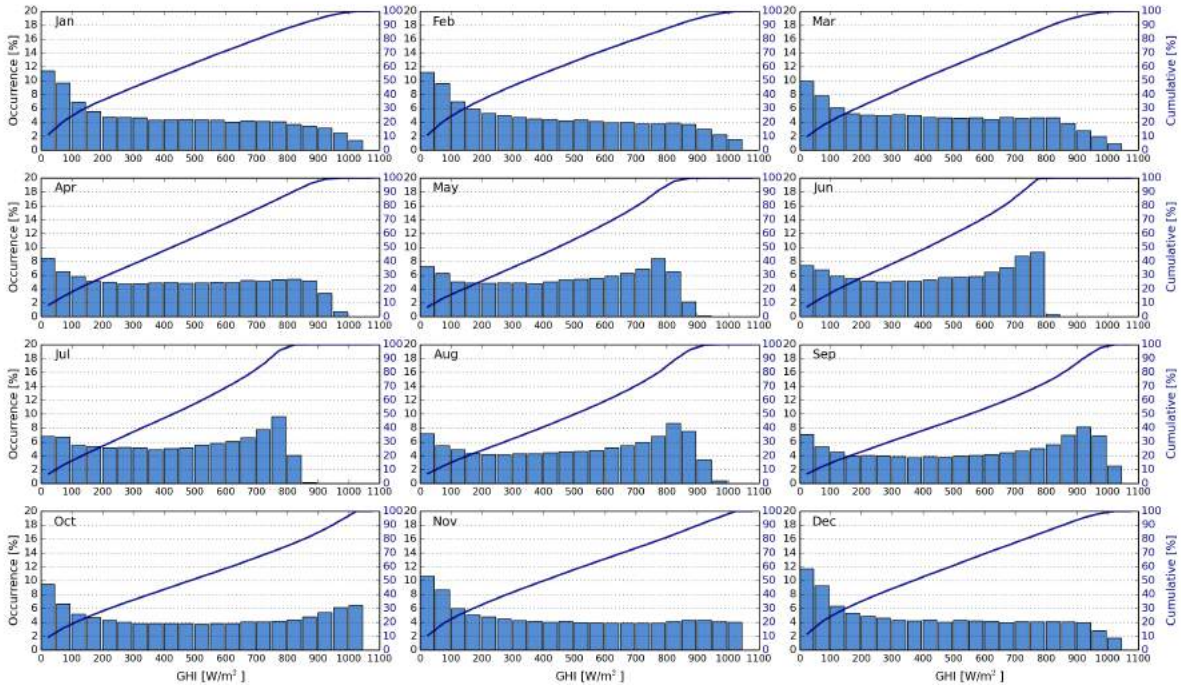

Figure XX: Histograms and cumulative distribution function of 15-minute GHI in Mount Makulu

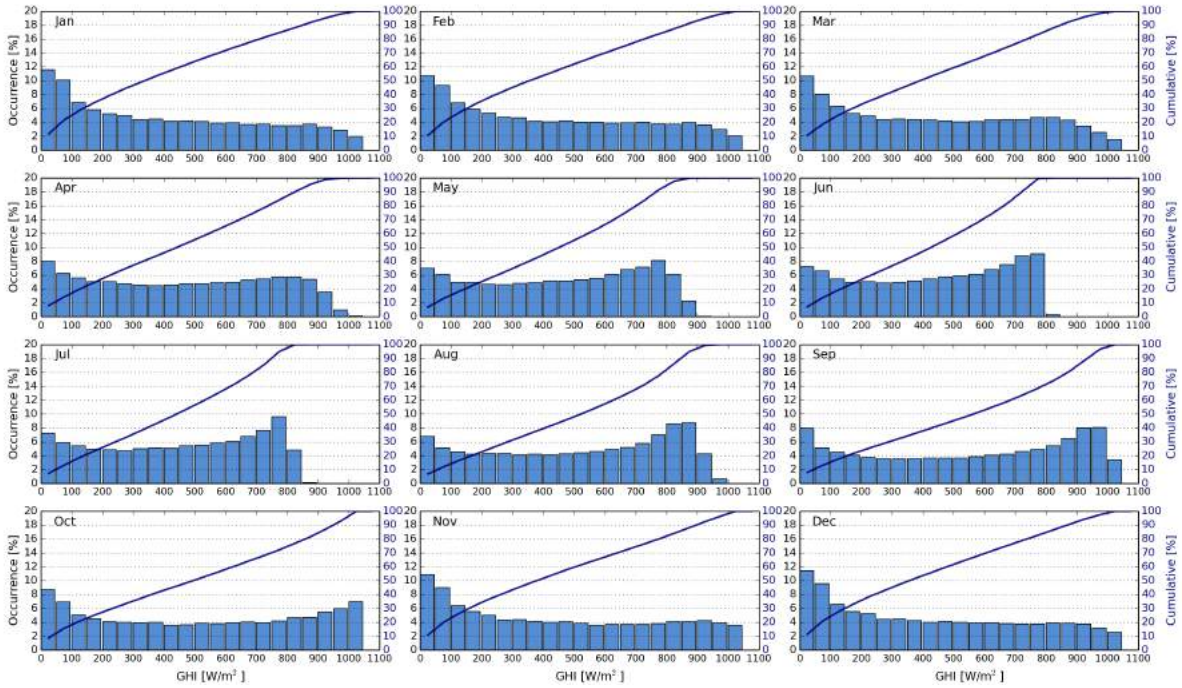

Figure XXI: Histograms and cumulative distribution function of 15-minute GHI in Mochipapa

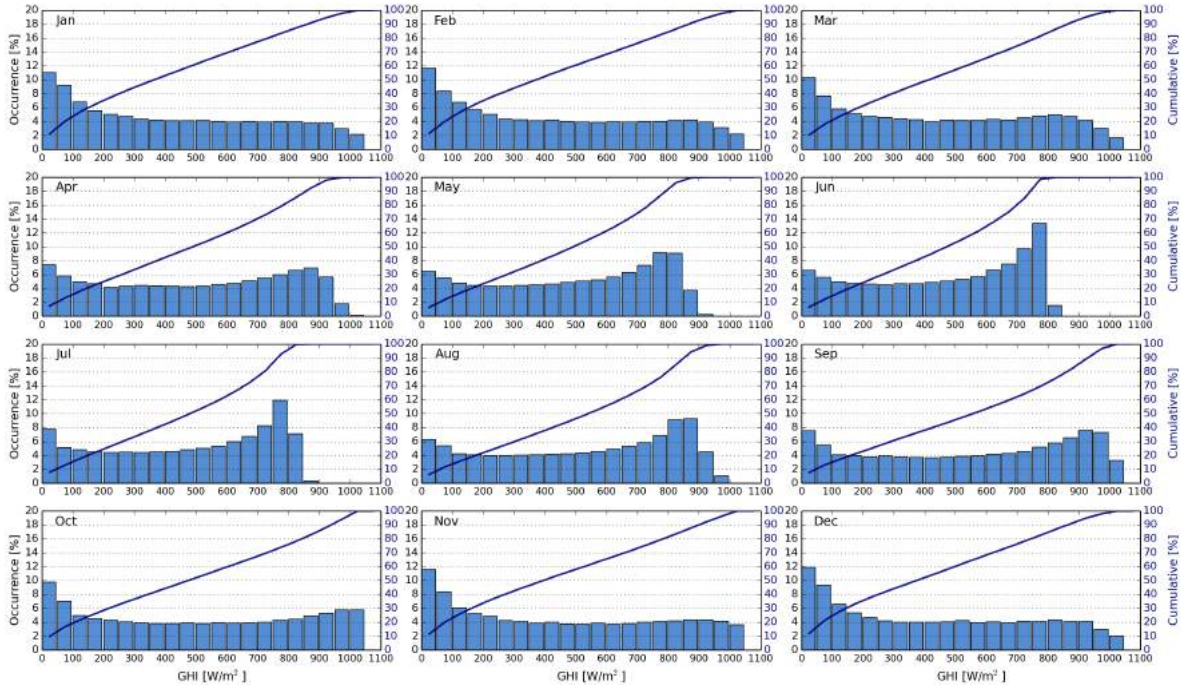

Figure XXII: Histograms and cumulative distribution function of 15-minute GHI in Longe

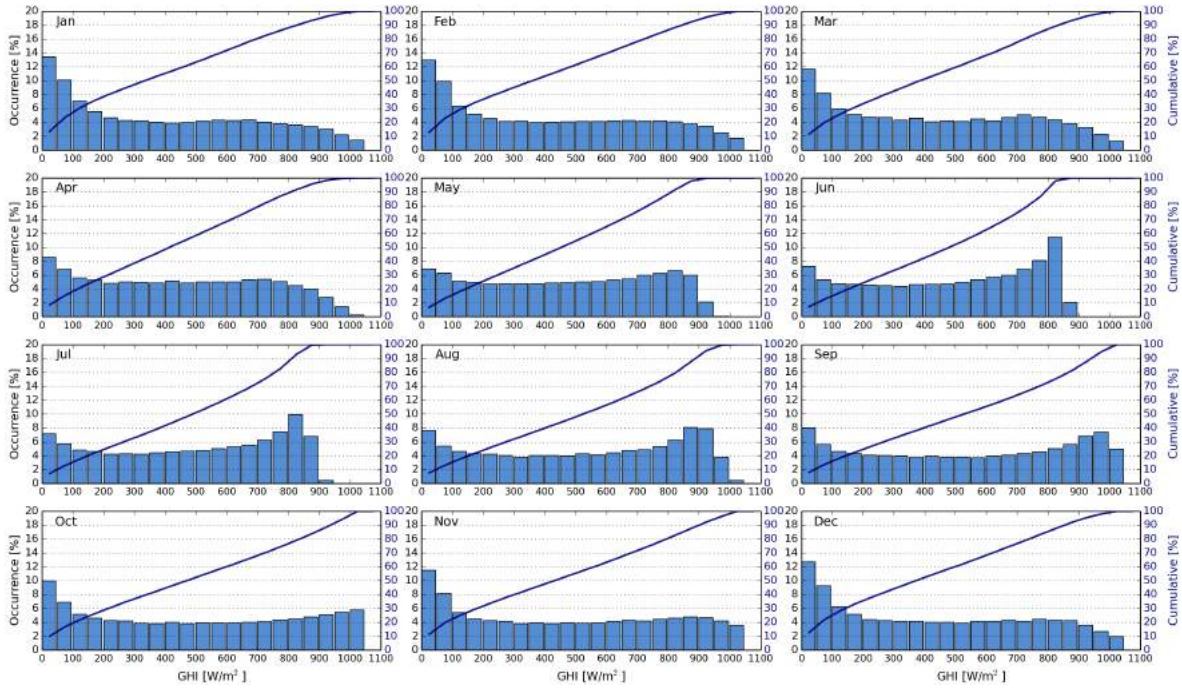

Figure XXIII: Histograms and cumulative distribution function of 15-minute GHI in Misamfu

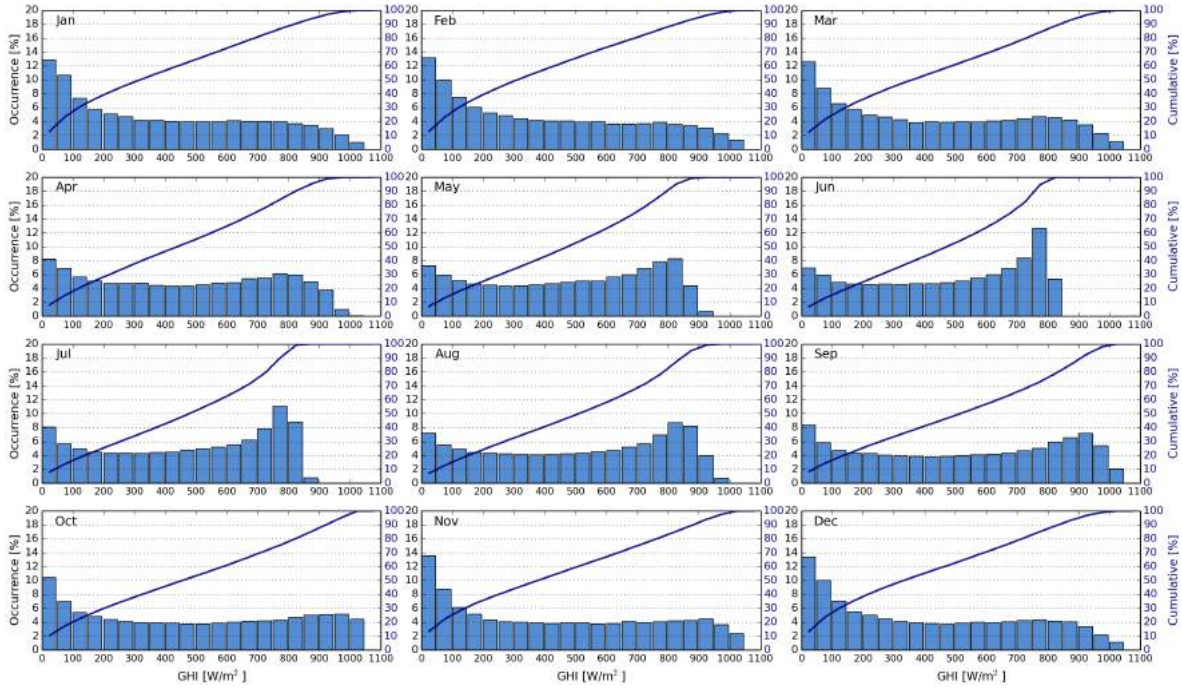

Figure XXIV: Histograms and cumulative distribution function of 15-minute GHI in Mutanda

Figures XIX to XXIV show monthly histograms (bars) and cumulative distribution (line) of 15-minute GHI values, calculated from Solargis time series. The values represent the occurrence of GHI values within 50 W/m^2 bins, ranging from 0 to 1100 W/m^2.

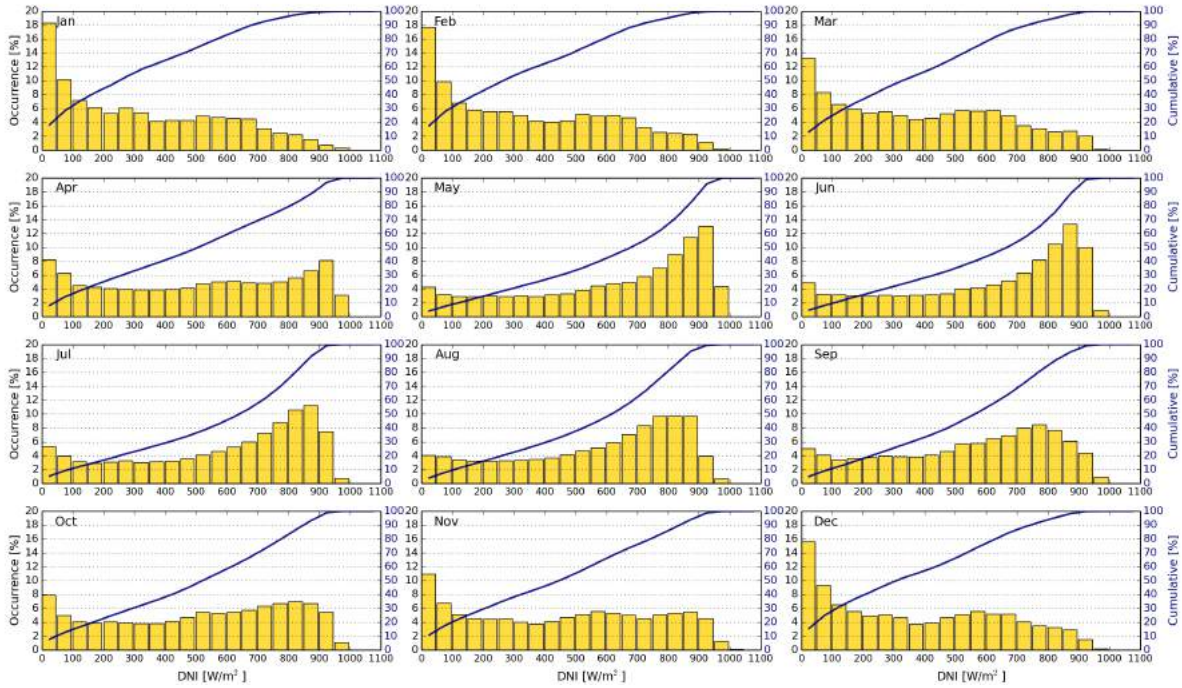

Figure XXV: Histograms and cumulative distribution function of 15-minute DNI in Lusaka UNZA

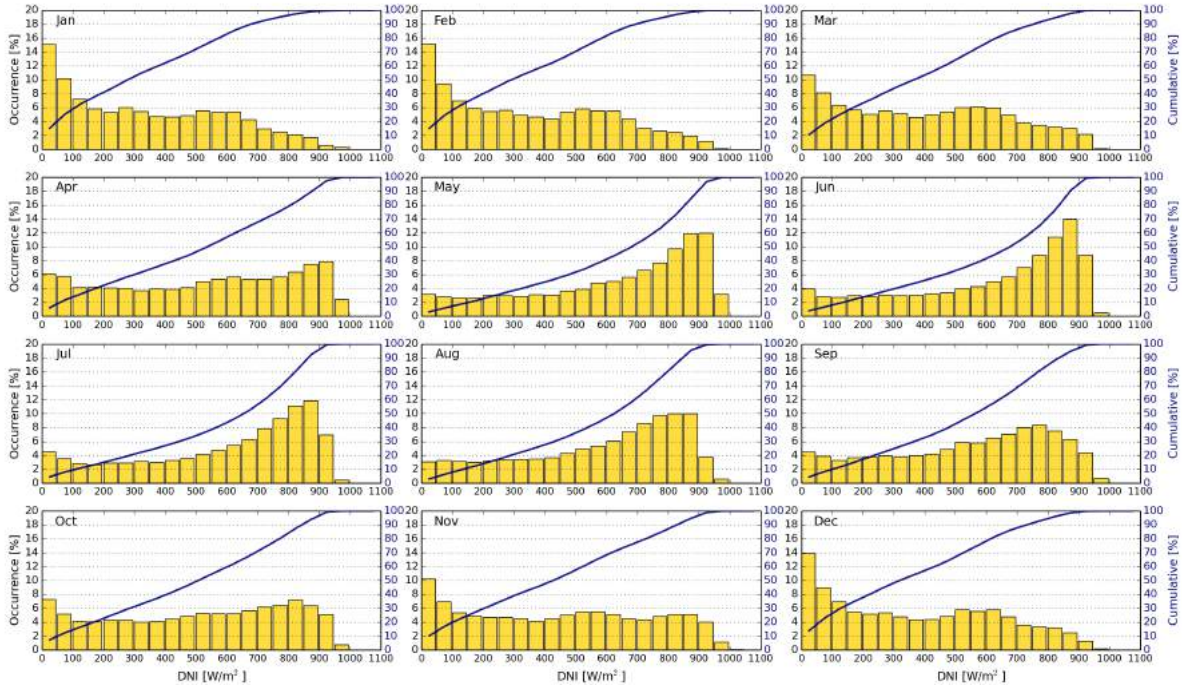

Figure XXVI: Histograms and cumulative distribution function of 15-minute DNI in Mount Makulu

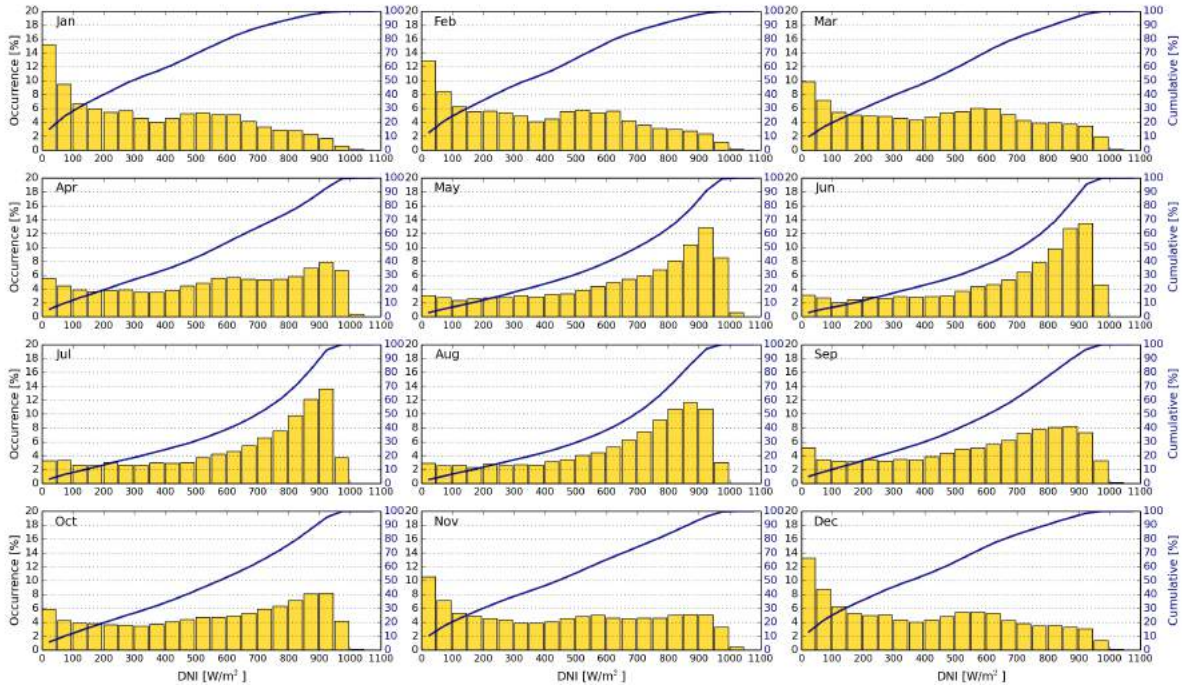

Figure XXVII: Histograms and cumulative distribution function of 15-minute DNI in Mochipapa

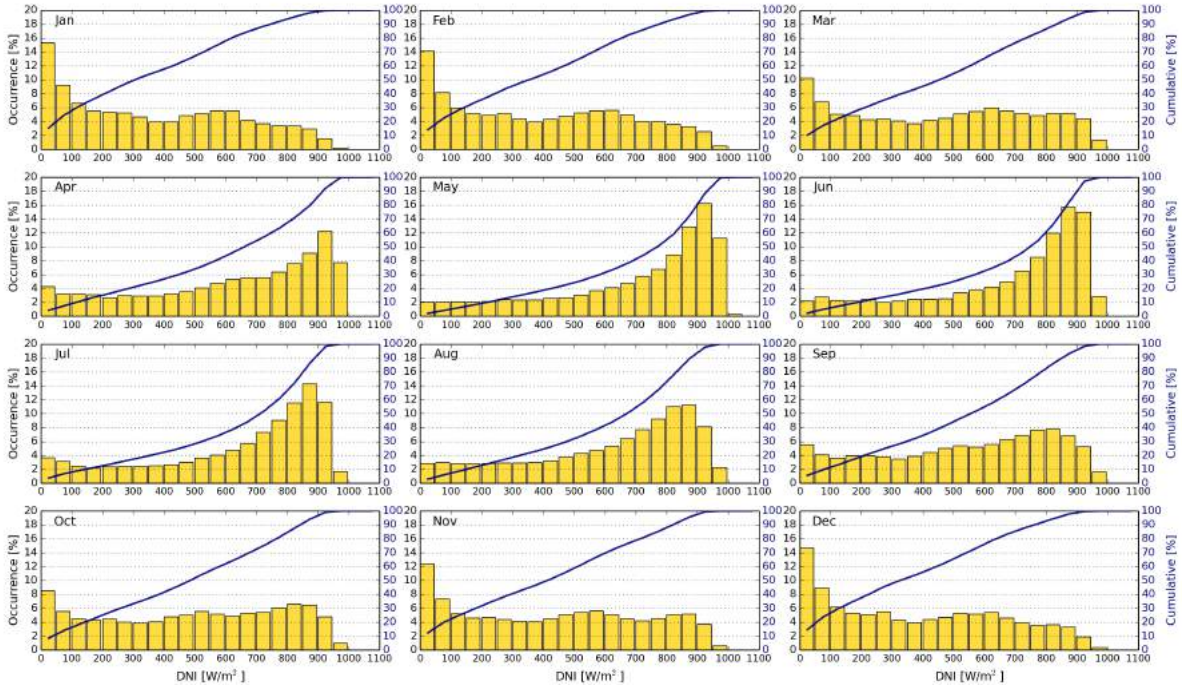

Figure XXVIII: Histograms and cumulative distribution function of 15-minute DNI in Longe

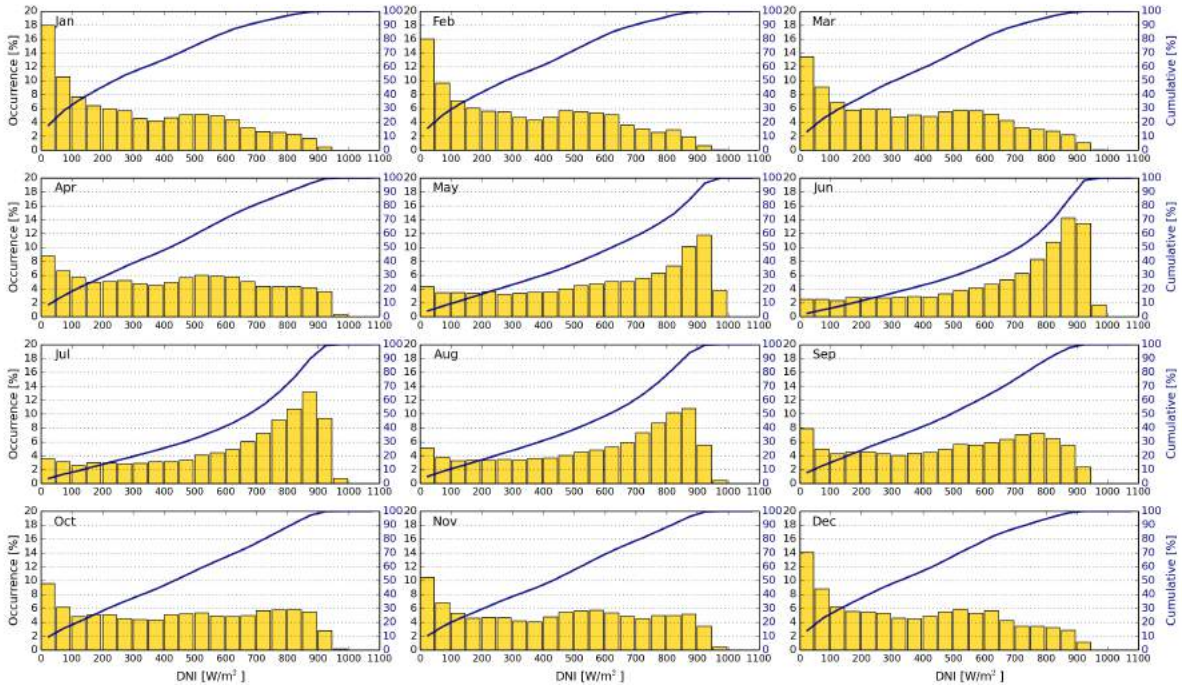

Figure XXIX: Histograms and cumulative distribution function of 15-minute DNI in Misamfu

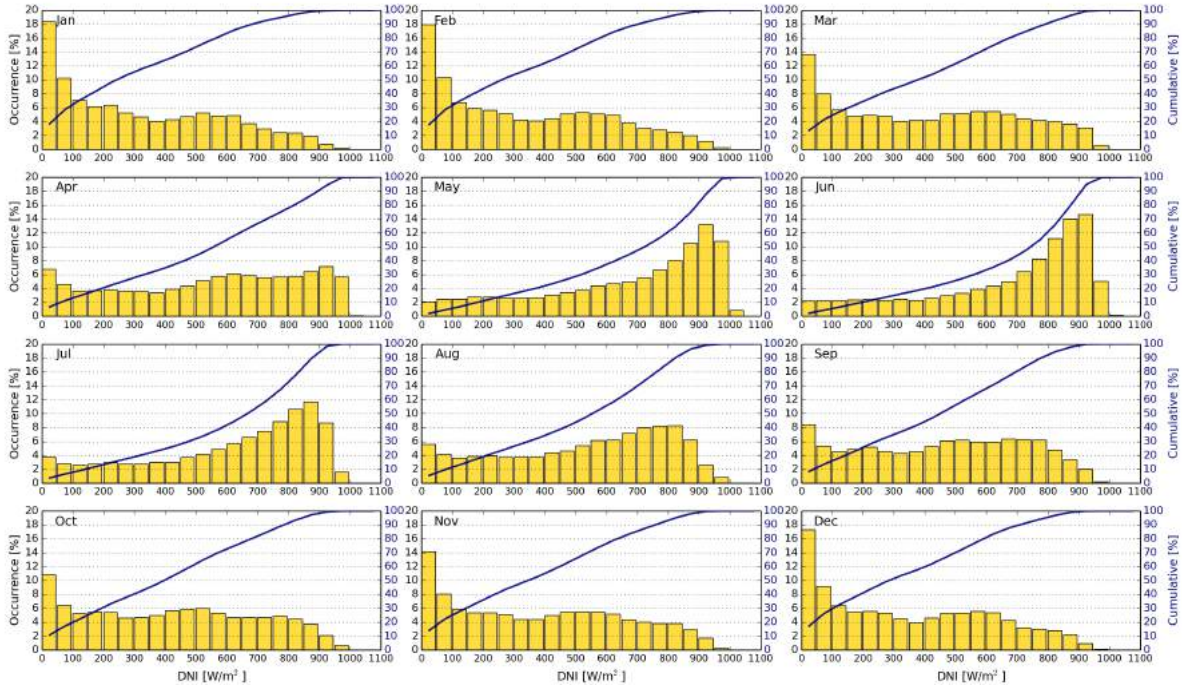

Figure XXX: Histograms and cumulative distribution function of 15-minute DNI in Mutanda

Figures XXV to XXX show monthly histograms (bars) and cumulative distribution (line) of 15-minute DNI values, calculated from Solargis time series. The values represent the occurrence of DNI values within 50 W/m^2 bins, ranging from 0 to 1100 W/m^2.

Frequency of occurrence of GHI and DNI measured and model values representing two years of ground measurements.

Figures XXXI to XLII show histograms comparing the measured values with the model GHI and DNI data. The period covered in these histograms is 24+ months (two full years of data, i.e. from 1 Dec 2015 to 31 Dec 2017):

- 1-minute measured vs. 15-min satellite-based model values
- 15-minute measured (aggregated from 1-min) vs. 15-min satellite-based values
- Daily measured (aggregated from 1-min) vs. daily satellite-based model values

Aggregation process deals with the missing values in the ground measurement in three steps:

1. Only those 1-minute measured data values that passed through quality control (Chapter 3.3) is taken into account (satellite time series does not have gaps.);
2. Aggregation of 1-minute measured data values into 15-minute slots (equivalent to satellite time slots) is applied if more than 15 valid data-points is available, otherwise the 15-minute data slot is ignored in further statistical comparison;
3. Daily aggregation of measured data represents the same 15-minute time slots in a day (passing through the two steps above), as those in the satellite-based data. Incorrect data slots found in the measurements are excluded in both the measured and model data.

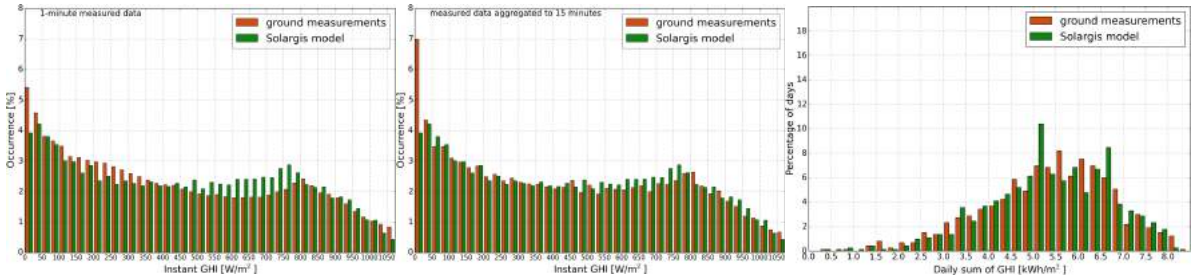

Figure XXXI: Measured vs. satellite-based GHI values in Lusaka UNZA
1-minute measured vs. 15-min satellite-based values.
15-minute measured (aggregated from 1-min) vs. 15-min satellite-based values
Daily measured (aggregated from 1-min) vs. daily satellite-based values

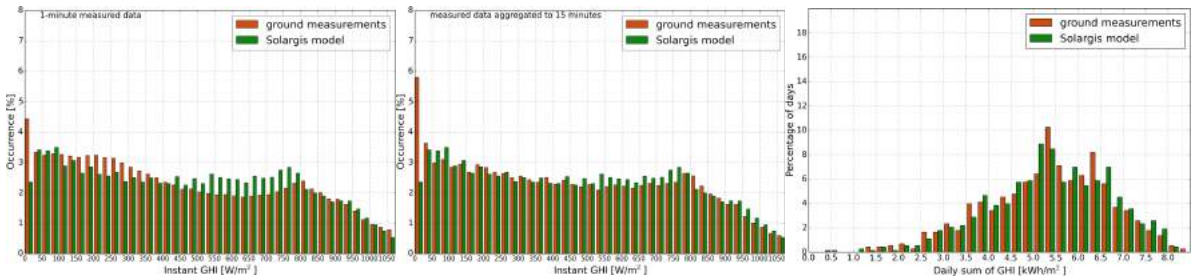

Figure XXXII: Measured vs. satellite-based GHI values in Mount Makulu
1-minute measured vs. 15-min satellite-based values.
15-minute measured (aggregated from 1-min) vs. 15-min satellite-based values
Daily measured (aggregated from 1-min) vs. daily satellite-based values

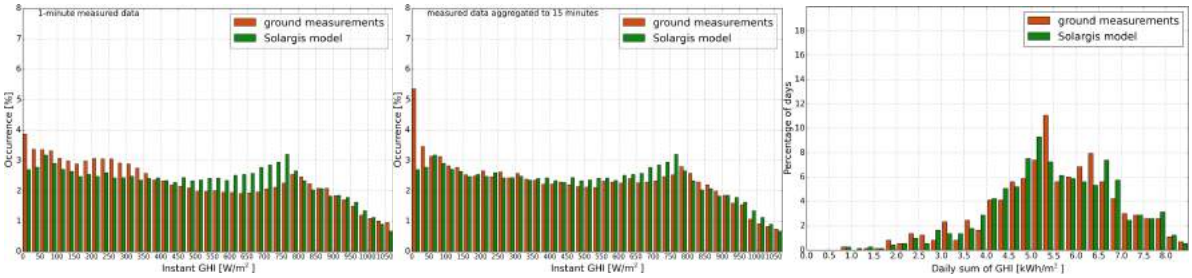

Figure XXXIII: Measured vs. satellite-based GHI values in Mochipapa
1-minute measured vs. 15-min satellite-based values.
15-minute measured (aggregated from 1-min) vs. 15-min satellite-based values
Daily measured (aggregated from 1-min) vs. daily satellite-based values

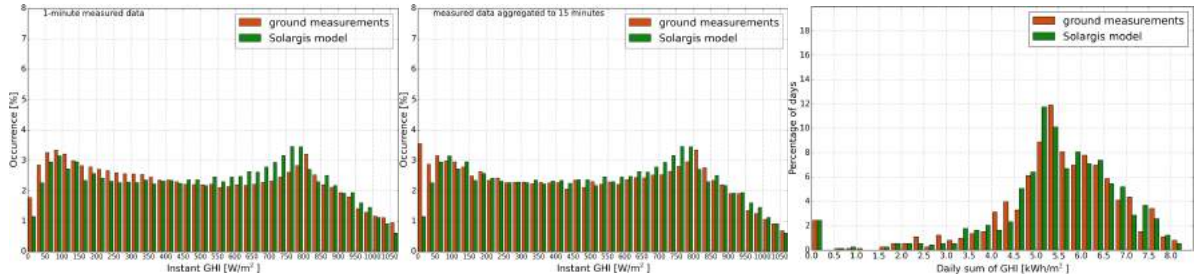

Figure XXXIV: Measured vs. satellite-based GHI values in Longe
1-minute measured vs. 15-min satellite-based values.
15-minute measured (aggregated from 1-min) vs. 15-min satellite-based values
Daily measured (aggregated from 1-min) vs. daily satellite-based values

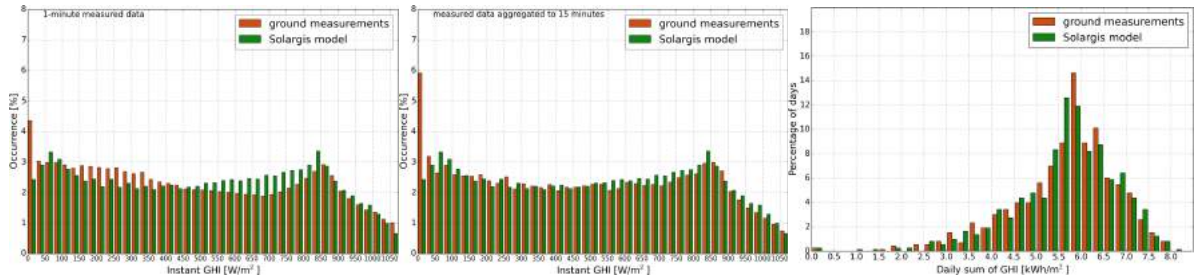

Figure XXXV: Measured vs. satellite-based GHI values in Misamfu
1-minute measured vs. 15-min satellite-based values.
15-minute measured (aggregated from 1-min) vs. 15-min satellite-based values
Daily measured (aggregated from 1-min) vs. daily satellite-based values

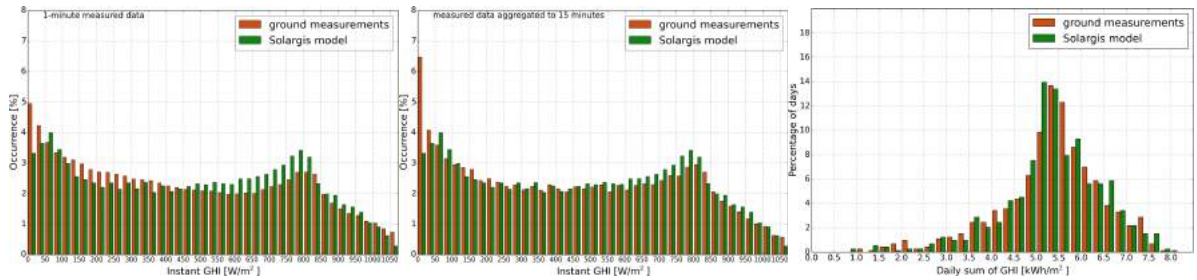

Figure XXXVI: Measured vs. satellite-based GHI values in Mutanda
1-minute measured vs. 15-min satellite-based values.
15-minute measured (aggregated from 1-min) vs. 15-min satellite-based values
Daily measured (aggregated from 1-min) vs. daily satellite-based values

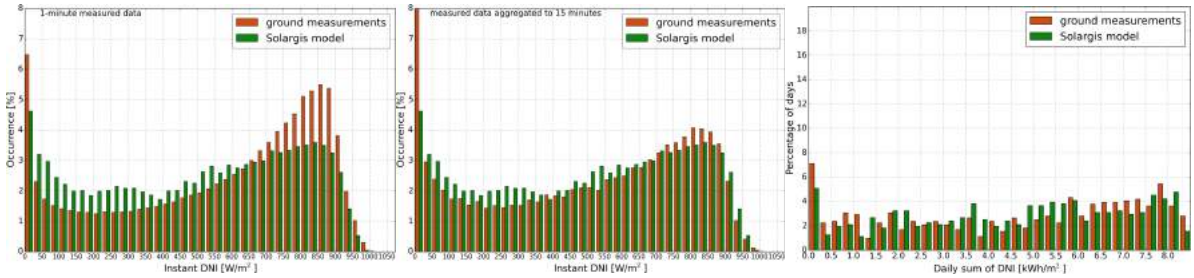

Figure XXXVII: Measured vs. satellite-based DNI values in Lusaka UNZA
1-minute measured vs. 15-min satellite-based values.
15-minute measured (aggregated from 1-min) vs. 15-min satellite-based values
Daily measured (aggregated from 1-min) vs. daily satellite-based values

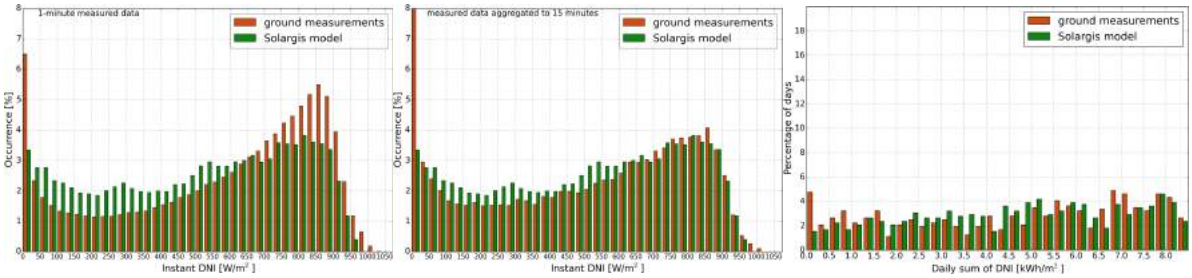

Figure XXXVIII: Measured vs. satellite-based DNI values in Mount Makulu
1-minute measured vs. 15-min satellite-based values.
15-minute measured (aggregated from 1-min) vs. 15-min satellite-based values
Daily measured (aggregated from 1-min) vs. daily satellite-based values

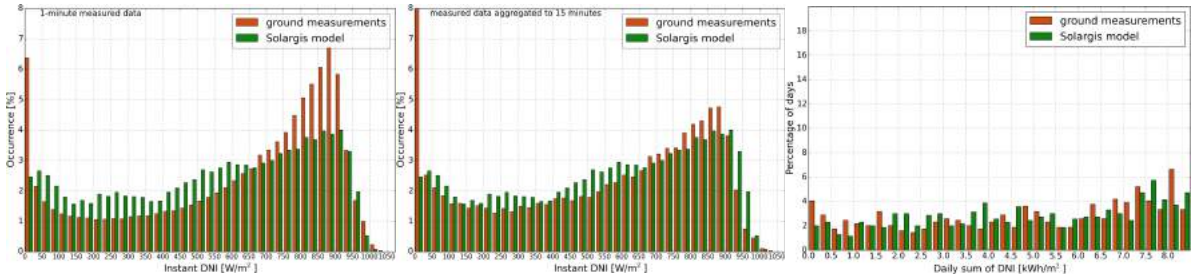

Figure XXXIX: Measured vs. satellite-based DNI values in Mochipapa
1-minute measured vs. 15-min satellite-based values.
15-minute measured (aggregated from 1-min) vs. 15-min satellite-based values
Daily measured (aggregated from 1-min) vs. daily satellite-based values

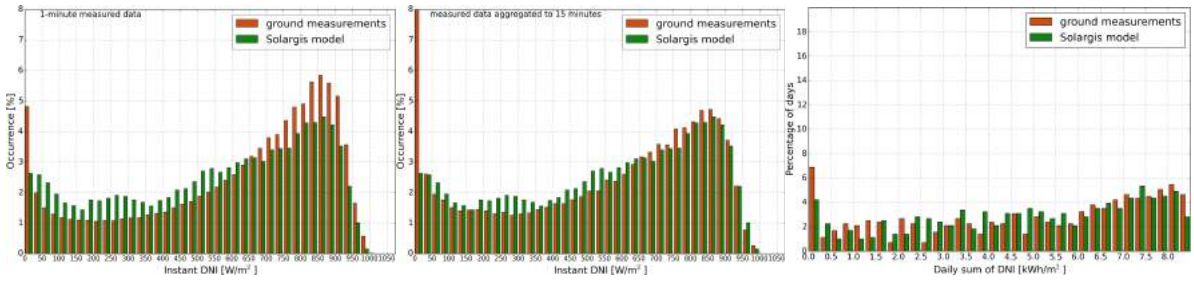

Figure XL: Measured vs. satellite-based DNI values in Longe
1-minute measured vs. 15-min satellite-based values.
15-minute measured (aggregated from 1-min) vs. 15-min satellite-based values
Daily measured (aggregated from 1-min) vs. daily satellite-based values

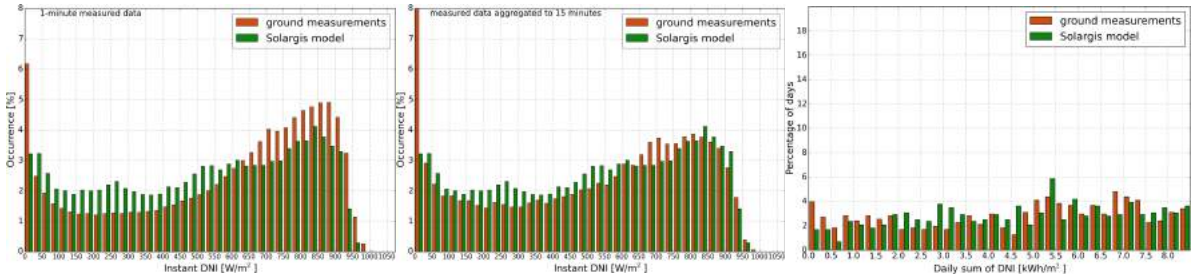

Figure XLI: Measured vs. satellite-based DNI values in Misamfu
1-minute measured vs. 15-min satellite-based values.
15-minute measured (aggregated from 1-min) vs. 15-min satellite-based values
Daily measured (aggregated from 1-min) vs. daily satellite-based values

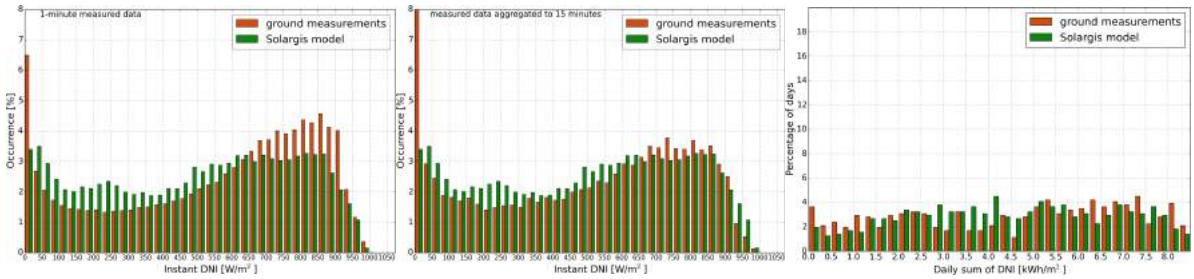

Figure XLII: Measured vs. satellite-based DNI values in Mutanda
1-minute measured vs. 15-min satellite-based values.
15-minute measured (aggregated from 1-min) vs. 15-min satellite-based values
Daily measured (aggregated from 1-min) vs. daily satellite-based values

Frequency of occurrence of GHI and DNI ramps

Figures XLIII to LIV show histograms of instantaneous changes (ramps) calculated from the measurements and compared to the instantaneous changes calculated for the model data. Figures show both negative (-) and positive (+) changes. Two versions for GHI and DNI are shown:

- Ramps calculated from 1-minute measured values compared to ramps calculated from 15-minute satellite-based data (figure on the left)
- Ramps calculated from 15-minute aggregated valid measurement compared to ramps calculated from 15-minute satellite-based data (figure on the right).

Occurrence of gaps in the measurements is managed in the same way as described about in this Chapter:

1. For measurements, only those 1-minute data values (measurements) that passed through quality control (Chapter 3.3) is taken into account (satellite time series does not have gaps.);
2. For measurements, the aggregation (averaging) of 1-minute measured data values into 15-minute slots (equivalent to satellite time slots) is applied if more than 15 valid data-points is available, otherwise the 15-minute data slot is ignored in further statistical comparison;

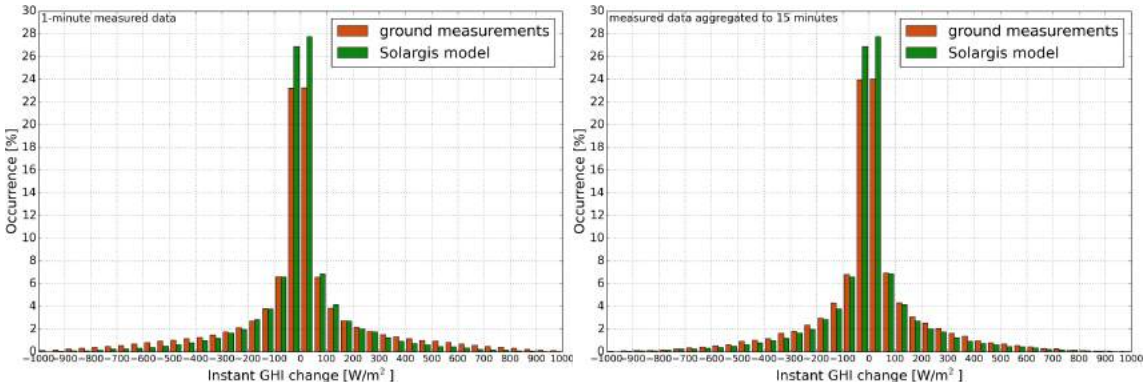

Figure XLIII: 1-minute and 15-minute GHI ramps (measured and satellite data) at Lusaka UNZA.

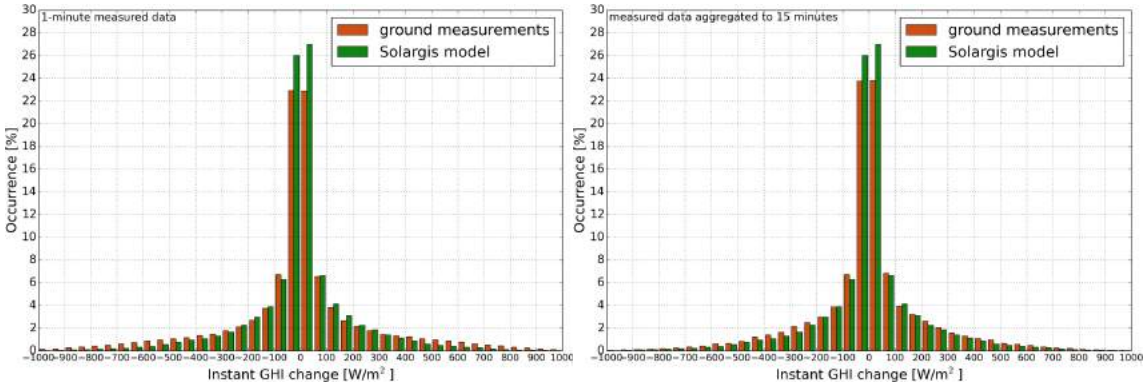

Figure XLIV: 1-minute and 15-minute GHI ramps (measured and satellite data) at Mount Makulu

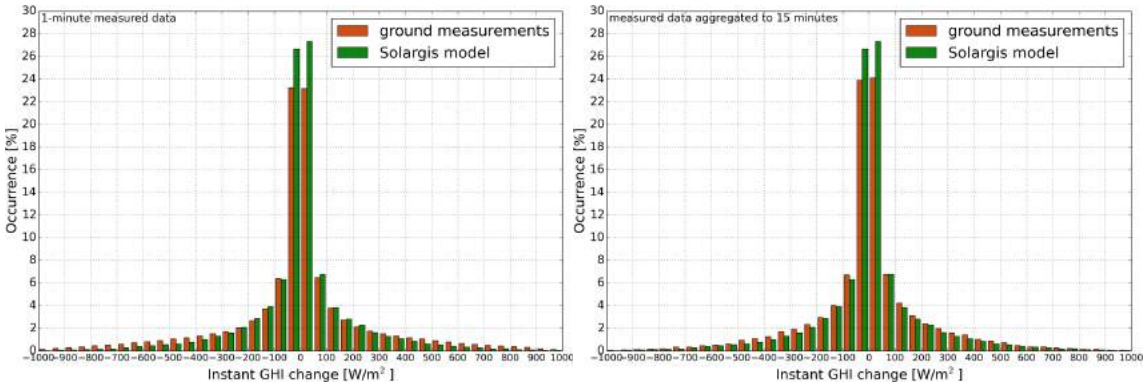

Figure XLV: 1-minute and 15-minute GHI ramps (measured and satellite data) at Mochipapa

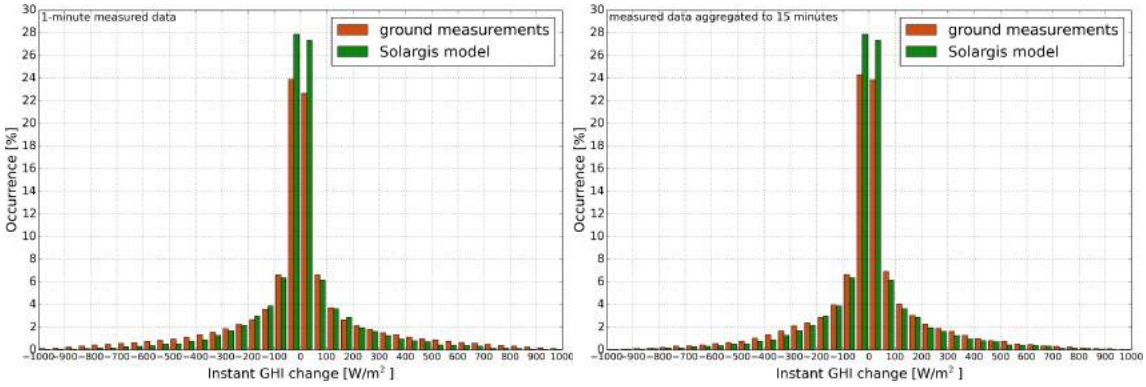

Figure XLVI: 1-minute and 15-minute GHI ramps (measured and satellite data) at Longe

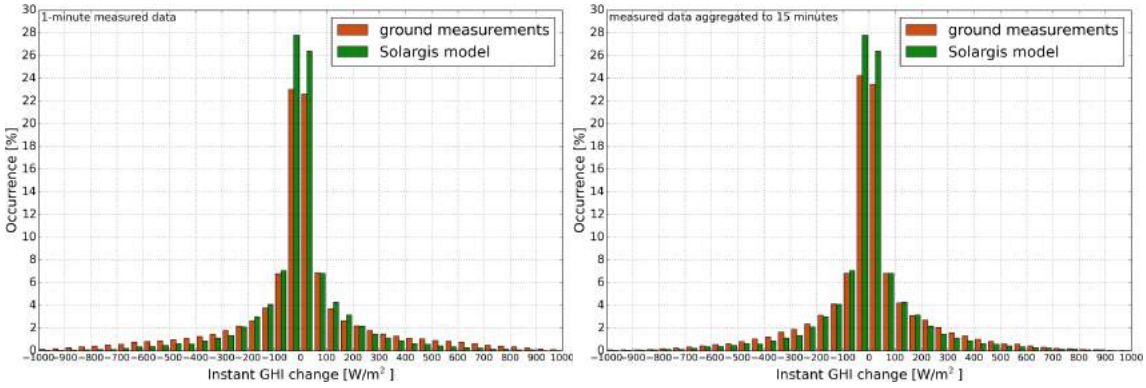

Figure XLVII: 1-minute and 15-minute GHI ramps (measured and satellite data) at Misamfu

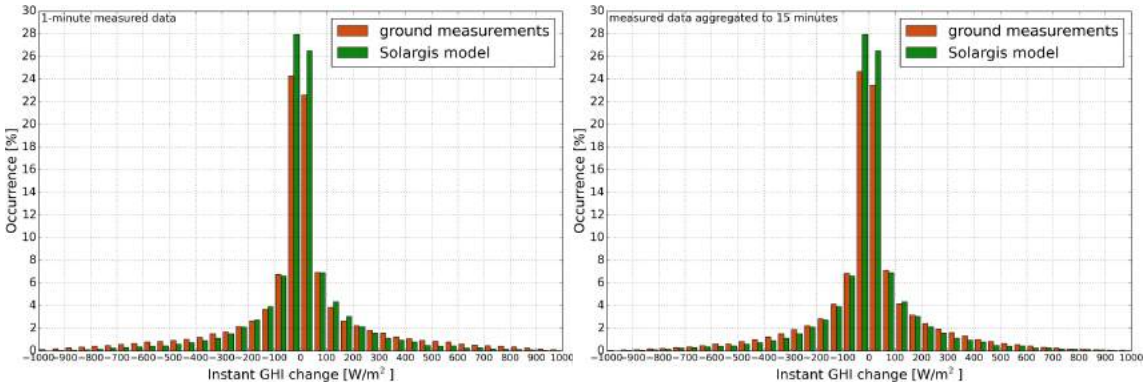

Figure XLVIII: 1-minute and 15-minute GHI ramps (measured and satellite data) at Mutanda

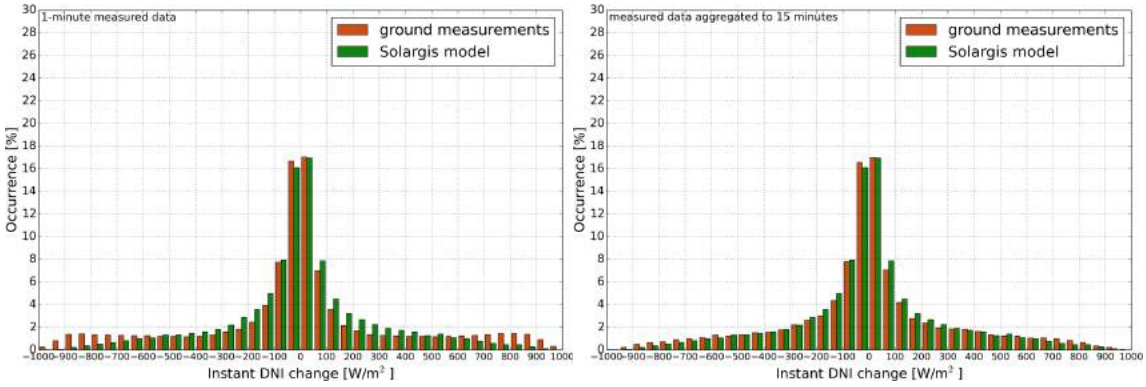

Figure XLIX: 1-minute and 15-minute DNI ramps (measured and satellite data) at Lusaka UNZA

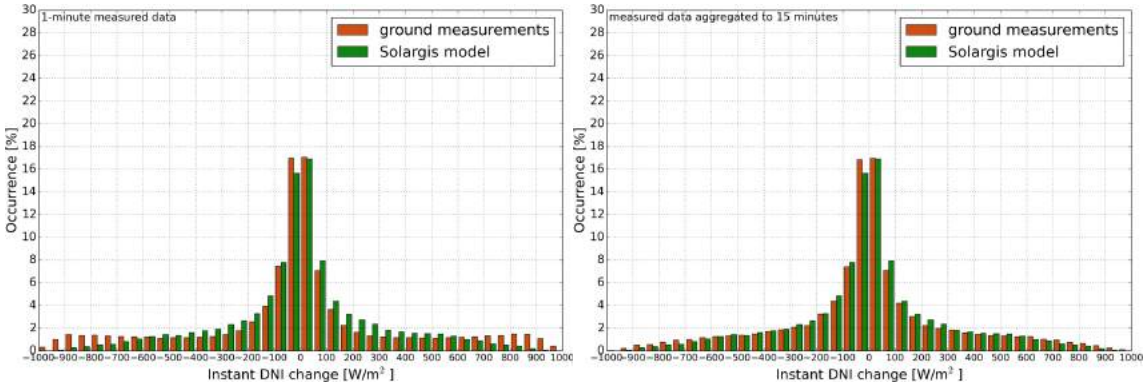

Figure L: 1-minute and 15-minute DNI ramps (measured and satellite data) at Mount Makulu

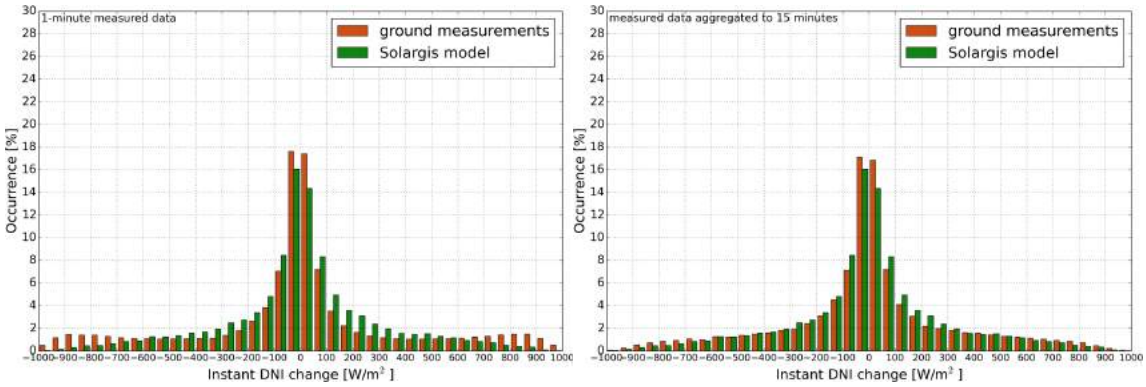

Figure LI: 1-minute and 15-minute DNI ramps (measured and satellite data) at Mochipapa

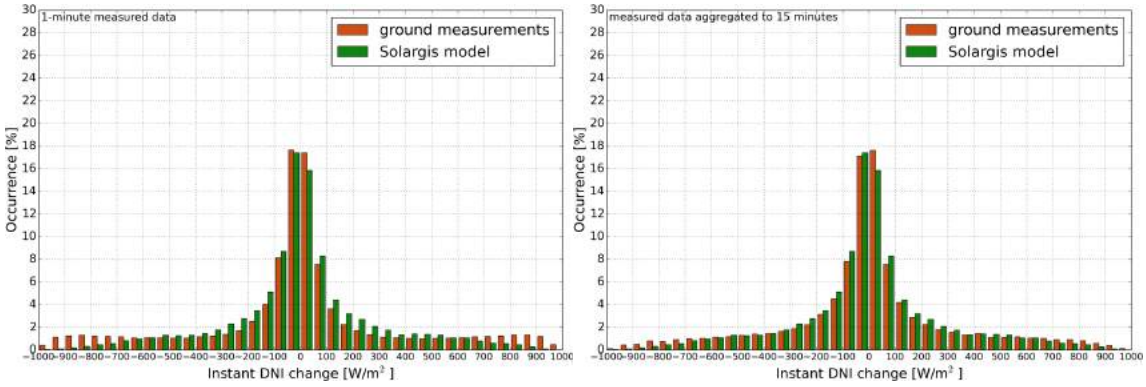

Figure LII: 1-minute and 15-minute DNI ramps (measured and satellite data) at Longe

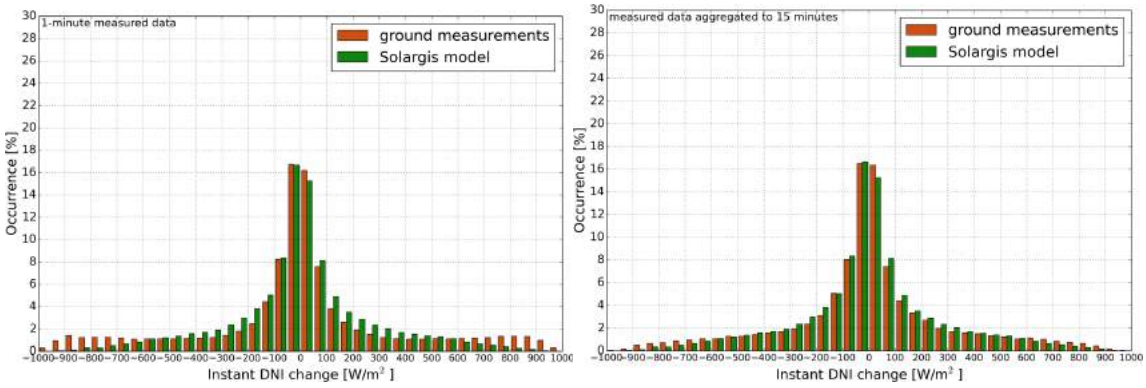

Figure LIII: 1-minute and 15-minute DNI ramps (measured and satellite data) at Misamfu

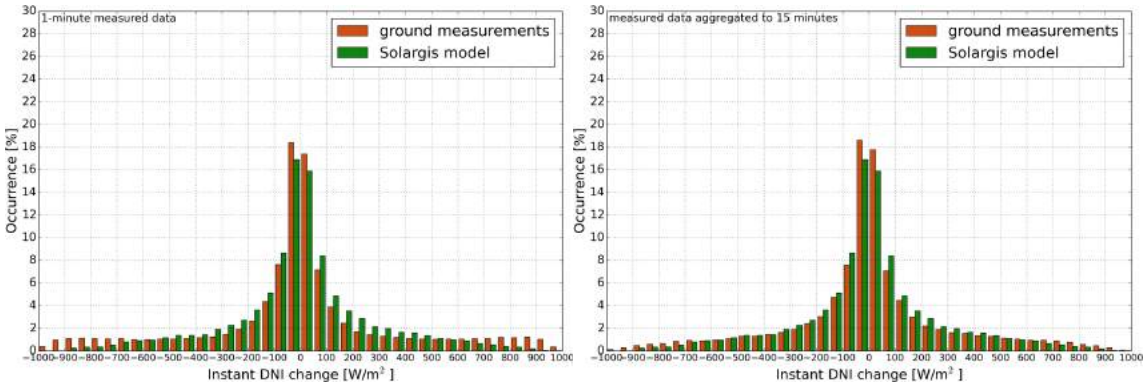

Figure LIV: 1-minute and 15-minute DNI ramps (measured and satellite data) at Mutanda

LIST OF FIGURES

LIST OF TABLES

REFERENCES

[1] NREL, 1993. User's Manual for SERI_QC Software-Assessing the Quality of Solar Radiation Data. NREL/TP-463-5608. Golden, CO: National Renewable Energy Laboratory.

[2] Younes S., Claywell R. and Muneer T, 2005. Quality control of solar radiation data: Present status and proposed new approaches. Solar Energy 30, 1533-1549.

[3] Perez R., Cebecauer T., Šúri M., 2013. Semi-Empirical Satellite Models. In Kleissl J. (ed.) Solar Energy Forecasting and Resource Assessment. Academic press. http://www.sciencedirect.com/science/article/pii/B9780123971777000024

[4] Cebecauer T., Šúri M., Perez R., High performance MSG satellite model for operational solar energy applications. ASES National Solar Conference, Phoenix, USA, 2010. http://solargis.com/assets/publication/2010/Cebecauer-Suri-Perez--ASES2010--High-performance-MSG-satellite-model-for-operational-solar-energy-applications.pdf

[5] Šúri M., Cebecauer T., Perez P., 2010. Quality Procedures of Solargis for Provision Site-Specific Solar Resource Information. Conference SolarPACES 2010, September 2010, Perpignan, France. http://solargis.com/assets/publication/2010//Suri-Cebecaue--Perez-SolarPACES2010--Quality-procedures-of-solargis-for-provision-site-specific-solar-resource-information.pdf

[6] Cebecauer T., Suri M., Gueymard C., Uncertainty sources in satellite-derived Direct Normal Irradiance: How can prediction accuracy be improved globally? Proceedings of the SolarPACES Conference, Granada, Spain, 20-23 Sept 2011.

[7] http://solargis.com/assets/publication/2011/Cebecauer-Suri-Gueymard--SolarPACES2011--Uncertainty-sources-in-satellite-derived-direct-normal-irradiance--How-can-prediction-accuracy-be-improved-globally.pdf

[8] Suri M., Cebecauer T., 2014. Satellite-based solar resource data: Model validation statistics versus user's uncertainty. ASES SOLAR 2014 Conference, San Francisco, 7-9 July 2014. http://solargis.com/assets/publication/2014//Suri-Cebecauer--ASES-Solar2014--Satellite-Based-Solar-Resource-Data--Model-Validation-Statistics-Versus-User-Uncertainty.pdf

[9] Ineichen P., A broadband simplified version of the Solis clear sky model, 2008. Solar Energy, 82, 8, 758-762.

[10] Benedictow A. et al. 2012. Validation report of the MACC reanalysis of global atmospheric composition: Period 2003-2010, MACC-II Deliverable D83.1.

[11] Molod, A., Takacs, L., Suarez, M., and Bacmeister, J., 2015: Development of the GEOS-5 atmospheric general circulation model: evolution from MERRA to MERRA2, Geosci. Model Dev., 8, 1339-1356, doi:10.5194/gmd-8-1339-2015

[12] GFS model. http://www.nco.ncep.noaa.gov/pmb/products/gfs/

[13] CFSR model. https://climatedataguide.ucar.edu/climate-data/climate-forecast-system-reanalysis-cfsr/

[14] CFSv2 model http://www.cpc.ncep.noaa.gov/products/CFSv2/CFSv2seasonal.shtml

[15] Cano D., Monget J.M., Albuisson M., Guillard H., Regas N., Wald L., 1986. A method for the determination of the global solar radiation from meteorological satellite data. Solar Energy, 37, 1, 31–39.

[16] Perez R., Ineichen P., Maxwell E., Seals R. and Zelenka A., 1992. Dynamic global-to-direct irradiance conversion models. ASHRAE Transactions-Research Series, pp. 354-369.

[17] Perez, R., Seals R., Ineichen P., Stewart R., Menicucci D., 1987. A new simplified version of the Perez diffuse irradiance model for tilted surfaces. Solar Energy, 39, 221-232.

[18] Ruiz-Arias J.A., Cebecauer T., Tovar-Pescador J., Šúri M., 2010. Spatial disaggregation of satellite-derived irradiance using a high-resolution digital elevation model. Solar Energy, 84,1644-57. http://www.sciencedirect.com/science/article/pii/S0038092X10002136

[19] Zelenka A., Perez R., Seals R., Renne D., 1997. Effective Accuracy of Satellite-Derived Hourly Irradiances. Theoretical Appl. Climatology, 62, 199-207.

[20] Espinar B., Ramírez L., Drews A., Beyer H. G., Zarzalejo L. F., Polo J., Martín L., Analysis of different comparison parameters applied to solar radiation data from satellite and German radiometric stations. Solar Energy, 83, 1, 118-125, 2009.

[21] Cebecauer T., Suri M., 2015. Site-adaptation of satellite-based DNI and GHI time series: overview and Solargis approach. SolarPACES conference, September 2015, Cape Town, North Africa. http://solargis.com/assets/publication/2015/Cebecauer-Suri--2015-SolarPaces--Site-adaptation-of-satellite-based-DNI-and-GHI-time-series--Overview-and-SolarGIS-approach.pdf

[22] Polo J., Wilbert S., Ruiz-Arias J.A., Meyer R., Gueymard C., Šúri M., Martín L., Mieslinger T., Blanc P., Grant I., Bolan J., Ineichen P., Remund J., Escobar R., Troccoli A., Sengupta M., Nielsen K.P., Renné D., Geuder N., Cebecauer T., 2016. Preliminary survey on site-adaptation techniques for satellite-derived and reanalysis solar radiation datasets. Solar Energy, 132, 25–37.

[23] Lohmann S., Schillings C., Mayer B., Meyer R., 2006. Long-term variability of solar direct and global radiation derived from ISCCP data and comparison with reanalysis data, Solar Energy, 80, 11, 1390-1401.

[24] Gueymard C., Solar resource assessment for CSP and CPV. Leonardo Energy webinar, 2010. http://www.leonardo-energy.org/webfm_send/4601

[25] Cebecauer T., Šúri M., 2015. Typical Meteorological Year Data: Solargis Approach. Energy Procedia, Volume 69, 1958-1969. http://dx.doi.org/10.1016/j.egypro.2015.03.195

[26] Sensor Verification Report Project: ESMAP Zambia. GeoSUN Africa, August 2016, reference No. 2012-026-1216-08.

SUPPORT INFORMATION

Background on Solargis

Solargis is a technology company supplying solar resource and meteorological data, software applications and consultancy services to solar energy industry. Our services are used globally in identification of optimum sites for development of solar power plants, for technical and financial evaluation and optimisation of solar energy production. We develop and operate own technology based on a new-generation high-resolution global meteorological database and software applications integrated within the Solargis® online information system. Accurate and standardised energy simulation data reduce the weather-related risks and costs in planning, performance evaluation, forecasting and management of distributed solar power systems.

Solargis is a technology company offering solar and meteorological data, software and consultancy services to solar energy. We support industry in the site qualification, planning, financing and operation of solar energy systems for more than 18 years. We develop and operate a new generation high-resolution global database and applications integrated within Solargis® information system. Accurate, standardised and validated data help to reduce the weather-related risks and costs in system planning, performance assessment, forecasting and management of distributed solar power.

Legal information

Considering the nature of climate fluctuations, interannual and long-term changes, as well as the uncertainty of measurements and calculations, company Solargis cannot take guarantee of the accuracy of estimates. Company Solargis has done maximum possible for the assessment of climate conditions based on the best available data, software and knowledge. Solargis® is the registered trademark of company Solargis. Other brand names and trademarks that may appear in this study are the ownership of their respective owners.

ISO 9001
LL-C (Certification)

Solargis is ISO 9001:2015 certified company for quality management.

Authors:	Marcel Suri Tomas Cebecauer Branislav Schnierer Artur Skoczek Daniel Chrkavy Nada Suriova
Maps:	Juraj Betak Veronika Madlenakova
Project manager:	Nada Suriova
Approved by:	Marcel Suri


SOLARGIS